Katholieke Universiteit Leuven

FACULTEIT WETENSCHAPPEN
Departement Chemie
Afdeling Coördinatiechemie

Spectroscopy of lanthanide ions in silica-based hybrid materials

Proefschrift ingediend voor het behalen van de graad van Doctor in de Wetenschappen

Kris Driesen

Leuven, 22 mei 2003

Promotoren

Prof. Dr. K. Binnemans

Prof. Dr. C. Görller-Walrand

Leden van de examencommissie:

Promotoren:	Prof. Dr. K. Binnemans
	Prof. Dr. C. Görller-Walrand
Andere leden:	Prof. Dr. G. Adriaenssens
	Prof. Dr. J. Mullens (L.U.C.)
	Prof. Dr. M. Van der Auweraer
	Prof. Dr. L. Vanquickenborne
	Prof. Dr. T. Verbiest

Acknowledgements:

I may have created the illusion that my PhD work was easy (or not) and that I have done everything by myself… This is untrue. A lot of people have helped me through this period and I would like to take this opportunity to thank them.

First of all I would like to thank my supervisors Prof. C. Görller-Walrand and Prof. K. Binnemans. They have given me the opportunity to start with an interesting project, supported me and provided the necessary equipment. Chemists are most of the time like children and like to play with toys, *big expensive* toys. Especially the arrival of the NIR-spectrofluorimeter made me happy.

Secondly I would like to thank Philip Lenaerts for helping me with the "almost always"-cracking silica sol-gel glasses. Many times our three-months work converted into thousands of worthless pieces (in a few minutes). If like they say in dutch: "scherven brengen geluk", I have a few good recipes. I would also like to thank Sofie Fourier for the hard work on the PEG-silica materials. Fortunately these samples did not crack.

Thirdly, I would like to thank all the people with whom I discussed during these four years. Thanks go to Dr. R. Van Deun, Dr. P. Nockemann, Dr. M. Van Bael (LUC), Dr. T. Vogth, K. Somers and Prof. J. Martens. I also would like to thank Prof. J. Mullens (LUC) for the use of his labs for the preparation of the SiO_2-TiO_2-GDLCs. P. Bloemen and L. Van Nerum helped with the analysis.

Fourthly, I would like to thank my colleagues and other people of the "200F". Besides the serious work done in the labs and technical talks in the corridors ☺, I must thank them for the good atmosphere. I'll try to summarize all in alphabetical order*: Antoine, Dries, Firmin, Georges, Jules, Jurgen, Katleen (10 years already!), Kelly, Ken, Koen 2x, Kristof, Leen, Liesbet, Linda, Pascal, Peter, Petra (& Frank), Philip, Pol, Rik, Sandy, Sofie, Tanja, Thomas…. I would like to express my appreciation to Rita for keeping order in the chaos and the administration.
Also at other places, like Italy or at the LUC, the atmosphere was good; thanks Daniel & Kristof, An, Dirk, John and Marlies.

Fiftly, I would like to thank my friends and my family for their support. And last but not least, special thanks go to my girlfriend Veerle.

(*) Disclaimer: In the light of "previous events", © the author reserves the right not to be responsible completeness or quality of the list provided **in the acknowledgement**.

Contents

Introduction

Materials doped with lanthanides are of particular interest for optical applications. The trivalent lanthanides ions are well known for the high colorimetric purity of their absorption and luminescence. Also very appealing is the near-infrared luminescence of Nd(III), Er(III) and Yb(III). Most materials, that are being used in applications, are inorganic lanthanide compounds like glasses and crystals. Well-known examples are the red luminescent phosphor Y_2OS_2:Eu(III) in CRT-tubes for color television and the near-infrared YAG:Nd(III) lasers. More recently, applications for luminescent organic complexes of lanthanides have been investigated. A good light-absorbing ligand can function as an antenna by transferring the absorbed energy from the ligand to the lanthanide ion and thus increasing the quantum yield. However these complexes must be doped in materials that are suitable for optical applications.

One of the older, but still appealing, inorganic materials is ordinary silica glass. It has a high optical transparency, has good mechanical properties and is very abundant… In search for a better process to make the perfect window glass, the sol-gel method gained a lot of attention. Despite the enormous efforts, this route has not lived up to the expectations. But the know-how of the sol-gel science is now used as a versatile route to small monoliths, gels, thin films and porous silica materials starting from silicon alkoxides. With the sol-gel process, one can make hybrid materials that bridge the gap between organic polymers and pure inorganic materials. Organoalkoxysilanes can be purchased with a large variety of subgroups that determine the properties of the material. The subgroups can be inert or organofunctional, hydrophilic or hydrophobic. As a bonus, “pure” inorganic materials can be doped with organic lanthanide coordination complexes due to the low processing temperatures. In this PhD thesis lanthanide doped hybrid silica materials are investigated.

Chapter 1 contains a literature overview, concerning the topics: sol-gel chemistry, lanthanide spectroscopy, lanthanide spectroscopy in sol-gels and liquid crystal displays. **Chapter 2** contains the instrumentation details and procedures.

The results are given in chapters 3 to chapter 6.

To start the study of lanthanide spectroscopy in silica-based materials the absorption properties of lanthanide ions doped in *pure silica sol-gel glasses* are discussed in **chapter 3**. Study of these glasses is useful because they contain few components. A lot of research has been done to develop strongly luminescent lanthanide doped sol-gel glasses. The absorption properties of the lanthanides were not studied in detail. However, these absorption properties can give additional information about the behaviour of lanthanide complexes in optical materials. Here the Judd-Ofelt theory, which is the standard theory to describe the intensities of f-f transition in lanthanide ions, is used to study the lanthanide ions and there behaviour in pure silica sol-gel glasses.

In **chapter 4** the absorption properties of lanthanide ions doped in a *hybrid material* are discussed. The preparation method is fast and allows a wide range of strong lanthanide complexes to be doped into this matrix. Large basic ligands are soluble in such hybrid materials. Again, the Judd-Ofelt analysis was used to investigate the lanthanide complexes. Some of the lanthanide complexes showed promising capacities and these are examined in the next chapter.

Both lanthanide ions and silica-based materials are currently being investigated for potential use in near-infrared (NIR) data transfer. In **chapter 5**, NIR-luminescence of lanthanide complexes doped in silica-based hybrid materials was studied.

In **chapter 6** another example of combining silica-based hybrid materials and lanthanides is given. *Glass dispersed liquid crystal* (GDLC) films doped with red-luminescent Eu(III) complexes were prepared and tested for employment as luminescent liquid crystal display.

Literature overview Chapter 1

1.1 Sol-gel chemistry

1.1.1 Introduction

Silicon is the seventh most abundant element in the universe and the second most abundant element in the earth crust. Silicon dioxide, also known as silica, is the naturally occurring oxide of silicon. A pure form is quartz. Silicon dioxide is also a constituent of many minerals found in nearly every geological environment. Historically it has been the spectroscopists favorite material used in e.g. lenses or cuvettes due to its wide optical transparency in the visual spectrum and beyond (~200-2500 nm).

Around 1845 Ebelmen reacted $SiCl_4$ with ethanol to form the metal alkoxide tetraethoxysilane (TEOS).[1] He found that the compound gelled when exposed to the atmosphere. In the late 1930's more extensive studies were started when scientists discovered that siloxane polymers containing organic side groups (silicones) could be prepared starting from organosilicon compounds. Driven by the idea of a low temperature fabrication method for windows and bricks, launched again in 1974, a new surge of interest in the gels appeared.[2,3]

Many specific applications of sol-gel materials include optics, protective and porous films, optical coatings, window insulators, dielectric and electronic coatings, high temperature superconductors, reinforcement fibers, and catalysts. Although the sol-gel method is successful in making all kinds of

metal oxides, this project is about hybrid silica materials prepared from silicon alkoxides.

A *sol* is a colloidal suspension of solid particles in a liquid. A *colloid* can be defined as a suspension in which the dimension of the dispersed phase is so small (1-1000 nm) that gravitation forces can be neglected and interactions are dominated by short-range forces (van der Waals or surface charges). A suitable definition of a *gel* is a two-component system that consists of a continuous solid and fluid phase of colloidal dimensions.[4] The sol-gel process thus involves the formation of a colloidal suspension (*sol*) and further polymerization of the sol to form an inorganic network in a continuous liquid phase (*gel*).

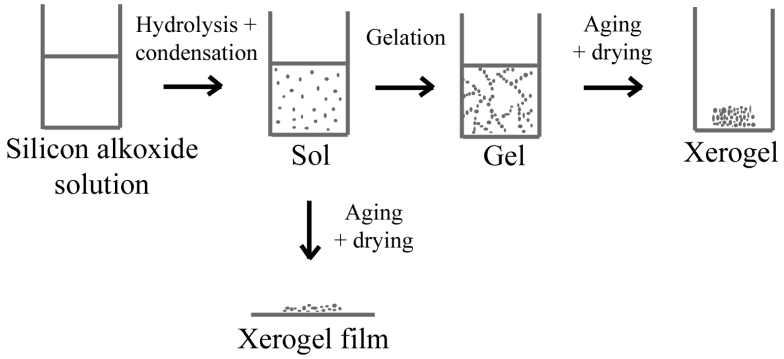

Figure 1.1: Possible processing routes for a silicon alkoxide solution.

A gel from which all volatile liquids have been removed is called a *xerogel*. Drying the gel to obtain a xerogel is not the only possible processing route. A far more important route is film formation. By spinning, spraying the sol or by dipping a substrate in the sol, a film can be made. Pore size, pore volume, surface area or thickness can be controlled. Other processing routes can be

used to make fibers or the extremely porous aerogels. Only silica xerogel monoliths or silica xerogel films are prepared in this project.

1.1.2 Hydrolysis and condensation of silicon alkoxides[4,5]

Silicon alkoxides react with water and undergo hydrolysis and polycondensation, leading to the formation of silicon oxides. The overall reaction scheme consists of three reactions. Beside the type of alkoxides used for hydrolysis, important reaction parameters are: the value of **r** (**r** = H_2O(mol)/Si(mol)), solvent, catalyst type, pH, temperature and pressure.

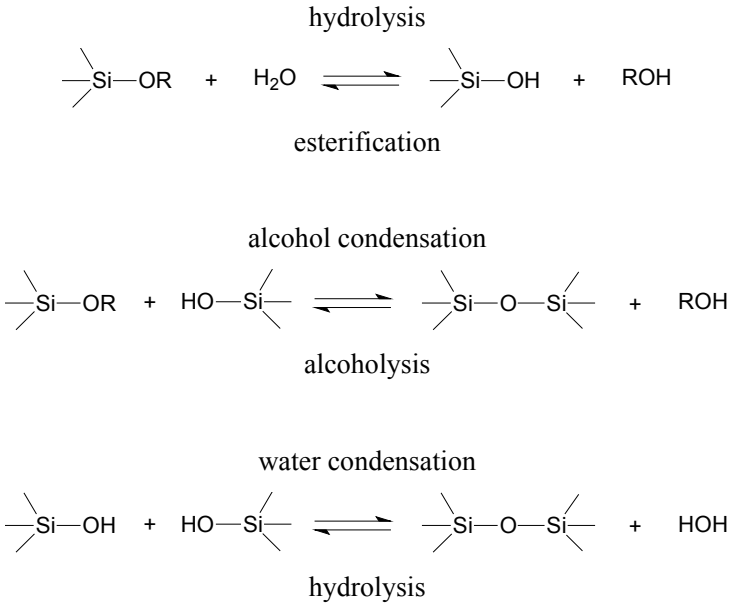

Scheme 1.1: Overall reaction scheme for silicon alkoxides and water.

Hydrolysis and catalysts

Water is used as a reagent in the hydrolysis reaction but is also a by-product of the condensation reaction. A molar ratio **r** = 2 is sufficient for a complete reaction. Under most conditions however, the hydrolysis of the alkoxide and the condensation reactions proceed simultaneously. Hydrolysis is incomplete even at ratios 2 < **r** < 10. The hydrolysis reaction starts with the nucleophilic attack of the oxygen atom of water on the silicon atom. The partial positive charge on silicon is +0.32. Alkoxysilanes and water are immiscible; therefore a solvent in which both components are soluble such as alcohols is used. The alcohol acts not simply as a solvent but participates in the reactions, as can be derived from the equations in scheme 1.1.

The hydrolysis can be specific acid or specific base catalyzed.[6] Mineral acids or ammonia are generally used as catalysts in sol-gel processing. Under basic conditions nucleophilic anions attack the silicon atom in a S_N2-type of reaction (scheme 1.2). Under acidic conditions an alkoxide group is protonated in a first step making the silicon more susceptible to a nucleophilic attack. The acid catalyzed hydrolysis is also believed to be a S_N2-type reaction (scheme 1.3).

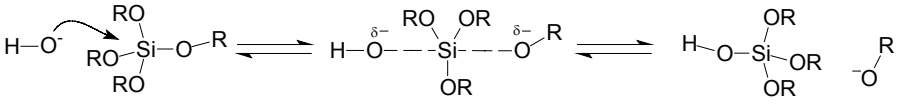

Scheme 1.2: Base catalyzed hydrolysis.

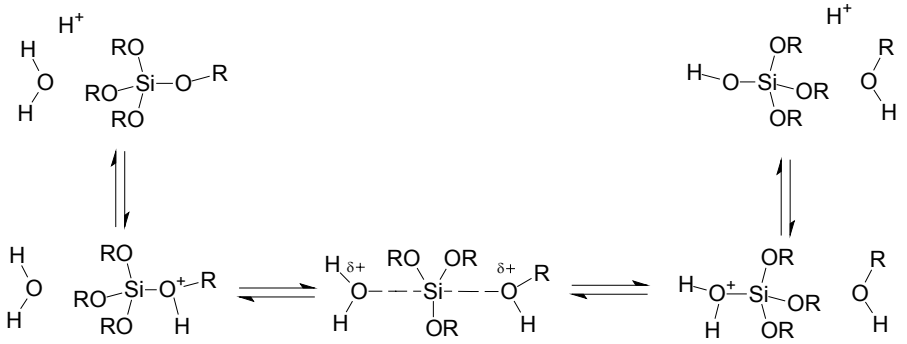

Scheme 1.3: Acid catalyzed hydrolysis.

Condensation and catalysts

Siloxane bonds are formed during polymerization. A water condensation route and an alcohol condensation route are possible. Both reactions are reversible but in alcohol-water solutions the depolymerization rate is low. Condensation rate is minimized near the isoelectric point (pH 1-3) and maximized near neutral pH. The most widely accepted mechanism for the base catalyzed condensation reaction involves the attack of a nucleophilic deprotonated silanol on a neutral silicate species.[4] Reactions occur between larger, more highly condensed species, which contain acidic silanols, and smaller species. In an acid catalyzed condensation, a neutral species attacks a protonated silanol situated on monomers, end groups of chains. The proposed reaction is S_N2-type.

Hydrolysis and condensation

The hydrolysis, condensation and depolymerization occur simultaneously. The pH-dependences of these reactions are schematically represented in figure 1.2.

The scheme can be divided in three pH regions: below pH 2, between pH 3-7 and above pH 7. At low pH (pH < 2) the hydrolysis is fast compared to the condensation and dissolution. Most monomer alkoxides are hydrolyzed before condensation at high **r**-ratios. Monomers react forming dimers. After monomers are depleted the condensation occurs via cluster-cluster aggregation. Dissolution is low and weakly branched structures are formed. At lower **r**-ratios, condensation starts before hydrolysis is complete. Unhydrolyzed OR groups reduce the functionality, more weakly branched structures are formed.
In contrast, for pH > 7, dissolution is fast and solubility is high. Dissolution provides a continual source of monomers and redistribution reactions. Condensation occurs preferentially between weakly acidic monomers and more strongly acidic larger species. Larger branched particles are formed. Understoichiometric additions of water cause unhydrolyzed sites in the growing clusters. At intermediate pH values a spectrum of structures is expected.

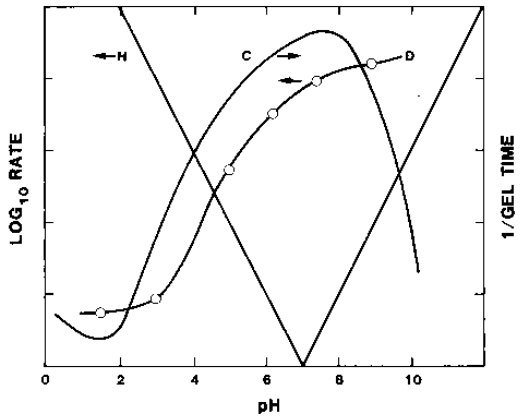

Figure 1.2: Schematic representation of the pH-dependences of hydrolysis (H), condensation (C) and dissolution (D).[7]

Precursors

The best studied silicon alkoxides are *tetraethoxysilane* ($Si(OC_2H_5)_4$, tetraethyl orthosilicate, TEOS) and *tetramethoxysilane* ($Si(OCH_3)_4$, tetramethyl orthosilicate, TMOS). To reduce the number of sites able to form Si-O-Si bonds or to introduce functionality *organoalkoxysilanes* are used. Hybrid *organically modified silicates* (ORMOSILs) can be prepared by using organoalkoxysilanes as precursors. Several organotrialkoxysilane or diorganodialkoxysilane precursors can be purchased. *Gelest Inc.* sells over 500 different types of organoalkoxysilanes. A few organoalkoxysilanes are given in table 1.1. Hydrolytic stability of the precursors is determined by inductive effects and by steric factors like alkyl chain length and degree of branching. The large difference between the hydrolysis reaction time of TEOS and TMOS is due to the retarding effect of the bulkier ethoxide group.

Table 1.1: Tetraalkoxysilane and organoalkoxysilane precursors for sol-gel synthesis.

Name	Abbreviation	Structure
tetraethoxysilane	TEOS	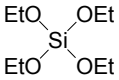
tetramethoxysilane	TMOS	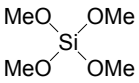
methoxy-T8-silsequioxane	T_8 cube	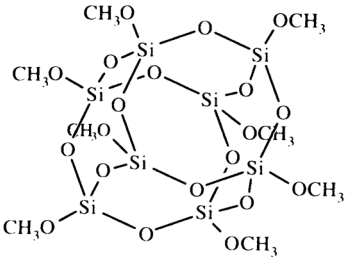
diethoxydimethylsilane	DEDMS	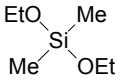
triethoxyethylsilane	TEES	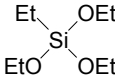
3-(glycidoxypropyl) trimethoxysilane	GLYMO/ GPTMS	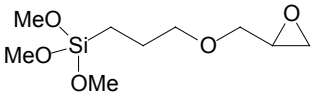
N-(2-Aminoethyl)-3-aminopropyl-trimethoxysilane		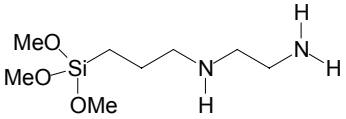

1.1.3 Gelation, aging, drying

After the formation of the sol a processing route can be chosen: e.g. the sol can be poured in a container and dried to make a xerogel or a substrate can be dipped in the sol to make a coating. The silica clusters continue to grow by condensation until the clusters collide. Now links can bridge clusters. After further links are formed a giant spanning cluster reaches across the fluid phase. This moment in time is called the *gel point*. Eventually the clusters overlap and become nearly immobile. The reactions continue after the gel point and the gel structurally changes. This process is called *aging*. The gel is strengthened, stiffened and shrinks (*synergesis*). When evaporation of the solvent is allowed (*drying*), in a first stage the network is forced to shrink by capillary tension. A second stage starts when the network is too stiff to shrink further. Now evaporation drives the liquid-vapor meniscus into the gel. Cracking is a major problem for most sol-gel based ceramics. Two important causes of stress are the non-uniform contraction and stress due to pore size distribution. If the gel dries starting from only one side, the pressure distribution is asymmetrical. The shape will be affected by this pressure distribution, by gravity and by adhesion to the mold or substrate. If the stress caused by non-uniform contraction exceeds the strength of the network, the drying gel cracks. Cracking is also attributed to the existence of a pore size distribution. As larger pores empty first, the higher tension in smaller pores creates stress that can crack the wall between pores.

Minimizing the capillary stress between pores or strengthening the network is important for crack-free drying. Several methods are proposed.[4,5]

- With slower evaporation, a large asymmetrical pressure distribution is avoided.
- Making larger pores and a smaller pore size distribution. Adding a *drying control chemical additive* (DCCA) like formamide or oxalic acid can narrow the pore size distribution.
- Strengthening the network by aging.
- With supercritical drying the liquid is removed from the network above the critical temperature and pressure of the liquid, where there is no distinction between the liquid and vapor phases. Capillary pressure is absent. The *aerogel* can be produced as large as the volume of the autoclave.
- Organoalkoxysilanes containing a flexible side group can be used as precursor. The side groups give the structure flexibility to avoid cracking.

After drying, the materials can be sintered or melted. There has been some discussion about the possible differences between glasses made by melting of conventional materials and sol-gel derived glass. After a gel has been melted it "forgets" its manner of preparation and acquires the equilibrium structure dictated by thermodynamics.[4,8]

1.1.4 ORMOSIL or CERAMER classification

The sol-gel technology is an important method to create organic/inorganic or hybrid materials. Other names are: *CERAMER* (from the combination of ceramic and polymer) and *ORMOCER* (organically modified ceramics). Focused on silicon materials the specific name is *ORMOSIL*. There have been several attempts to classify hybrids. Sanchez and Ribot[9] in their seminal paper classify the hybrids by the bonding between the organic and inorganic parts of the network:

> Class I: hybrids where organic molecules are blended into the inorganic network.
> Class II: hybrids where inorganic and organic constituents are linked via covalent bonds.

Mackenzie[10] has a similar classification but makes a differentiation whether the organic part is entrapped before gelation or impregnated into the pores after gelation.

> Type A: An organic substance like a dye is mixed into the sol-gel liquid solution and on gelation the organic substance is trapped.
> Type B: A porous oxide gel is formed first; an organic substance is impregnated into the pores of the gel.
> Type C: The organic substance is attached to the oxide gel.

Wojcik and Klein have another classification scheme for transparent hybrid gels.[11] Four major classes are presented but there are also several subclasses based on preparation methods.

Covalently bonded organic/inorganic gels = type C, Class I
Organic/inorganic interpenetrating networks = type A, Class II
Polymer impregnated gels = type B, Class II
Organic doped gels = type A, Class II

Although the classification scheme by Sanchez and Ribot is a very simplified one, it is the only one that is widely used.

1.2 Lanthanide spectroscopy

1.2.1 Introduction

Lanthanides are the series of elements from La (Z = 57) to Lu (Z = 71). The trivalent lanthanide ions are known for their sharp electronic transitions in the near-UV, visible and near-infrared spectral regions. These transitions are 4f-4f transitions. Most of the transitions are *induced electric dipole transitions* (ED), some are *magnetic dipole transitions* (MD) but both have low intensity. The ED transitions are intraconfigurational and therefore forbidden by the Laporte selection rule. The MD transitions have an inherent low intensity. Another important aspect about the valence shell is that the filled 5s- and 5p-orbitals outside the 4f-shell shield the 4f-orbitals. Because the f-electrons are only moderately perturbated by their surroundings, the transitions appear as sharp lines. This also results in a longer lifetime of the exited state and therefore trivalent lanthanides show strong luminescence with a high coloric purity. However, the low absorbance is a drawback for good luminescence but this can be bypassed through the antenna effect. Several aspects of lanthanide spectroscopy are discussed in the following paragraphs.

1.2.2 Free-ion and crystal field

The +III oxidation state is the most important one in lanthanide chemistry and spectroscopy. The ground electronic configuration of the trivalent lanthanide ions is $[Xe]4f^N$. A central field approximation is used to describe the free ion

system. Each electron is considered to move in the field of the nucleus and the mean central field due to the charge distribution of the other electrons. The most important perturbations are electron repulsion and spin-orbital coupling. In the *Russell-Saunders coupling scheme* the electron repulsion is considered to be a lot larger than the spin-orbital coupling. The individual orbital angular momenta and electronic spin angular momenta of all the electrons combine into a total atomic orbital angular momentum *L* and a total spin angular momentum *S*. The total angular moment *J* is given by the coupling of *L* and *S*. This scheme is not correct for the lanthanides but neither is the *j-j coupling scheme* where the spin-orbital coupling is larger than electron repulsion. A more correct scheme is the *intermediate coupling scheme*. The coulombic and spin-orbital interactions are simultaneously introduced. Terms with the same *J* but different *L* and *S* can mix. Thus *L* and *S* are no longer valid quantum numbers.

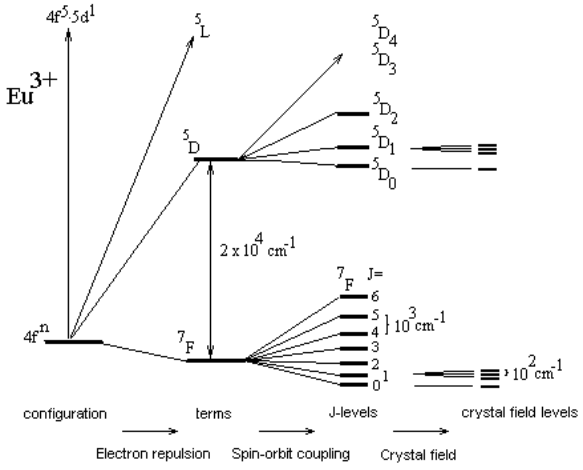

Figure 1.3: Splitting of the energy levels of Eu(III).

When a lanthanide is surrounded by a coordinating environment, all the electrons of the system, other than those of the lanthanide ion itself, destroy the spherical symmetry of the "free-ion". This effect is the crystal-field perturbation. Taking only the first coordination sphere into account is a good approximation due to the good shielding of the f-electrons. The individual *J*-levels are split up further by the crystal field. *J*-mixing is allowed. Thus *L* and *S* and *J* are no longer valid quantum numbers but for convenience the name of the mixed term is derived from the largest contributing term. This crystal field fine structure can be seen in a crystal matrix at low temperature but is seldom seen in other host materials. Average energy gaps introduced between the levels by the perturbations are ER ($\approx 10^{4\text{-}5}$ cm^{-1}) > SOC ($\approx 10^{3\text{-}4}$ cm^{-1}) > CF ($\approx 10^{2}$ cm^{-1}). When the lanthanide is placed in a magnetic field, there is an additional perturbation: the *Zeeman perturbation*. All degeneracy is destroyed.

1.2.3 Coordination chemistry

The coordination chemistry of lanthanide ions only slightly depends on the type of lanthanide ion. The coordination numbers and symmetry are more determined by the ligand characteristics. Most of the minor deviations are due to the variation in ionic radius. Coordination numbers range from six to twelve, eight and nine are the most common coordination numbers. Lanthanides are hard Lewis acids and preferably coordinate with hard Lewis bases like oxygen. Bonding of nitrogen and especially sulphur to lanthanide ions is much weaker. Negative charges on the donor atom or large ground-state dipole moments on the ligands improve the bonding. Unfortunately this includes water molecules

and hydroxide ions and these are hard to remove from the first coordination sphere. The ligands can be mono- or multidentate.

1.2.4 Judd-Ofelt theory of induced electric dipole transitions

The spectroscopic active lanthanide ion can interact with the electric field component of the light through an induced electric dipole. This transition (and the electric dipole operator) has odd parity. Intraconfigurational electric dipole transitions are forbidden by the Laporte selection rule. But by mixing states of different parity into the f^N configuration the selection rule is relaxed. These transitions are therefore called *induced electric dipole transitions*.

The induced electric dipole transitions are described by the Judd-Ofelt theory.[12,13] Judd considered the odd part of the crystal-field potential as the perturbation for mixing states of different parity. The Judd-Ofelt theory is a static coupling mechanism. The full expression for dipole strengths between two crystal field levels in an isotropic system is given in formulae 1.1-1.2.

$$D = e^2 \left| \left\langle l^N \psi J M \left| \hat{D}_p^{(1)} \right| l^N \psi' J' M' \right\rangle \right|^2 = e^2 \sum_{k,q,\lambda \text{ even}} (2\lambda+1) \left| A_{kq} \right|^2 \frac{1}{2k+1} \times \Xi^2(k,\lambda) \left| \left\langle l^N \psi J \left\| U^\lambda \right\| l^N \psi' J' \right\rangle \right|^2 \quad (1.1)$$

$$\text{with} \quad \Xi^2(k,\lambda) = 2 \sum_{n'l'} (2l+1)(2l'+1)(-1)^{l+l'} \begin{Bmatrix} l & \lambda & k \\ l & l' & 1 \end{Bmatrix} \begin{pmatrix} l & 1 & l' \\ 0 & 0 & 0 \end{pmatrix} \begin{pmatrix} l' & k & l \\ 0 & 0 & 0 \end{pmatrix} \times \frac{\left\langle nl \left| \hat{f} \right| n'l' \right\rangle \left\langle nl \left| \hat{r}^k \right| n'l' \right\rangle}{\Delta(n'l')} \quad (1.2)$$

The complete derivation of these formulae and the used symbols are explained elsewhere.[14]

If the exact intensity of transitions at the crystal-field level is known, A_{kq} parameters can be calculated. However crystal-field fine structure of lanthanide ions is not resolved in solutions and glasses. In the simplest form of the Judd-Ofelt theory, the induced ED-transitions can be characterized by the three phenomenological intensity parameters Ω_λ ($\lambda = 2, 4, 6$). Knowledge of minimally three transition bands, which can consist of different *J*-levels, is sufficient for calculating the Ω_λ-parameters. The simple Judd-Ofelt expression for the theoretical dipole strength D_{calc} between *J*-multiplets is given in formula 1.3 and 1.4.

$$D_{calc} = \frac{10^{36}}{2J+1}\frac{\left(n^2+2\right)^2}{9n}e^2 \sum_{\lambda=2,4,6} \Omega_\lambda \left|\left\langle J \left\| U^{(\lambda)} \right\| J' \right\rangle\right|^2 \qquad (1.3)$$

$$\text{with} \quad \Omega_\lambda = (2\lambda+1)\sum_{k,q}\left|A_{kq}\right|^2 \Xi^2(k,\lambda)\frac{1}{2k+1} \qquad (1.4)$$

Dipole strengths are expressed in *Debye*^{2} (D^2). The factor 10^{36} is used for the conversion between D^2 units and esu^2 cm^2 ($1D = 10^{-18}$ esu cm). Correction for a dielectric medium (*n* is the refractive index) is incorporated in the factor $\frac{\left(n^2+2\right)^2}{9n}$. The degeneracy of the ground state equals $2J+1$. The squared reduced matrix elements $\left|\left\langle J \left\| U^{(\lambda)} \right\| J' \right\rangle\right|^2$ can be calculated and have been tabulated by Carnall *et al.*.[15,16,17,18] The Ω_λ-parameters can be determined by a least-squares fit of calculated dipole strength against experimental dipole strengths extracted from the absorption spectra.

The formula to calculate the experimental dipole strength D_{exp} is:

$$D_{exp} = \frac{1}{108.9}\int \frac{\varepsilon(\bar{\nu})}{\bar{\nu}} d\bar{\nu} \qquad (1.5)$$

The origin of factor 108.9 is described in detail elsewhere.[14]

In cases where an MD transition is present, the magnetic dipole intensity must be subtracted. The Ω_λ-intensity parameters represent the square of the charge displacement due to induced electric dipole transitions. Theoretical calculations and comparisons between lanthanides in different host materials or surrounded by different ligands have linked these parameters to both short- and long-range properties. The Ω_2-parameter is associated with short-range coordination effects and its value increases with increasing coordination number, higher basic character of the ligand and higher covalence of the bonding. The Ω_2-parameter depends on the ligand type: oxygen donor > nitrogen-oxygen donor > sulphur donor > aqua ion. There is an inverse relationship between the length of the ligand-lanthanide bond and the Ω_2-parameter. The Ω_4- and Ω_6-parameters depend on long-range effects. More rigid matrices have lower Ω_4- and Ω_6-values. Table 1.2 gives an overview of properties related to the different parameters.

The Judd-Ofelt theory as proposed originally by Judd and Ofelt is limited to the assumption of one-electron, one-photon interaction and is not valid in lanthanide systems with polyatomic ligands with highly anisotropic charge distributions. Reid and Richardson developed a more general theory, additional parameters are required but the phenomenological Ω_λ-parameters remain valid.[19]

1.2.5 Hypersensitivity

The dipole strengths of most transitions in lanthanide ions are little affected by the environment, but some transitions are very sensitive to small changes in the ligand coordination sphere. These "*hypersensitive*" transitions are characterized by high squared reduced matrix elements $\left|\left\langle J\left\|U^{(2)}\right\|J'\right\rangle\right|^2$ and are therefore connected to the Ω_2-parameter. The other transitions are more related to the Ω_4- and Ω_6-parameters.

Important luminescent transitions for optical applications like the $^5D_0 \rightarrow {}^7F_2$ of Eu^{3+} (ca. 615 nm) are hypersensitive and a lot of effort is used to increase their intensities. Jørgenson and Judd noted that hypersensitive transitions obey the selection rules $|\Delta S| = 0$, $|\Delta L| \leq 2$ and $|\Delta J| \leq 2$.[20] These are also the selection rules for pure quadrupole transitions but the hypersensitive transitions do not have a quadrupole character. The hypersensitivity is reflected by the value of the Ω_2-parameter, related to $\left|\left\langle J\left\|U^{(2)}\right\|J'\right\rangle\right|^2$. These Ω_2-parameters and the hypersensitive transitions are an important spectroscopic probe for coordination changes.

Table 1.2: Properties related to the different Judd-Ofelt parameters.

Ω_2 The Ω_2-parameter is connected to short-range effects and hypervalence.[21]

- ✓ Coordination number [22,23,24]
  Higher coordination number, higher Ω_2
- ✓ Basic character of the ligand [22,23,25]
  Higher basic character, higher Ω_2
- ✓ Binding atom of the ligand [26]
  oxygen > nitrogen + oxygen > nitrogen > sulphur > aqua-ion
  Harder Lewis base character, higher Ω_2
- ✓ Symmetry [24,27]
  Lower symmetry, higher Ω_2
- ✓ Metal-ligand bond distance [22]
  Smaller distance, higher Ω_2
- ✓ Covalence [21]
  More covalent bond, higher Ω_2

Ω_4 The Ω_4-parameter is connected to long-range effects.[21]

- ✓ Rigidity [28]
  Less rigid matrices, higher Ω_4
  Rigidity increases in the following order: coordination complexes < halide vapours < hydrated ions < viscous solutions < glasses < crystalline mixed oxides

Ω_6 The Ω_6-parameter is connected to long-range effects.[21]

- ✓ Rigidity [28]
  Less rigid matrices, higher Ω_6
  Rigidity increases in the following order: coordination complexes < halide vapors < hydrated ions < viscous solutions < glasses < crystalline mixed oxides
- ✓ Covalence [29]
  Less covalent bond, higher Ω_6

Table 1.3: Most important hypersensitive transitions.

Ion	Hypersensitive transition	Wavenumber/Wavelength
Nd^{3+}	$^4G_{5/2} \leftarrow {}^4I_{9/2}$	17300 cm^{-1}/586 nm
Sm^{3+}	$^4F_{1/2}$, $^4F_{3/2} \leftarrow {}^6H_{5/2}$	6400 cm^{-1}/1562 nm
Eu^{3+}	$^5D_1 \leftarrow {}^7F_1$	18700 cm^{-1}/535 nm
	$^5D_2 \leftarrow {}^7F_0$	21500 cm^{-1}/465 nm
	$^5D_0 \rightarrow {}^7F_2$	16300 cm^{-1}/613 nm
Dy^{3+}	$^6F_{11/2} \leftarrow {}^6H_{15/2}$	7700 cm^{-1}/1299 nm
Ho^{3+}	$^5G_6 \leftarrow {}^5I_8$	22100 cm^{-1}/451 nm
	$^3H_6 \leftarrow {}^5I_8$	27700 cm^{-1}/361 nm
Er^{3+}	$^2H_{11/2} \leftarrow {}^4I_{15/2}$	19200 cm^{-1}/521 nm
	$^4G_{11/2} \leftarrow {}^4I_{15/2}$	26400 cm^{-1}/378 nm

1.2.6 Antenna effect

If the ligand contains a light-absorbing organic group, the photonic energy absorbed by the chromophore can be transferred to the lanthanide ion. This photosensitization can eliminate the absorption bottleneck of the lanthanide luminescence. Well-known sensitizers are 2,2'-bipyridine, 1,10-phenanthroline and β-diketones. The photosensitization mechanism is given in figure 1.4.
Important parameters in this mechanism are: ligand-metal distance, ligand oxidation, the gap between the T_1-levels and the lanthanide energy levels, and the rate of energy back donation.

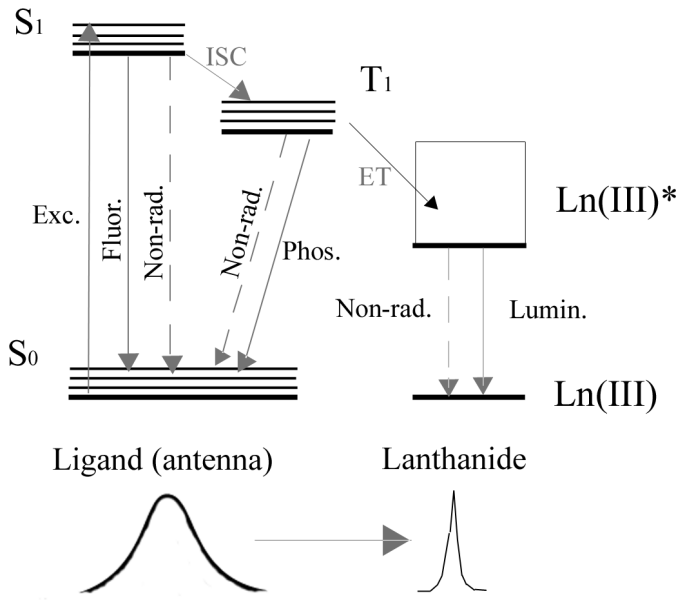

Figure 1.4: Antenna effect in lanthanide complexes.

In complexes with Eu(III) or Yb(III), which have low reduction potentials, another mechanism is also plausible: a *ligand-to-metal charge transfer* (LMCT). In the case of europium, the LMCT-state (ligand^{+}-Eu(II)) decays nonradiatively. In the case of ytterbium, the charge recombination (ligand^{+}-Yb(II) to ligand-Yb(III)*) leaves Yb(III) in an exited state.[30]

1.2.7 Magnetic dipole transitions

Magnetic dipole (MD) transitions occur by interaction of the lanthanide ion with the magnetic field component of the light. During a magnetic dipole transition a charge is displaced over a curved path. The intensity is low because it is proportional to the square of a small transition dipole moment. The magnetic dipole operator is even under inversion. Therefore an intraconfigurational MD f-f transition is allowed, but has an intrinsic low intensity.

1.3 Lanthanide spectroscopy in sol-gels

1.3.1 Introduction

For years sol-gel materials have been doped with lanthanide complexes. The first articles appeared mid 1980's when the research in quality sol-gel devices for opto-electronic and laser applications started.[31] The sol-gel approach allows the silica matrix to be doped in high concentration at a low temperature. The sols are homogenous and exact compositions can be made.

Eu(III) and Tb(III) salts were used in most cases because of their intense visible red and green luminescence.[e.g.31,32,33] Additionally Eu(III) can be used as a probe for local environmental changes, the $^5D_1 \rightarrow {}^7F_0$ transition is site selective.[34] But high dopand levels 0.5-12.5% ($gEu/gSiO_2$) were necessary to give sufficient intensity. Later, Eu(III) complexes with ligands like bipyridyls, phenanthrolines and β-diketones were used.[e.g.33,35] By using the antenna effect, the luminescence yield is improved. The visible luminescence of Pr(III) and Sm(III) is less studied. More recently a lot of effort is devoted to *near-infrared luminescence* (NIR-luminescence) of Er(III) and Nd(III) in sol-gel materials.[e.g.36,37,38] There are possible applications in NIR data communication technology. Optical fibers can be made by the sol-gel technique and lanthanide doped optical fibers can be used to improve the NIR-signal.

Most luminescence studies are done with fibers, powders or small samples. Making bulk samples is time-consuming and not so important for luminescence. Less interest is devoted to the absorption properties of the lanthanides in sol-gel materials. While the Judd-Ofelt theory is common for lanthanides studied in other materials, only few results have been published for

sol-gel materials.[39,40,41,42,43] Ho(III), Nd(III) and Er(III) that are now well studied in sol-gel materials are ideal for the Judd-Ofelt analysis. A possible reason is the necessity to exactly know the path length and concentration of the lanthanide in the shrinked xerogel. The volume of the wet xerogels is only a fraction of the initial sol volume and thus the concentration of the lanthanide increases during shrinkage. Important is also that the lanthanides must be doped in high concentration due to the low absorption cross-section. Another possibility is a longer path length but then it is more difficult to avoid cracking and long drying times are necessary.

1.3.2 Influence of the matrix composition

The classification schemes discussed in chapter 1 (see 1.1.4) divide hybrid sol-gel materials on the basis of their composition or preparation method. However, for lanthanide doped materials the interaction between the matrix and the lanthanide complex is more important than the type of bond between the inorganic and organic phase. Hybrids type I and II silica sol-gel materials have been used.

Most silica matrices containing lanthanides are prepared with TEOS or TMOS and organoalkoxysilanes or organic additives in low concentration to enhance the mechanical properties of the matrix. If a stable lanthanide complex is introduced, the lanthanides preferably coordinate to the ligand and not to the silica matrix.[e.g.[34] [42,44,45]]

Silica matrices are also prepared with organoalkoxysilanes or organic components in high concentration. Again, if a stable lanthanide complex is introduced, the lanthanides are preferably coordinated to the ligand and not to

the hybrid matrix. The hybrid matrix may have periodic functional porosity introducing local differences in lanthanide solubility. For example: more hydrophilic and more hydrophobic parts can coexist.[46,47]

By using lanthanide ethoxides like $Ln(OEt)_3$ mixed with organoalkoxysilanes, the lanthanides ions can be incorporated directly in the matrix.[48] Often silica hybrid matrices are prepared with organoalkoxysilanes or organic components that can coordinate with the lanthanide itself. The authors claim higher homogeneity.e.g.[49]

Generally the choice of the silica matrix (type of ORMOSIL) is more important for improving solubility, faster processing time and the desired application, than for improving the luminescence yield.

1.3.3 Drying

Drying improves the luminescence by removing the water out of the first coordination sphere.[34] Spectra of the lanthanides in a wet gel resemble the spectra of diluted compounds in an aqueous solution. The spectra of lanthanides in samples heated to 1000°C resemble those in glasses prepared by melting. Some silanol (Si-OH) groups are retained by the system even after high temperature annealing.

1.3.4 Ligand

The ligand plays an important role in the photophysics of lanthanide complexes as the luminescence intensity improves noticeably when the ligand is more able

to shield the lanthanide from the quenching of surrounding (water) molecules.[31] Because the antenna effect is very useful, the majority of the ligands contain a chromophoric unit. Frequently used ligands are: bipyridyl, phenanthroline, crown ethers and β-diketones.[50] The same rules for lanthanide luminescence stand as for other matrices or solutions. Not only the effectiveness of the antenna is important, but also the solubility. As the water based silica sol-gels contain a large amount of water and ethanol, solubility in these solvents is an important issue. Using organoalkoxysilanes as building blocks in the silica backbone of the sol-gel can circumvent this problem.

1.4 Liquid crystal displays

1.4.1 Introduction

We use *liquid crystal displays* (LCDs) almost every day. They are present in laptop computers, mobile phones, calculators,… LCDs are becoming even more common because they offer some real advantages over other display technologies: they are thinner, lighter and draw much less power than *cathode-ray tube* (CRT) screens.

Liquid crystals are sometimes referred to as the "fourth state" of matter following gases, liquids and solids. The *liquid-crystalline phase* or *mesophase* is a state of matter, which exists between the organized solid and the isotropic liquid. The molecules are orientationally ordered but are in dynamic motion. They can point in any direction and move anywhere in the liquid. A well-known example is 5CB (4-pentyl-4´-cyanobiphenyl). On a microscopic level, the rodlike 5CB molecules (figure 1.5) are locked in place and aligned when the sample is a solid. When the sample becomes liquid-crystalline, the molecules are free to translate and can rotate somewhat. However, the molecules remain more or less aligned. When the sample finally melts to a liquid, all orientation is lost. The values for the solid-liquid crystal and liquid crystal-liquid transition temperatures are 22.5 °C and 35.0 °C respectively.

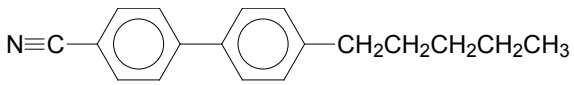

Figure 1.5: Structure of 4-pentyl-4´-cyanobiphenyl (5CB).

There are several liquid crystal phases that depend on the molecular properties of the substance. The least ordered phase is the nematic phase, like the one in 5CB. The molecules all point more or less in the same direction but no further ordering is present (e.g. layers). The orientation of the molecule can be changed by an external electric or magnetic field. LCDs are based on switching in an electric field. There are several types of LCD: dynamic scattering mode display, twisted nematic display, dispersed liquid crystal display… The only one discussed in next paragraph is the dispersed liquid crystal display.[51]

1.4.2 Dispersed liquid crystal display

Dispersed liquid crystal displays (DLCDs) are a newer type of LCD. This type of LCD involves micrometer-sized droplets of a nematic liquid crystal in a solid, isotropic matrix. There are two requirements. First, the refractive index of the matrix (n_g) must be similar to the refractive index of polarized light perpendicular to the director of the liquid crystal ($n_\perp$). Secondly, the matrix must induce the director of the liquid crystal in the droplets to orient parallel to the surface of the matrix. A schematic view of the liquid crystal orientation in ON and OFF state is given in figure 1.6. When no external electric field is applied, light propagating through the cell encounters droplets with a refractive index different from the refractive index of the matrix. Incoming light is scattered. When an electric field is present, the electric field direction of the light is perpendicular to the director in the droplets, giving the droplets a refractive index equal to that of the matrix ($n_g = n_\perp$). There is no light scattering.

A polymer matrix can be used to make a *polymer dispersed liquid crystal* display (PDLC) but *glass dispersed liquid crystal* display (GDLC) can be produced by a sol-gel method.

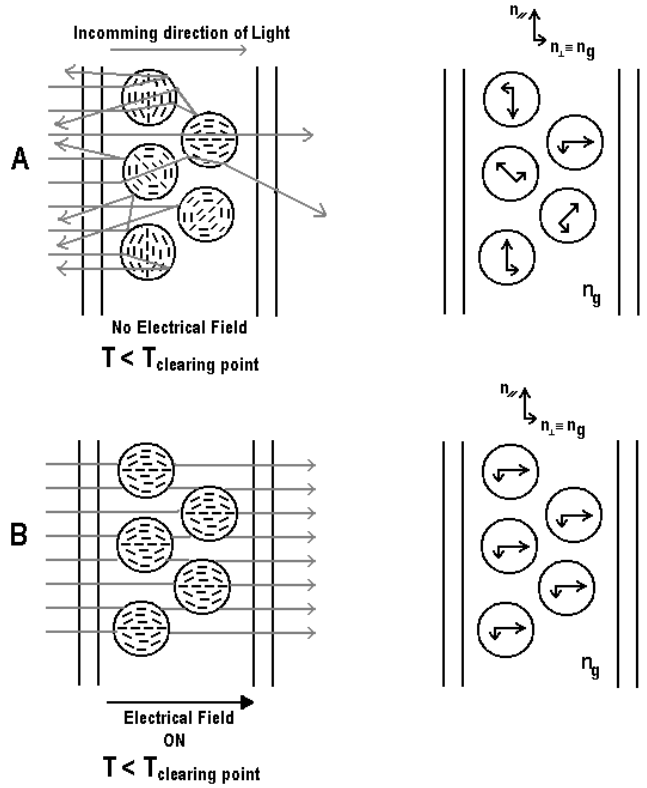

Figure 1.6: Illustration of a switching GDLC. The incoming light is scattered in the OFF state (A). The incoming light passes the GDLC layer when an electric field is applied (B). The refractive indexes of the liquid crystal ($n_{\perp}$ and $n_{//}$) and the matrix (n_g) are indicated on the right side.

The LCD can be illuminated by ambient light or backlight. Colors can be introduced by color filters or dyes/phosphors inside the matrix or inside the liquid crystal micro-droplets.

1.4.3 Sol-gel glass dispersed liquid crystals

Liquid crystals have been used to trap organic molecules in materials by the sol-gel process, but larger cavities can also be introduced by providing a molecular oriented surface using organic side groups in ORMOSILs.[52] At the surface of these cavities nematogenic compounds can be aligned. This was first demonstrated by Levy and Otón.[53,54] The thin films were prepared by mixing water, TEOS, 5CB and an organoalkoxysilane: *triethoxyethylsilane* (TEES). The materials have dispersed droplets filled with 5CB that are 0.1 to 15 μm in diameter. Si-CH_2-CH_3 groups make the orienting surface on the pore cage. The hydrophobic inner surface of the pores gives orientation to the surface molecules. The orientation in the pore is radial with the director pointing to the sphere center. This orientation leads to a discontinuity at the center. Difference in transmission of less than 20% is found when an electric field of >100V is applied. The contrast ratio is 5-10:1. Newer studies use different precursors to lower the voltage and to decrease the differences between the refractive index of the matrix and the liquid crystals.[55,56,57,58,59,60,61,62] GDLCs were also doped with dyes.[63,64] For matrix dopands rhodamine 6G, fluorescein and oxazine-1 were used. The liquid crystal microdroplets were doped using a B3 dye specifically designed for liquid crystal doping.

REFERENCES

[1] Ebelmen, M., *Ann. Chim. Phys.*, 2003, **15**, 319.

[2] Nogami, M. and Moriya Y., *J. Non-Cryst. Solids*, 1980, **37**, 191.

[3] Yoldas, B. E., *J. Mater. Sci.*, 1977, **12**, 1203.

[4] Brinker, C. J. and Scherer, G. W., *Sol-Gel Science*, Academic Press, San Diego **1990**.

[5] Hench, L. and Ulrich, D., *Science of Ceramic Chemical Processing*, John Wiley & Sons, New York **1986**, 54-200.

[6] Pohl, E. R. and Osterholtz, F. D., in *Molecular Characterization of Composite Interfaces* ,(Ishida, H. and Kumar, G.), Plenum, New York **1985**, 157.

[7] Brinker, C. J., *J. Non-Cryst. Solids*, 1988, **100**, 30.

[8] Weinberg, M. C., *Mat. Res. Soc. Symp. Proc.*, 1986, **73**, 431.

[9] Sanchez, C. and Ribot, F., *New. J. Chem.*, 1994, **18**, 1007.

[10] Mackenzie, J. D., *J. Sol-Gel Sci. Technol.*, 1994, **2**, 81.

[11] Wojcik, A. B. and Klein, L. C., *Appl. Organomet. Chem.*, 1997, **11**, 129.

[12] Judd, B. R., *Phys. Rev.*, 1962, **127**, 750.

[13] Ofelt, G., *J. Chem. Phys.*, 1962, **37**, 511.

[14] Görller-Walrand, C. and Binnemans, K., in *Handbook on the Physics and Chemistry of Rare Earths*, *Vol. 25*, (Gschneidner, K. jr. and Eyring, L.), Elsevier, Amsterdam **1998**, 101-264.

[15] Carnall, W. T., Fields, P. R., and Rajnak, K., *J. Chem. Phys.*, 1968, **49**, 4443.

[16] Carnall, W. T., Fields, P. R., and Rajnak, K., *J. Chem. Phys.*, 1968, **49**, 4447.

[17] Carnall, W. T., Fields, P. R., and Rajnak, K., *J. Chem. Phys.*, 1968, **49**, 4450.

[18] Carnall, W. T., Fields, P. R., and Rajnak, K., *J. Chem. Phys.*, 1968, **49**, 4424.

[19] Reid, M. F. and Richardson, F. S., *Chem. Phys. Lett.*, 1983, **95**, 501.

[20] Jorgensen, C. and Judd, B. R., *Mol. Phys.*, 1964, **8**, 281.

[21] Oomen, E. and van Dongen, A., *J. Non-Cryst. Solids*, 1989, **111**, 205.

[22] Henrie, D., Fellows, D., and Choppin, G., *Coord. Chem. Rev.*, 1976, **18**, 199.

[23] Karraker, D., *Inorg. Chem.*, 1967, **7**, 473.

[24] Bel'tyukova, S., Nazarenko, N., Gritsai, T., and Lozanova, E., *Russian. J. Inorg. Chem.*, 1981, **55**, 117.

[25] Fellows, D. and Choppin, G., *J. Coord. Chem.*, 1974, **4**, 79.

[26] Surana, S. S. L, Mathur, P. C., Mehta, P. C., and Sandon, S. P., *Appl. Phys.*, 1975, **6**, 363.

[27] Krupke, W. F., *Phys. Rev. B*, 1966, **145**, 325.

[28] Jorgensen, C. and Reisfeld, R., *J. Less-Common Met.*, 1983, **93**, 107.

[29] Reisfeld, R. and Jorgensen, C., *Laser and Excited States of Rare Earths*, Springer, Berlin **1977**.

[30] Horrocks, W., Bolender, J., Smith, W., and Supkowsky, R., *J. Am. Chem. Soc.*, 1997, **119**, 5972.

[31] Levy, D., Reisfeld, R., and Avnir, D., *Chem. Phys. Lett.*, 1984, **109**, 593.

[32] Bredol, M., Kynast, U., and Ronda, C., *Adv. Mater.*, 1991, **3**, 361.

[33] Li, W. L., Li, W., Yu, G., Wang, Q. G., and Jin, R., *J. Alloys Compds.*, 1993, **192**, 34.

[34] Campostrini, R., Carturan, G., Ferrari, M., Montagna, M., and Pilla, O., *J. Mater. Res.*, 1992, **7**, 745.

[35] Matthews, L. R. and Knobbe, E. T., *Chem. Mater.*, 1993, **5**, 1697.

[36] Fujiyama, T., Hori, M., and Sasaki, M., *J. Non-Cryst. Solids*, 1990, **121**, 273.

[37] Gaponenko, N. V., Mudryi, A. V., Sergeev, O. V., Borisenko, V. E., Stepanova, E. A., Baran, A. S., Rat'ko, A. I., Pivin, J. C., and McGilp, J. F., *Spectrochimica Acta A*, 1998, **54**, 2177.

[38] Lai, D. C., Dunn, B., and Zink, J. I., *Inorg. Chem.*, 1996, **35**, 2152.

[39] Patra, A., Reisfeld, R., and Minti, H., *Mater. lett.*, 1998, **37**, 325.

[40] Perry, C. C. and Aubonnet, S., *J. Sol-Gel Sci. Technol.*, 1998, **13**, 593.

[41] Sokolnicki, J., Urbanski, B., and Legendziewicz, J., *J. Alloys Compds.*, 2000, **300-301**, 450.

[42] Strek, W., Legendziewicz, J., Lukowiak, E., Maruszewski, K., Sokolnicki, J., Boiko, A. A., and Borzechowska, M., *Spectrochimica Acta A*, 1998, **54**, 2215.

[43] Viana, B., Koslova, N., Aschehoug, P., and Sanchez, C., *J. Mater. Chem.*, 1995, **5**, 719.

[44] Zhang, H., Fu, L., Wang, S., Meng, Q., Yang, K., and Ni, J., *Mater. lett.*, 1999, **38**, 260.

[45] Li, H. H., Inoue, S., Ueda, T., Machida, K., and Adachi, G. Y., *Bull. Chem. Soc. Jpn.*, 2000, **73**, 251.

[46] Jin, T., Inoue, S., Tsutsumi, S., Machida, K., and Adachi, G. Y., *J. Non-Cryst. Solids*, 1998, **223**, 123.

[47] Qiang, G. D. and Wang, M. Q., *J. Am. Ceram. Soc.*, 2000, **83**, 703.

[48] Westin, G., Wijk, M., Moustiakimov, M., and Kritikos, M., *J. Sol-Gel Sci. Technol.*, 1998, **13**, 125.

[49] de Zea Bermudez, V., Carlos, L. D., Duarte, M. C., Silva, M. M., Silva, C. J. R., Smith, M. J., Assunçao, M., and Alcacer, L., *J. Alloys Compds.*, 1998, **275-277**, 21.

[50] Klonkowski, A. M., Lis, S., Hnatejko, Z., Czarnobaj, K., Pietraszkiewicz, M., and Elbanowski, M., *J. Alloys Compds.*, 2000, **300-301**, 55.

[51] Collings, P. and Hird, M., *Introduction to Liquid Crystals*, Taylor&Francis, London **1997**, 271.

[52] Avnir, D., Le Strat, V., and Reisfeld, R., *J. Phys. Chem.*, 1984, **88**, 5956.

[53] Levy, D., Serna, C. J., and Oton, J. M., *Mater. lett.*, 1991, **10**, 470.

[54] Oton, J. M., Serrano, A., Serna, C. J., and Levy, D., *Liq. Cryst.*, 1991, **12**, 733.

[55] Levy, D., Pena, J. M. S., Serna, C. J., and Oton, J. M., *J. Non-Cryst. Solids*, 1992, **147-148**, 646.

[56] Levy, D., *J. Non-Cryst. Solids* , 1992, **147-148**, 508.

[57] Levy, D., Serrano, A., and Oton, J. M., *J. Sol-Gel Sci. Technol.*, 1994, **2**, 803.

[58] Levy, D. and Esquivias, L., *Adv. Mater.*, 1995, **7**, 120.

[59] Pena, J. M. S., Olias, E., Quintana, X., and Oton, J. M., *Mol. Cryst. Liq. Cryst.*, 1997, **299**, 337.

[60] Whang, W., *Gel-glass dispersed liquid crystals*, 30-12-1997, US pat. nr. 5,702,636.

[61] Hori, M. and Toki, M., *J. Sol-Gel Sci. Technol.*, 2000, **19**, 349.

[62] Levy, D., *Mol. Cryst. Liq. Cryst.*, 2000, **354**, 159.

[63] Levy, D., Del Monte, F., Quintana, X., and Oton, J. M., *J. Sol-Gel Sci. Technol.*, 1997, **8**, 1063.

[64] Haruvy, Y. and Webber, S. E., *Chem. Mater.*, 1991, **10**, 470.

Instrumentation and procedures Chapter 2

2.1 Instrumentation

2.1.1 UV/VIS/NIR

UV/VIS/NIR absorption spectra have been measured on a Shimadzu UV-3100, an AVIV 17 DS or on a Cary 5000e spectrophotometer.

2.1.2 Luminescence, luminescence lifetime

The luminescence and lifetime spectra of Eu(III) have been recorded on an Edinburgh Instruments FS-900 spectrofluorimeter. This UV/VIS instrument is equipped with a xenon arc lamp, a microsecond flashlamp and a red-sensitive photomultiplier (300-850 nm).

The NIR-luminescence and lifetime spectra of the other lanthanides have been recorded on an Edinburgh Instruments FS-920 spectrofluorimeter equipped with a Xenon arc lamp, a Continuum Minilite II YAG(Nd) laser with a Continuum Jaguar C dye-laser, a double excitation monochromator, a photomultiplier (300-700 nm) and a Hamamatsu R5509-72 NIR-photomultiplier (600-1700 nm). The dye-laser has a guaranteed output greater than 100 μJ per pulse (10 Hz) across the full tuning range (370-850 nm) The pulse width is around 5 ns.

2.1.3 CHN elemental analysis

Elemental analyses (Carbon-Hydrogen-Nitrogen) were performed on a CE-Instrument EA-1110 elemental analyser.

2.1.4 Microscopy

Optical textures were observed with an Olympus BX60 polarising microscope equipped with a Linkam THMS600 hot stage and a Linkam TMS93 programmable temperature controller. A mounted Olympus digital photo camera was used to take digital images.

2.2 Procedures

2.2.1 Volume measurement

When a body is immersed in a fluid like water (or mercury), it experiences an apparent loss of weight equal to the weight of the water it displaces (Archimedes' principle). It can easily be shown that this principle leads to a very simple way of measuring the relative density of a solid, which is denser than water. First the effective weight is measured. Secondly the weight of the same piece of solid is measured when it is completely immersed in pure water. Density can be calculated. This exposes the sample to water. If the immersion

water is exchanged with the water contained within the sol-gel pores, the lanthanide complexes can be exchanged. This leads to an error.

The measurement of the volumes of the silica sol-gel glasses was therefore done with a micrometer screw and a caliper. This is the fastest and most convenient method to measure the volume. A cross section of the average structure of the disk shaped glasses is displayed in figure 2.1.

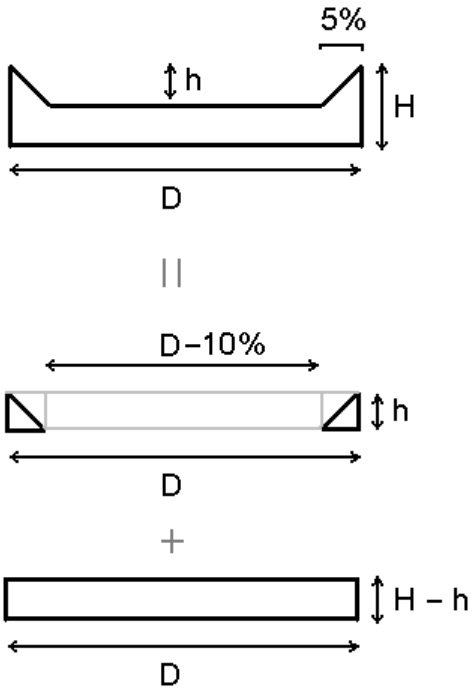

Figure 2.1: Schematic view of the cross-section of an average sol-gel glass sample.

The three values *D*, *H* and *h* are precisely measured. The volume is calculated in two parts. The first part is the cylinder with diameter *D* and height *H-h*. The second part is approximated. The volume of the outer ring is calculated by

subtracting the inner cylinder (diameter *D*-10% and height *h*) from the total cylinder (diameter *D* and height *h*). The volume of this ring is divided by two. The two parts are added to give a good approximation for the volume. Sufficiently precise results were obtained by this procedure.

2.2.1 Judd-Ofelt calculations

For the Judd-Ofelt analysis, experimental dipole strengths were extracted by integration of the lanthanide spectra in *Origin*©. The fitting of the parameters was done by a standard least-squares method in *Mathcad*©. The method minimizes the absolute differences between the experimental and the calculated values.

2.3 Safety notification

Working with alkoxysilanes is very dangerous. TMOS is one of the fastest reacting alkoxysilanes and is therefore representative for the necessary safety measurements:

Acute hazards/symptoms	Prevention	First aid
1. Flammable (R 10)	Avoid open flames and sparks (S16).	Powder, water spray
2. Above 20°C explosive vapour/air mixtures may be formed.	Use a closed system, ventilation (S16).	
3. The substance can be absorbed into the body by inhalation (R26) of its vapour and by ingestion. A harmful contamination of the air can be reached very quickly on evaporation of this substance at 20°C. The substance irritates severely the eyes, the skin and the respiratory tract (R37/38/41).	Local exhaust. Safety goggles, or eye protection in combination with breathing protection. Protective gloves (S36/37/39). Protective clothing.	Remove contaminated clothes. Rinse and wash with water and soap (S26/28A). Rinse mouth. Do NOT induce vomiting. The effects may be delayed. Medical observation is indicated (S45). The substance may have effects on the kidneys and liver. Inhalation of vapour may cause lung oedema.

3.1 Introduction

Pure silica sol-gel glasses were chosen as a first host matrix because this is the most simple silica sol-gel glass. Although the synthesis of the glasses is slow and cracking an important problem, it is a good reference because these glasses are well studied and there are no other precursors used than TEOS. These silica sol-gel glasses have been doped with mostly Eu(III) and Tb(III) salts and complexes, ligands like bipyridyls, phenanthrolines and β-diketones were used.[e.g.[1,2,3,4]] Eu(III) can be used as a probe for local environmental changes, the fine structure of the $^5D_1 \rightarrow {}^7F_0$ transition is site selective.[5] While Judd-Ofelt theory is common for lanthanides studied in other materials, only few results are published for sol-gel materials.[6,7,8,9,10] Especially Nd(III), Er(III) and Ho(III) that are now well studied for their NIR-luminescence, are ideal candidates for Judd-Ofelt analysis. Judd-Ofelt parameters of lanthanide ions in sol-gel materials have not been studied in detail before. It is interesting to see what influence local structural changes have on these intensity parameters.

3.2 Preparation of the lanthanide complexes

3.2.1 Bipyridyl complexes

The lanthanide(III) bipyridyl complexes, $[Ln(bipy)_2]Cl_3 \cdot 2H_2O$ (bipy = 2,2'-bipyridine or bipyridyl; Ln = Nd, Ho, Er, Dy, Sm), were prepared according to a method described by Qian *et al.*.[11] 2,2'-Bipyridine (figure 3.1) was added to a hot (60 °C) ethanol solution containing an equivalent amount of the corresponding hydrated lanthanide chloride salt. The precipitate was filtered, then washed several times with cold ethanol and dried in a vacuum oven. The complexes were characterized by IR spectrometry and by CHN elemental analysis.

3.2.2 Phenanthroline complexes

The lanthanide(III) phenanthroline complexes $[Ln(phen)_2]Cl_3 \cdot 2H_2O$ (phen = 1,10-phenanthroline; Ln = Nd, Sm, Dy, Ho and Er) were prepared by adding 1,10-phenanthroline (figure 3.1) to a warm (60 °C) ethanol solution containing an equivalent amount of the corresponding hydrated lanthanide chloride salt. The precipitate was filtered, then washed several times with cold ethanol and dried in a vacuum oven. The complexes were characterized by IR spectrometry and by CHN elemental analysis.

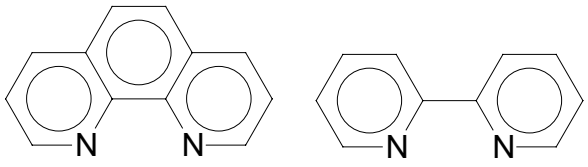

Figure 3.1: Structure of 1,10-phenanthroline (left) and 2,2'-bipyridine (right).

3.2.3 Nitrate complexes

An exact quantity of Ln_2O_3 was dissolved in a concentrated HNO_3 solution. The solution was diluted by an ammonia solution to pH = 2 and to a volume of exactly 25 mL. This solution was used to react with the TEOS.

3.3 Preparation of the pure silica sol-gel glasses

This is the most simple silica sol-gel glass. TEOS is the most used starting product for these glasses. TEOS is mixed with ethanol and acidified water is slowly added. Ethanol is added because TEOS and water are immiscible. The procedure roughly follows methods described in the literature.[12,13,14,2,15,16] No sufficient details about aging time, used vessels, exact volumes, drying time and temperature were given in the literature. These very important parameters were therefore experimentally optimized. Drying temperature, pH and time appeared to be the most critical parameters. Table 3.1 gives an overview of the parameters that were changed.

Criteria for a sample of good quality are:

1. Crack free: this is necessary to measure the volume exactly and to have a clear optical path. Cracks cause light scattering.

2. Sufficient long path lengths (> 0.5 mm) and/or good dopant solubility: a shorter path length means that the concentration of the lanthanide complexes must be higher because the molar absorptivities of the lanthanide complexes are low. The path length must be measured precisely.

3. Acceptable fabrication time: this is the drawback for pure silica sol-gels, a drying time of more than 4 months is too long.

Figure 3.2: Slow cracking of a Nd(III) doped silica sol-gel (diameter 4 cm).

Table 3.1: Tested parameters in the sol-gel synthesis process.

Parameter	Induced change	Range	Optimum
pH	Speed of the hydrolysis and condensation reactions change	pH 1-7	2-3 If the pH is too high (> pH 3.5) the starting solution is turbid when adding water and gel time is fast
Sol Temperature	Faster hydrolysis and condensation	18-100 °C	50 °C The samples gelled noticeably faster (few days)
Aging time	Longer aging time gives less chance of cracking	1-20 days	2 days The aging process can help but drying time and temperature is more critical
Volume of sample	A larger volume gives long drying time but the path length is longer	0.25-20mL	4 mL This volume was necessary to keep the drying times low but at the same time give a sufficient long path length
Drying temperature	The samples dry faster	18-100 °C	18 °C All the samples dried at elevated temperature cracked
Drying time	Slower drying gives less cracks	1 hour-6 months	> 45 days for 4 mL of sol. These long drying times are necessary

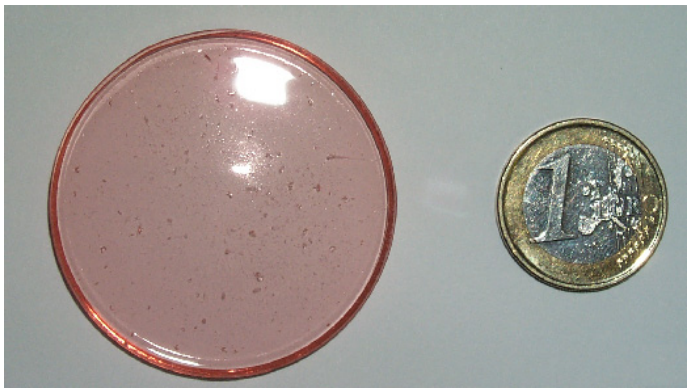

Figure 3.3: A six-month drying period is necessary
to obtain large sol-gel glasses.

The SiO_2 sol-gel glasses were obtained by hydrolysis of the precursor TEOS. For the acid-catalyzed sol preparation, exactly measured volumes of TEOS (160 mL, obtained from Aldrich), ethanol (120 mL) were mixed. To this mixture an aqueous HCl or HNO_3 solution (80 mL) was slowly added, resulting in a solution with pH = 2 and a H_2O/precursor ratio (**r**) of 6.2. An excess of water (**r** >> 2) decreases the gel-time and makes the lanthanide complex more soluble in the starting solution. Disadvantage is a longer drying time (90 days total drying time) needed to obtain crack-free monoliths. This mixture was heated at reflux during 6 days, and after this period divided into batches of 40 mL. The lanthanide complexes were dissolved in these solutions. Of each solution, 4 mL quantities were divided over small glass vials (diameter 2.4 cm, height 5 cm). The vials were closed with Parafilm®. After one week, the Parafilm® cover was perforated several times with a needle and the solvent was allowed to evaporate.

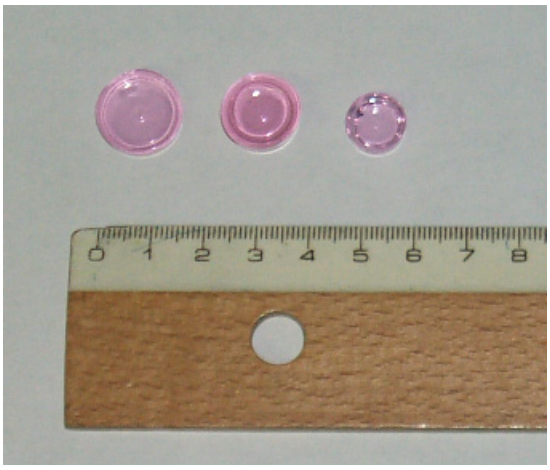

Figure 3.4: Shrinkage of the sol-gel.

After ca. 90 days transparent monolithic glass samples were obtained, most of them free of cracks. After drying the average volume of the gels shrunk to 10% (up to 85 % smaller in height and 55% smaller in diameter) of the original volume.

The bipyidine and phenanthroline complexes can be dissolved in the sol before gellation.[17] The lanthanide nitrate solutions with pH 2 are directly added to the TEOS and ethanol instead of using acidified water. Several lanthanide doped samples are shown in figure 3.5. The final lanthanide concentration in the dried gel varied between 0.1 and 2.2 mol/L.

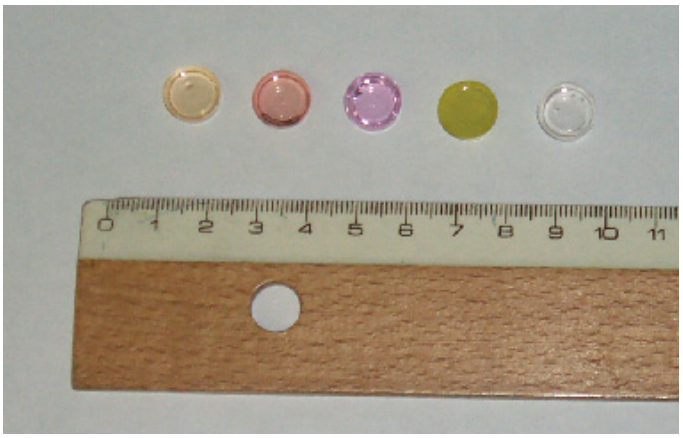

Figure 3.5: Er(III), Ho(III), Nd(III), Pr(III) and Eu(III) doped silica sol-gel glass.

3.4 The lanthanide doped silica sol-gel glass spectra

3.4.1 Cluster formation

Cluster formation is a problem for Judd-Ofelt analysis. The spectroscopic properties of neighbouring lanthanide ions change if the lanthanide ions form clusters.[18] This is possible with samples where the lanthanide concentration is high. Some authors reported cluster formation in sol-gel glasses at higher concentrations.[9] The concentration versus dipole strength plot is then non-linear. Examples are given for Pr(III) where the product composition is higher than x = 5% (xPr_2O_3-$(100-x)SiO_2$).

If cluster forming is present, the calculated dipole strengths and the Judd-Ofelt parameters are incorrect. Samples of $Nd(NO_3)_3$ were prepared with different concentrations. The dipole strength is calculated for different concentrations and shown in figure 3.6. Dipole strength of the transitions $^4F_{5/2} \leftarrow {}^4I_{9/2}$ and $^4S_{3/2} \leftarrow {}^4I_{9/2}$ does not vary in function of the concentration. The $^4G_{5/2} \leftarrow {}^4I_{9/2}$ transition is hypersensitive and small environmental changes should induce small changes in the dipole strength. No changes are detected. It is clear that cluster forming is absent in the measurable concentration range of these pure silica sol-gels.

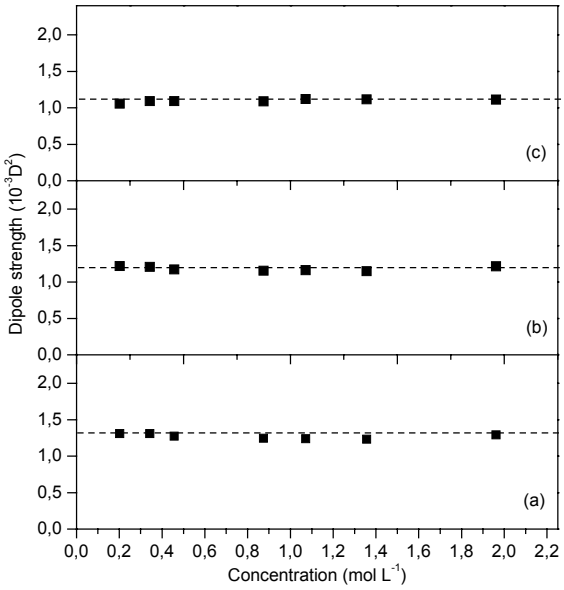

Figure 3.6: Dipole strength of three transitions: (a) $^4F_{5/2} \leftarrow {}^4I_{9/2}$, (b) $^4S_{3/2} \leftarrow {}^4I_{9/2}$ and (c) $^4G_{5/2} \leftarrow {}^4I_{9/2}$ of Nd(III) at different concentration in pure silica sol-gels.

3.4.2 $Nd(NO_3)_3$ doped silica sol-gel glass

Absorption spectra of the lanthanide-doped glasses were recorded between 300 and 1500 nm. Figure 3.7 shows the photo-physical behaviour of one of the complexes in the glass during a heat treatment. An absorption spectrum of a $Nd(NO_3)_3$ sol-gel glass at room temperature (a), after a heat treatment of 36 hours at 50 °C in air (b), after 36 hours at 70 °C (c), after 36 hours at 100 °C (d) and after one month exposure to air (e) is shown.

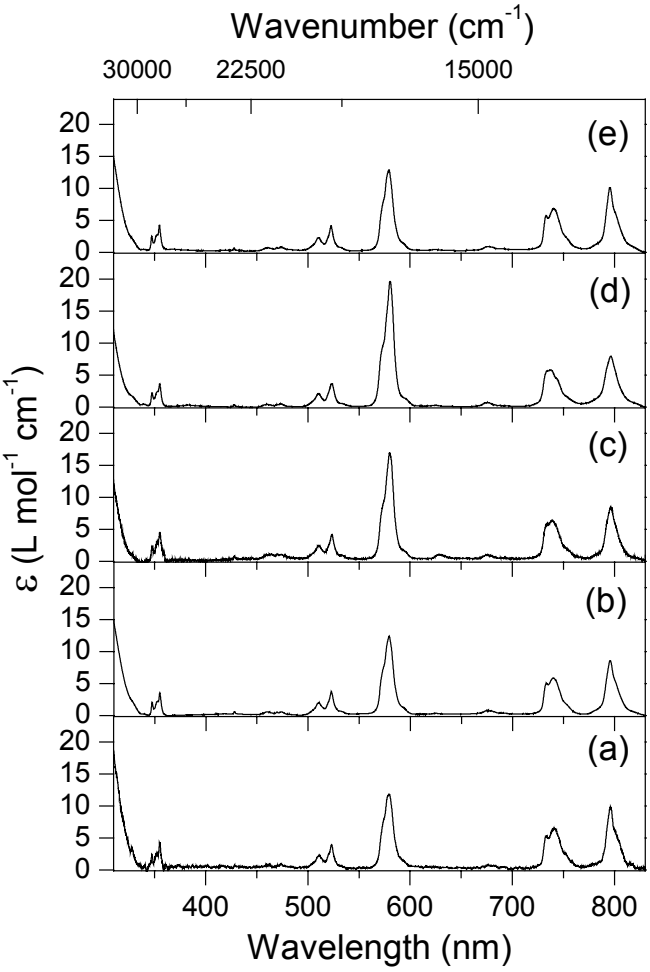

Figure 3.7: Absorption spectrum of a SiO_2:$Nd(NO_3)_3$ sol-gel glass at room temperature (a), after a heat treatment of 36 hours at 50 °C in air (b), after 36 hours at 70 °C (c), after 36 hours at 100 °C (d) and after one month exposure to air after heat treatment (e).

The narrow, weak absorption bands are characteristic of the trivalent lanthanides ions in glasses. If the absorption spectra, taken after the different drying temperatures 18 °C, 50 °C, 70 °C and 100 °C are compared, it is clear that some transitions increased in intensity. This phenomenon is previously reported for the luminescence of Eu(III) and Tb(III) doped sol-gel glasses during heat treatment.[e.g.[2,5,17]] This intensity increase was assigned to the evaporation of ethanol and more importantly, of water molecules. These molecules quench the lanthanide luminescence.

A more detailed look at some intense absorption $Nd(NO_3)_3$ transitions is given in figure 3.8 and figure 3.9. The shape of the $^4F_{5/2} \leftarrow {}^4I_{9/2}$ and $^4S_{3/2} \leftarrow {}^4I_{9/2}$ transitions is changed during heating. The maximum intensity lowers and some transitions broaden. Important is that the overall intensity for these transitions is not changed very much. If we look at another part in the spectrum (figure 3.9) of Nd^{3+}, we can see an important increase in intensity of the $^4G_{5/2} \leftarrow {}^4I_{9/2}$ transition. The intensity is doubled.

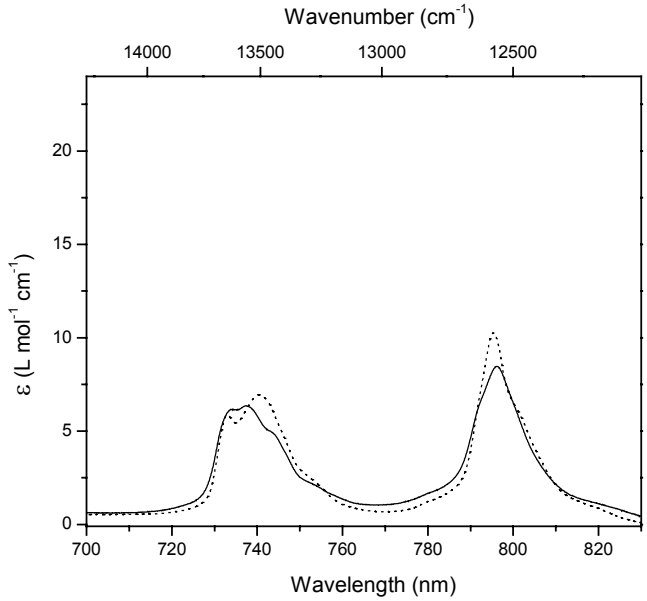

Figure 3.8: The $^4F_{5/2} \leftarrow {}^4I_{9/2}$ and $^4S_{3/2} \leftarrow {}^4I_{9/2}$ transitions of $Nd(NO_3)_3$ in pure silica sol-gel glasses change during the heating. The dotted and solid lines represent the spectrum before and after drying respectively.

This is typical behaviour of hypersensitive transitions, hence their name. These transitions are sensitive to small local changes. The lanthanide ions occupy different low symmetry sites and are surrounded by water molecules in the wet gel. At higher temperatures the water leaves the structure and the lanthanide ions are more embedded in the glass network. The silica structure closes around the lanthanide sites and causes distortion of the local crystal field. There are strong inhomogeneities from site to site because the number and positions of the oxygens and not reacted hydroxyls are different. Some

transitions can broaden. This broadening is also visible in luminescence spectra.[5,11,19]

After the heat treatment and one month exposure to air, the spectrum is almost the same as before heat treatment. This can be related to the hygroscopic character of the silica sol-gels. Water is reabsorbed. Throwing a well-dried sol-gel in demineralized water can reproduce this phenomenon. The dopant concentration is no longer the same, but the spectrum resembles the spectrum of the wet silica sol-gels.

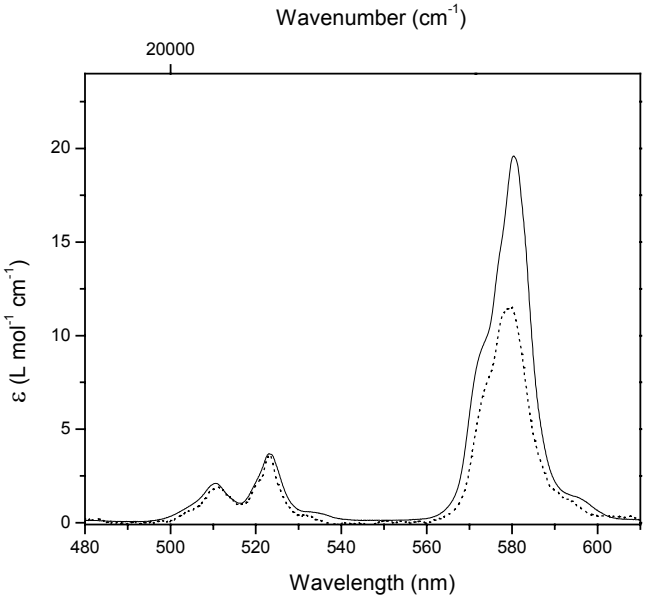

Figure 3.9: The $^4G_{5/2} \leftarrow {}^4I_{9/2}$ transition of $Nd(NO_3)_3$ at 580 nm in pure silica sol-gel glasses change during the heating. The dotted and solid lines represent the spectrum before and after drying respectively.

3.4.3 $[Ln(phen)_2]Cl_3$ and $[Ln(bipy)_2]Cl_3$ doped silica sol-gel glasses

Absorption spectra of the lanthanide-doped glasses have been recorded between 300 and 1500 nm. An absorption spectrum of a SiO_2: $[Ho(phen)_2]Cl_3$ sol-gel glass at room temperature (a), after a heat treatment of 36 hours at 50 °C in air (b), after 36 hours at 70 °C (c), after 36 hours at 100 °C (d) and after one month exposure to air (e) is shown in figure 3.10. The cut-off in the UV spectrum that appears in all the $[Ln(phen)_2]Cl_3$ and $[Ln(bipy)_2]Cl_3$ doped glasses is due to ligand absorption. Similar behaviour is observed in spectra of both phenanthroline and bipyridyl complexes. Some transitions broaden and other increase in intensity like in $Ln(NO_3)_3$ doped glasses.

Some authors attribute the increment in luminescence intensity of $Eu(bipy)_2Cl_3$-doped glasses to the mobility of the ligands in the silica pores at higher temperature and in situ formation of the complex.[11] Here, an increment in absorption intensity was observed with and without a ligand. But there is a remarkable difference in the fine structure of the hypersensitive transitions.

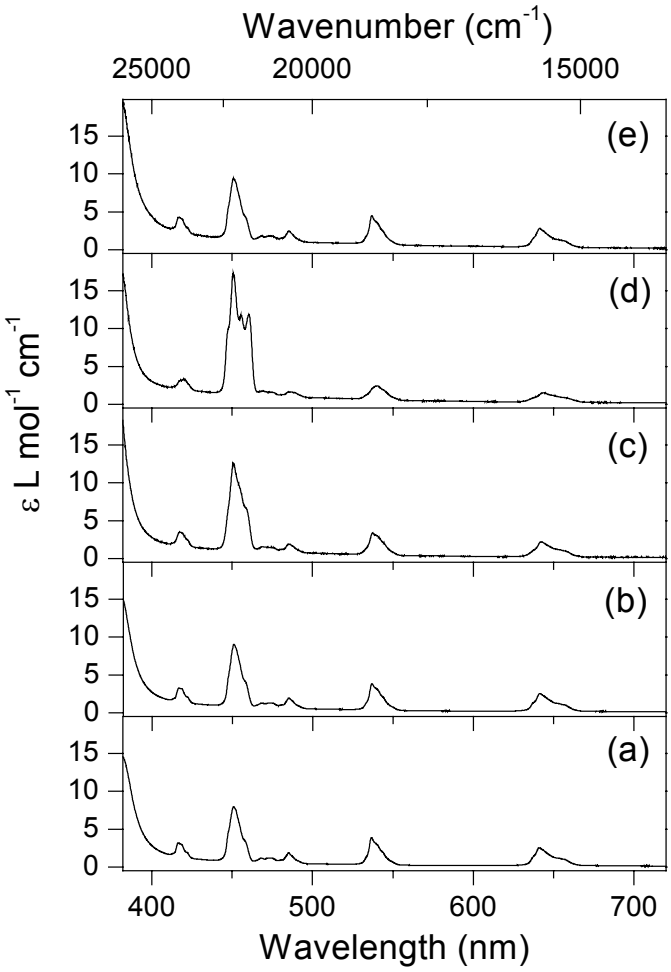

Figure 3.10: Absorption spectrum of a SiO_2:$[Ho(phen)_2]Cl_3$ sol-gel glass at room temperature (a), after a heat treatment of 36 hours at 50 °C in air (b), after 36 hours at 70 °C (c), after 36 hours at 100 °C (d) and after one month exposure to air (e).

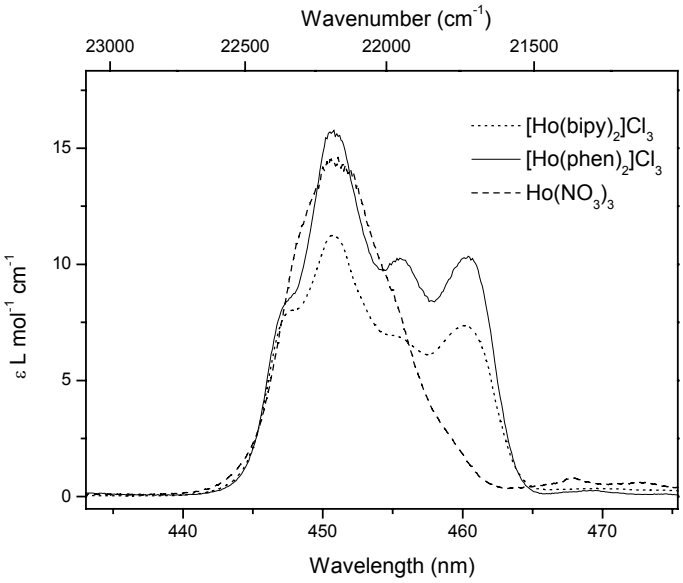

Figure 3.11: Fine structure for the hypersensitive transition $^5G_6 \leftarrow ^5I_8$ of Ho(III) at 450 nm after heat treatment.

This is most apparent in the hypersensitive transition at 450 nm of Ho(III) (figure 3.11). At a higher drying temperature the fine structure improves, whereas fine structure is absent in the $Ho(NO_3)_3$ doped glass. This fine structure can be attributed to the surrounding bipyridyl and 1,10-phenanthroline. There is a difference in intensity for bipyridyl and 1,10-phenanthroline.

3.4.4 Judd-Ofelt analysis of the pure silica sol-gel spectra

Judd-Ofelt calculations can be used to rationalize the transition intensities in disordered systems like glasses.[20,21] The dipole strengths of the transitions were extracted from the absorption spectrum. The exact knowledge of the concentration of the doped ion is necessary. The Ω_λ-parameters can be determined via a least-squares fit, minimizing the sum of the squares of the differences between the experimental and calculated dipole strengths. The procedure is explained in chapter 1 p16. In general the intensities of the induced electric dipole transitions in lanthanide ions are little affected by the environment. In the sol-gel glasses some bands broadened during heat treatment, but some peaks increased in intensity.

The intensity of the hypersensitive transitions is mainly described by the Ω_2-parameter. Hypersensitive transitions are the $^4G_{5/2} \leftarrow {}^4I_{9/2}$ transition of Nd(III) (586 nm or 17300 cm^{-1}), the $^6F_{11/2} \leftarrow {}^6H_{15/2}$ transition of Dy(III) (1298 nm or 7700 cm^{-1}), the $^5G_6 \leftarrow {}^5I_8$ transition of Ho(III) (451 nm or 22100 cm^{-1}) and the $^2H_{11/2} \leftarrow {}^4I_{15/2}$ and $^4G_{11/2} \leftarrow {}^4I_{11/2}$ transitions of Er(III) (at 521 and 378 nm or 19200 cm^{-1} and 26400 cm^{-1} respectively). Sm(III) also has a hypersensitive transition but the transition is situated at 1562 nm where a broad absorption band of the sol-gel matrix is situated (overtone of OH vibrations). The hypersensitive transition cannot be resolved and integrated. As a consequence it was impossible to calculate the Ω_2-parameter of Sm(III). All calculated parameters are given in table 3.2-3.4. There is a remarkable increase in the Ω_2-parameters during the heat treatment. There are several factors that can influence hypersensitive transitions (see chapter 1, table 1.2). An increase of the basic character of the coordinated ligand results in an increased absorption

intensity. Decreasing metal-ligand bond distances also results in an intensity enhancement. The greater the number of ligands, the higher the enhancement of intensity. The intensity of the hypersensitive transitions increases as electrolyte concentration increases. The observed changes can be explained by these considerations. When the sol-gel is heated, water and ethanol are expelled out of the gel matrix. As the glass shrinks and polymerization continues, the pore size and the metal ligand bond distance decrease. The coordination sphere changes: water molecules are removed from the direct surrounding of the lanthanide ions and the covalent character of the Ln(III)-ligand bounding increases. The transitions become more intense. Higher initial values of the Ω_2-parameter in table 3.2 to 3.5 for the $Ln(NO_3)_3$ complexes can be explained by a higher electrolyte concentration due to the different synthesis methods.

Table 3.2: Judd-Ofelt parameters of the silica sol-gel glasses doped with $Ln(NO_3)_3$, before and after heat treatment.

Ligand	Ion	parameter[a]	18°C	50°C	70°C	100°C	recovery
NO_3	Nd	Ω_2	4.8 ± 0.4	5.4 ± 0.7	7.8 ± 0.4	9.9 ± 0.4	5.5 ± 0.6
		Ω_4	4.2 ± 0.4	4.1 ± 0.8	4.9 ± 0.4	4.4 ± 0.5	4.1 ± 0.7
		Ω_6	7.2 ± 0.3	7.3 ± 0.6	6.7 ± 0.3	7.5 ± 0.4	7.9 ± 0.5
	Sm	Ω_2	-	-	-	-	-
		Ω_4	4.1 ± 0.6	4.1 ± 0.6	4.4 ± 0.7	3.9 ± 0.8	3.4 ± 0.7
		Ω_6	2.0 ± 0.3	2.1 ± 0.3	2.3 ± 0.4	2.7 ± 0.4	2.3 ± 0.4
	Dy	Ω_2	1.9 ± 0.4	2.9 ± 0.4	6.1 ± 0.3	7.6 ± 0.4	2.9 ± 0.4
		Ω_4	1.7 ± 0.4	1.7 ± 0.4	1.6 ± 0.3	2.1 ± 0.4	1.8 ± 0.4
		Ω_6	2.9 ± 0.3	3.0 ± 0.3	3.0 ± 0.2	2.7 ± 0.3	3.1 ± 0.3
	Ho	Ω_2	3.5 ± 0.5	3.9 ± 0.6	6.5 ± 0.6	9.1 ± 0.7	3.7 ± 0.7
		Ω_4	1.8 ± 0.8	1.9 ± 0.8	2.1 ± 0.9	2.0 ± 0.9	2.4 ± 0.9
		Ω_6	1.9 ± 0.6	2.0 ± 0.6	2.0 ± 0.6	1.8 ± 0.7	2.2 ± 0.7
	Er	Ω_2	3.6 ± 0.3	4.3 ± 0.3	6.0 ± 0.3	6.5 ± 0.3	4.0 ± 0.3
		Ω_4	0.4 ± 0.4	0.6 ± 0.4	0.7 ± 0.5	0.7 ± 0.4	0.6 ± 0.4
		Ω_6	1.0 ± 0.2	0.9 ± 0.2	0.9 ± 0.3	1.0 ± 0.2	1.0 ± 0.2

[a] All intensity parameters are in 10^{-20} cm^2.

Table 3.3: Judd-Ofelt parameters of the silica sol-gel glasses doped with $[Ln(bipy)_3]Cl_3$, before and after heat treatment.

Ligand	Ion	parameter[a]	18°C	50°C	70°C	100°C	recovery
bipy	Nd	Ω_2	0.3 ± 0.4	2.2 ± 0.5	3.3 ± 0.6	5.6 ± 0.5	0.7 ± 0.7
		Ω_4	4.7 ± 0.7	6.0 ± 0.7	5.8 ± 0.9	5.8 ± 0.7	5.7 ± 0.9
		Ω_6	4.6 ± 0.4	5.8 ± 0.4	5.3 ± 0.5	4.8 ± 0.5	5.8 ± 0.5
	Sm	Ω_2	-	-	-	-	-
		Ω_4	3.8 ± 0.2	3.5 ± 0.2	3.9 ± 0.2	3.6 ± 0.2	3.3 ± 0.2
		Ω_6	1.6 ± 0.1	1.6 ± 0.1	1.9 ± 0.1	1.8 ± 0.1	1.7 ± 0.1
	Dy	Ω_2	1.6 ± 0.4	2.9 ± 0.4	3.2 ± 0.3	6.7 ± 0.3	2.3 ± 0.6
		Ω_4	0.4 ± 0.5	0.1 ± 0.5	0.4 ± 0.3	0.4 ± 0.3	0.3 ± 0.7
		Ω_6	2.8 ± 0.2	2.7 ± 0.3	2.9 ± 0.2	2.9 ± 0.2	3.2 ± 0.4
	Ho	Ω_2	2.2 ± 0.1	2.6 ± 0.2	4.7 ± 0.2	8.9 ± 0.2	2.1 ± 0.2
		Ω_4	2.5 ± 0.2	2.7 ± 0.3	2.5 ± 0.3	2.5 ± 0.3	2.6 ± 0.4
		Ω_6	2.5 ± 0.1	2.4 ± 0.2	2.1 ± 0.1	2.0 ± 0.2	2.5 ± 0.2
	Er	Ω_2	2.0 ± 0.3	4.5 ± 0.4	5.7 ± 0.2	9.3 ± 0.3	3.7 ± 0.4
		Ω_4	0.6 ± 0.4	1.3 ± 0.6	1.7 ± 0.4	1.3 ± 0.5	1.1 ± 0.6
		Ω_6	1.2 ± 0.3	1.2 ± 0.4	1.1 ± 0.2	0.8 ± 0.3	1.5 ± 0.4

[a] All intensity parameters are in 10^{-20} cm^2.

Table 3.4: Judd-Ofelt parameters of the silica sol-gel glasses doped with $[Ln(phen)_3]Cl_3$, before and after heat treatment.

Ligand	Ion	parameter[a]	18°C	50°C	70°C	100°C	recovery
phen	Nd	Ω_2	1.3 ± 0.4	2.2 ± 0.4	4.7 ± 0.4	5.8 ± 0.4	1.8 ± 0.5
		Ω_4	5.0 ± 0.6	5.3 ± 0.6	5.3 ± 0.6	6.0 ± 0.6	5.2 ± 0.8
		Ω_6	4.6 ± 0.3	5.1 ± 0.3	5.1 ± 0.3	5.0 ± 0.3	5.5 ± 0.4
	Sm	Ω_2	-	-	-	-	-
		Ω_4	3.0 ± 0.2	3.4 ± 0.3	4.1 ± 0.1	4.7 ± 0.2	3.0 ± 0.3
		Ω_6	2.7 ± 0.1	2.6 ± 0.1	2.4 ± 0.1	2.3 ± 0.1	2.7 ± 0.1
	Dy	Ω_2	0.7 ± 0.2	0.8 ± 0.2	1.5 ± 0.1	5.0 ± 0.5	2.1 ± 0.1
		Ω_4	0.7 ± 0.3	0.5 ± 0.3	1.0 ± 0.1	0.5 ± 0.6	1.3 ± 0.2
		Ω_6	2.7 ± 0.2	3.2 ± 0.2	2.1 ± 0.1	2.1 ± 0.3	2.6 ± 0.1
	Ho	Ω_2	3.1 ± 0.2	4.5 ± 0.2	5.8 ± 0.2	12.0 ± 0.2	3.4 ± 0.3
		Ω_4	2.5 ± 0.3	2.3 ± 0.3	3.0 ± 0.3	2.2 ± 0.3	2.9 ± 0.4
		Ω_6	2.5 ± 0.2	2.0 ± 0.2	2.3 ± 0.2	2.0 ± 0.2	2.7 ± 0.2
	Er	Ω_2	1.2 ± 0.3	2.6 ± 0.4	4.0 ± 0.2	6.2 ± 0.2	2.0 ± 0.3
		Ω_4	0.6 ± 0.3	1.1 ± 0.4	1.2 ± 0.2	0.8 ± 0.3	1.0 ± 0.3
		Ω_6	0.7 ± 0.2	1.1 ± 0.3	1.0 ± 0.2	0.7 ± 0.2	0.9 ± 0.2

[a] All intensity parameters are in 10^{-20} cm^2.

When the samples are measured again after one month, the Ω_2-parameter values drop but do not recover fully. The hygroscopic sol-gel reabsorbs water. The values are situated between the values before drying and after drying at 50°C. The remaining differences can be attributed to the loss of ethanol molecules and irreversible condensation reactions. The hygroscopic properties and intensity recovery is important when using these lanthanide doped silica sol-gel glasses in optical applications. Transition probabilities of hypersensitive transitions become smaller when water is reabsorbed. Moreover, the water molecules quench the luminescence, especially in the near infrared region.

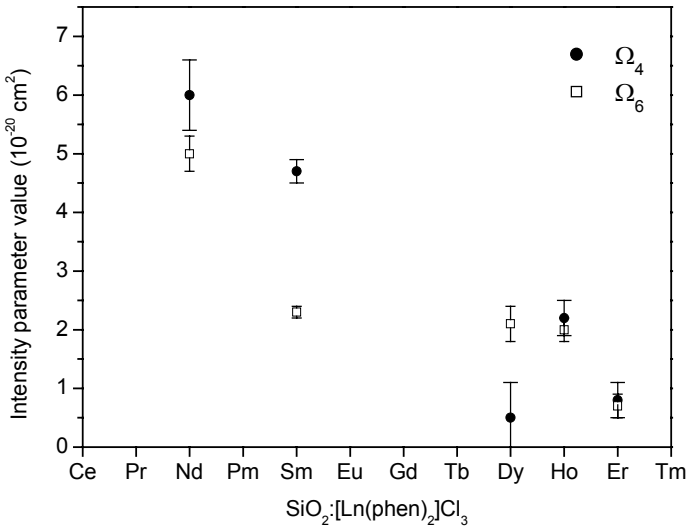

Figure 3.12: The change of the Ω_4- and Ω_6-intensity parameters in $[Ln(phen)_2]Cl_3$ (Ln = Nd, Sm, Dy, Ho, Er) doped silica sol-gel glass over the lanthanide series after heat treatment at 100 °C for 36 hours.

The Ω_4- and Ω_6-parameters describe the intensities of the other f-f transitions. These intensities do not increase; some bands broaden. The Ω_6-parameter is related to the rigidity of the medium in which the lanthanide ion is embedded. The rigidity of the matrix increases in the following order: coordination complexes < halide vapours < hydrated ions < viscous solutions < glasses < crystalline mixed oxides. Tables with phenomenological intensity parameters Ω_λ in various host matrices are presented elsewhere.[22] The parameters change during the treatment but the changes are minor and in a random way. The parameters change slightly (table 3.2-3.4) when the ligand is changed except Ω_6 in $Nd(NO_3)_3$. The fact that the lanthanide is in a sol-gel silica glass has a stronger effect on the Ω_6-parameter than the ligand. The Ω_4-parameter is also mainly dependent upon long-range effects and can be related to the bulk properties of the glass. Differences between the samples with other ligands are minor. In figure 3.12 the Ω_4- and Ω_6-parameters of the $[Ln(phen)_2]Cl_3$ complexes have been compared for the different lanthanides. The values of both Ω_4 and Ω_6 of the lighter lanthanides are larger than those of the heavy lanthanides. This phenomenon can be expected due to the contraction of the 4-shell from Ce(III) to Lu(III). The radial integrals in the expressions of the Judd-Ofelt parameters decrease from Nd to Er.[22,23] This behaviour is the same for all the complexes. Sometimes a minimum for the parameters at Gd(III) or Eu(III) occurs. Because these ions are not included, the minimum is situated between Sm(III) or Dy(III).

3.5 Conclusion

Silica sol-gel glasses were doped with $[Ln(bipy)_2]Cl_3$, $[Ln(phen)_2]Cl_3$ and $Ln(NO_3)_3$ complexes. Cluster formation was tested and is absent in the measured concentration range. During a heat treatment the intensities of the majority of the f-f transitions remained constant, whereas the intensities of the hypersensitive transitions increased. Judd-Ofelt parameters have been calculated. The Ω_2-parameter increased upon heat treatment due to a change in the coordination sphere of the Ln(III). This is caused by water leaving the sol-gel glass and the lanthanide surroundings. When drying, the fine structure is lost for the $Ln(NO_3)_3$ doped glass but is improved for the hypersensitive transitions when the lanthanide is coordinated to 1,10-phenanthroline or bipyridyl. The coordination improves when the water leaves the first coordination sphere. The Ω_4- and Ω_6-parameters remain constant during heat treatment and are more influenced by matrix effects than by the surrounding ligands. Almost total recovery of the initial intensity occurs when the samples are exposed to air at room temperature after the heat treatment. This is important for spectroscopic applications.

It was demonstrated that Judd-Ofelt parameters are not only interesting to compare results between different materials or different complexes, but these parameters can also be used to detect structural changes within one material.

REFERENCES

[1] Li, W. L., Li, W., Yu, G., Wang, Q. G., and Jin, R., *J. Alloys Compds.*, 1993, **192**, 34.

[2] Matthews, L. R. and Knobbe, E. T., *Chem. Mater.*, 1993, **5**, 1697.

[3] Levy, D., Reisfeld, R., and Avnir, D., *Chem. Phys. Lett.*, 1984, **109**, 593.

[4] Bredol, M., Kynast, U., and Ronda, C., *Adv. Mater.*, 1991, **3**, 361.

[5] Campostrini, R., Carturan, G., Ferrari, M., Montagna, M., and Pilla, O., *J. Mater. Res.*, 1992, **7**, 745.

[6] Patra, A., Reisfeld, R., and Minti, H., *Mater. lett.*, 1998, **37**, 325.

[7] Perry, C. C. and Aubonnet, S., *J. Sol-Gel Sci. Technol.*, 1998, **13**, 593.

[8] Sokolnicki, J., Urbanski, B., and Legendziewicz, J., *J. Alloys Compds.*, 2000, **300-301**, 450.

[9] Strek, W., Legendziewicz, J., Lukowiak, E., Maruszewski, K., Sokolnicki, J., Boiko, A. A., and Borzechowska, M., *Spectrochimica Acta A*, 1998, **54**, 2215.

[10] Viana, B., Koslova, N., Aschehoug, P., and Sanchez, C., *J. Mater. Chem.*, 1995, **5**, 719.

[11] Qian, G. D., Wang, M. Q., and Wang, M., *J. Photochem. Photobiol. A*, 1997, **107**, 121.

[12] Chang, S. Y. and Ring, T. A., *J. Non-Cryst. Solids*, 1992, **147-148**, 56.

[13] Higginbotham, C., Pike, C. F., and Rice, J. K., *J. Chem. Educ.*, 1998, **75**, 461.

[14] Li, H. H., Inoue, S., Machida, K. I., and Adachi, G. Y., *Chem. Mater.*, 1999, **11**, 3171.

[15] Murtagh, M. T., Kwon, H. C., Shahriari, M. R., Krikah, M., and Ackley, D. E., *J. Mater. Res.*, 1998, **13**, 3326.

[16] Nogami, M. and Moriya Y., *J. Non-Cryst. Solids*, 1980, **37**, 191.

[17] Jin, T., Tsutsumi, S., Deguchi, Y., Machida, K., and Adachi, G. Y., *J. Alloys Compds.*, 1997, **252**, 59.

[18] Simpson, J. R, in *Rare Earth Doped Fiber Lasers and Amplifiers on Optical Engineering* ,(Digonnet, M.), Marcel Dekker inc., New York **1993**, 4.

[19] Meng, Q., Zhang, H., Fu, L. S., and Yang, K., *J. Inorg. Mater.*, 1999, **14**, 630.

[20] Judd, B. R., *Phys. Rev.*, 1962, **127**, 750.

[21] Ofelt, G., *J. Chem. Phys.*, 1962, **37**, 511.

[22] Görller-Walrand, C. and Binnemans, K., in *Handbook on the Physics and Chemistry of Rare Earth*s, *Vol. 25*, (Gschneidner, K. jr. and Eyring, L.), Elsevier, Amsterdam **1998**, 101-264.

[23] Krupke, W. F., *Phys. Rev. B*, 1966, **145**, 325.

4.1 Introduction

The sol-gel process allows preparation of silica-based materials at ambient temperature. Pure SiO_2 glass can be made by hydrolysis and polymerisation of silicon alkoxides. The resulting silica materials are transparent and have good mechanical properties. Bulk glass, coatings, fibres can be made, but there are some drawbacks like the low solubility of lanthanide complexes in this matrix and the low pH needed for the hydrolysis reaction. The cracking of the material and the water present in the pores also causes problems, making long drying times necessary.[1] These materials were discussed in chapter 3.

One way to overcome the solubility problems of lanthanide complexes, with large basic ligands, is to neutralize the solution after hydrolysis and to introduce organic parts in the material. Flexible organic parts are good to avoid cracking. The properties of the *inorganic-organic hybrid materials* depend on the chemical nature of the different components.[2,3] *Polyethylene glycol* (PEG, figure 4.1a) can be introduced in the silica matrix by simple mixing the PEG with the silica precursors.[4,5,6,7,8,9] PEG-200 (average molecule weight = 200) is a viscous liquid that is soluble in water and is able to form complexes with metal cations. No covalent bonds are formed between the PEG-chains and the silica backbone and these materials are therefore class I hybrids.[2] The PEG-silica sol-gels are transparent, easily made and have good mechanical and optical properties. The solubility of the ligands can be improved by using a buffered solution for the sol-gel synthesis.

Related hybrid materials called *ureasils* have PEG chains covalently bonded in the silica network through urea bridges.[10,11,12,13,14,15] The urea bridges are able to bind the lanthanides strongly and ureasils are therefore unsuited for this work (figure 4.1b). Small silica clusters are formed at the network nodes, the polymer chains are in a folded state inside these clusters and in a nearly extended state between different clusters. Lanthanide ions preferentially coordinate to the urea bridges.

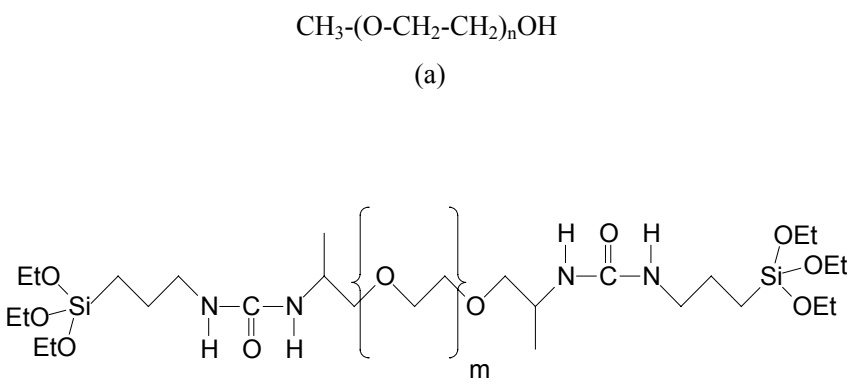

Figure 4.1: Structure of PEG (a) and structure of a precursor for Ureasils(b).

4.2 Preparation of the lanthanide complexes

4.2.1 Bipyridyl and phenanthroline complexes

The preparation of lanthanide(III) phenanthroline and bipyridyl complexes $[Ln(phen)_2]Cl_3 \cdot 2H_2O$ and $[Ln(bipy)_2]Cl_3 \cdot 2H_2O$ (phen = 1,10-phenanthroline; bipy = 2,2'-bipyridine; Ln = Nd, Sm, Dy, Ho and Er) is described in chapter 3.

4.2.2 Chloride salts

An exactly measured quantity of Ln_2O_3 was dissolved in a concentrated solution of HCl. Repetitive evaporation of the solution and redissolving in water removed the excess of hydrogen chloride. Finally a neutral water solution with a known quantity of Ln(III) was obtained.

4.2.3 Dpa complexes

For the $Na_3[Ln(dpa)_3]$ complexes, pyridine-2,6-dicarboxylic acid (dipicolinic acid) is dissolved in a warm 0.2 mol/L NaOH solution. The pH must be around pH = 7 or 8. The resulting solution is further concentrated by evaporation of the water and the pH is measured again. Before cooling down, an equivalent quantity (Ln:dpa ratio 1:3) of the lanthanide salt is added. Small crystals appear after a few minutes. The precipitate was filtered, then washed several times with cold water and dried in a vacuum oven. The dried complexes were

characterized by CHN elemental analysis. The dipicolinate ligand crystallizes with lanthanides in a complex of D_3-symmetry.[16] The three tridentate dipicolinate molecules allow the lanthanide ion to obtain coordination number 9 and to saturate the first coordination sphere without the need of water molecules.

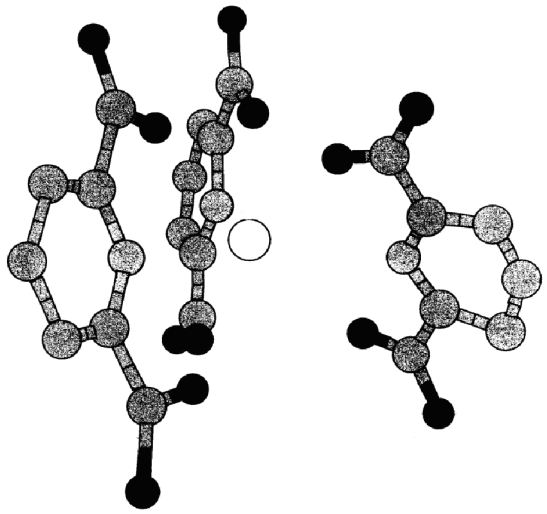

Figure 4.2: Crystal structure of the $Na_3[Ln(dpa)_3]$ Complex, Van Meervelt *et al.*[16]

4.3 Preparation of the PEG-silica sol-gels

The PEG-silica sol-gels were synthesized by hydrolysis and polymerization of the monomeric precursor tetramethylorthosilicate (TMOS, purchased from Fluka) with water and PEG-200 (purchased from Fluka).[5] First, a solution *A* was made by mixing 8 mL of TMOS with 2 mL of water containing hydrochloric acid or nitric acid to obtain pH = 2. This solution was stirred for 1 hour. In solution *B*, PEG was mixed with water or a buffered water solution in a 80% (w/w) composition. An equivalent quantity of Na_2HPO_4 and NaH_2PO_4 was used to make the buffer (pH = 6.33). The final solution *C* was prepared by mixing 8 mL of solution *A* with 40 mL of solution *B*. Stirring was continued for 20 min. A lanthanide complex can be added in this stage. 3 mL portions of solution *C* were poured in disposable PMMA (polymethylmethacrylate) UV-cuvettes. All volumes were exactly pipetted and the masses were exactly measured, because the lanthanide concentrations have to be known for the Judd-Ofelt analysis. Parafilm® was used to seal the cuvettes for direct measurement and aluminium foil was used for the cuvettes in the oven (50°C). The solutions gelled after a few hours. No higher heating temperature was used because otherwise the PMMA cuvettes would melt. The buffered PEG-silica sol-gel method was used for the dipicolinate, bipyridyl and phenanthroline complexes. When $LnCl_3$ was added to a neutralized sol-gel, lanthanide phosphates precipitated. Therefore pH = 2 was used for these samples. The influence of this lowered pH on the results was tested by comparing spectra at different pH but no differences were detected. Another experiment was done with different equivalents (1-20) of phenanthroline or bipyridyl added to a fixed lanthanide concentration. Exact amounts of ligand were added to a solution *B* containing a fixed concentration of Ln(III).

4.4 The lanthanide doped PEG-silica spectra

Absorption spectra were recorded at room temperature using a Shimadzu UV-3100 spectrophotometer. Three absorption spectra of each sample were recorded: one before gelation, one after 24 hours of drying at 50 °C and a third one after a month of drying at 50 °C. During this month of heat treatment the volume of the sol-gels shrunk further to between 85% and 95% of the starting volume. Also spectra of $[Ln(phen)_2]Cl_3$ and $[Ln(bipy)_2]Cl_3$ were recorded in solution *B* and in pure PEG-200. These complexes dissolve well in pure PEG-200.

4.4.1 Cluster formation

If cluster formation is present the calculated dipole strengths and the Judd-Ofelt parameters are not correct. This phenomenon was discussed in more detail in chapter 3. The linear behaviour of dipole strength versus concentration is given in figure 4.3. Again no deviations were detected. A concentration around 0.05 mol/L was chosen for the experiments to avoid solubility problems for the dipicolinate complexes. This concentration in combination with the 1 cm cell path length was enough to obtain reproducible parameters.

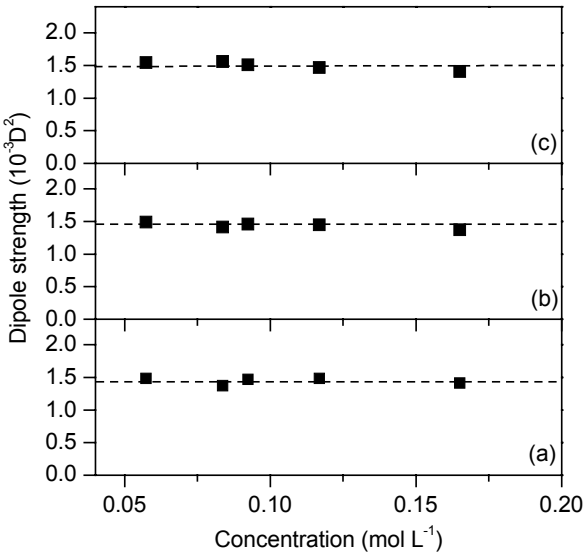

Figure 4.3: Dipole strength of three transitions: (a) $^4F_{5/2} \leftarrow {}^4I_{9/2}$, (b) $^4S_{3/2} \leftarrow {}^4I_{9/2}$ and (c) $^4G_{5/2} \leftarrow {}^4I_{9/2}$ of Nd(III) at different concentration in PEG-silica sol-gels.

4.4.2 $LnCl_3$ doped PEG-silica sol-gels

There was little difference between the spectra of the final solution *C* and the gelled samples that stayed in the oven for 24 hours. Small changes appeared only after a few weeks of drying, whereas in the pure silica sol-gel glasses the drying had more influence. Again only the hypersensitive transition showed an increase in intensity when the water evaporated.

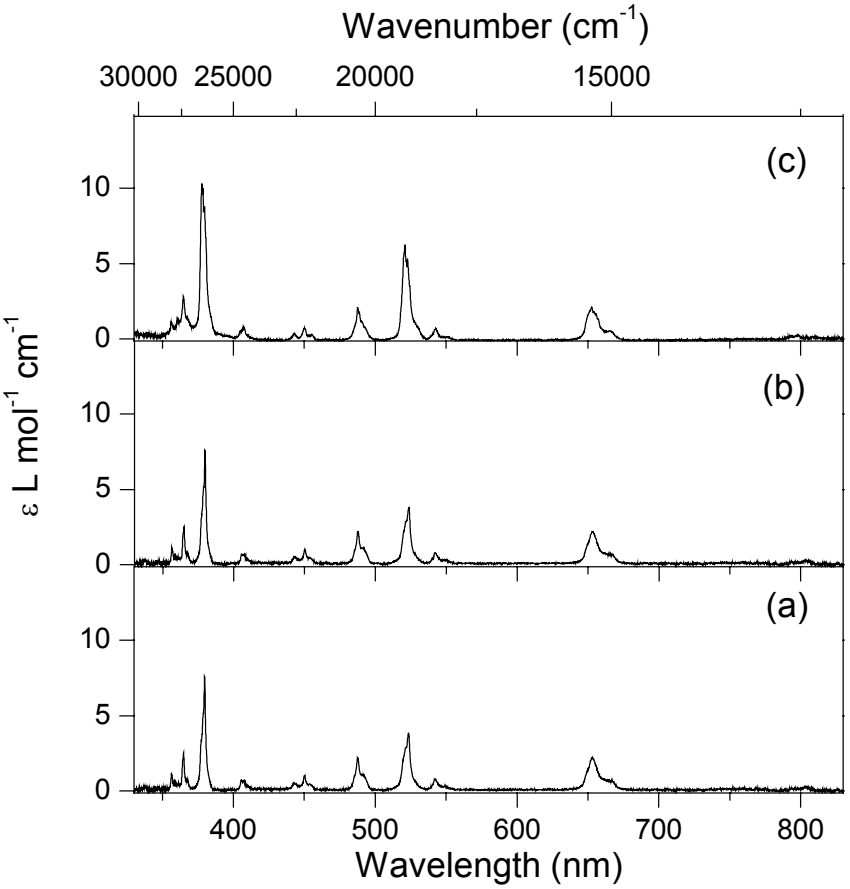

Figure 4.4: Absorption spectrum of a $ErCl_3$ doped PEG-silica sol-gel at room temperature before drying (a), after a heat treatment of 24 hours at 50 °C in air (b), after a heat treatment of one month in air at 50 °C (c).

4.4.3 $[Ln(phen)_2]Cl_3$ and $[Ln(bipy)_2]Cl_3$ doped PEG-silica sol-gels

1,10-Phenanthroline and especially bipyridyl dissolves well in these hybrid sol-gel materials. At very high concentrations crystals appear in the sol-gel after drying the samples with phenanthroline, this is shown in picture 4.5. For the measurements the concentrations of phenanthroline were kept below 0.4 mol/L to avoid this problem.

Figure 4.5: Picture of a $[Er(phen)_2]Cl_3$ doped sample at high concentration.

At first sight there was no difference in the spectra for the samples containing $[Ln(phen)_2]Cl_3$ or $[Ln(bipy)_2]Cl_3$ or even $LnCl_3$. Therefore, the influence of high concentrations of the ligands on the dipole strength, while the Nd(III) concentration was kept constant (0.02 mol/L), was investigated (figure 4.6-4.9). An extra amount of 1,10-phenanthroline influenced the dipole strength of the hypersensitive transition $^4G_{5/2} \leftarrow {}^4I_{9/2}$.

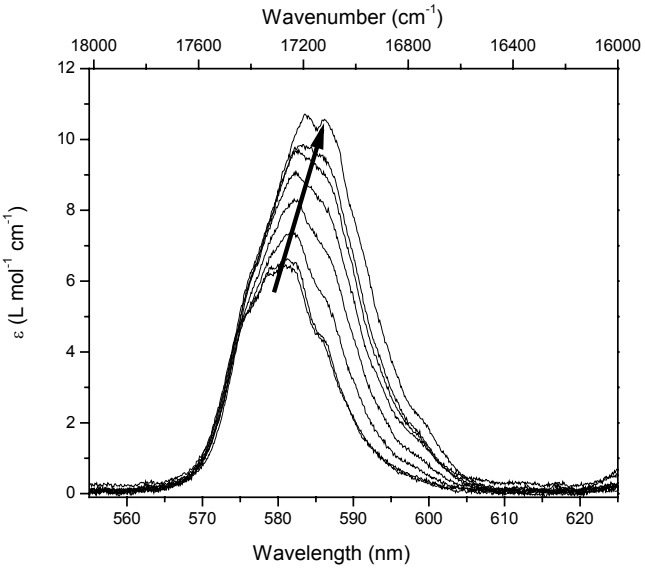

Figure 4.6: The intensity and shape of the $^4G_{5/2} \leftarrow {}^4I_{9/2}$ transition of Nd(III) changes by addition of 1,10-phenanthroline. The arrow indicates the increase in intensity from a 1:1 to a 1:20 ratio (Ln:phen).

For this transition the intensity nearly doubles. The intensity of the non-hypersensitive transitions does not change as a function of the 1,10-phenanthroline content. Only the appearance of the peaks and the fine structure changed. Other lanthanides show similar behaviour. To analyze the intensity increase, the dipole strength in function of the Nd:phen ration is shown in figure 4.8. There is a plateau in the dipole strength when the ligand concentration is twelve times the lanthanide concentration (0.02 mol/L). This behaviour is concentration dependent. At a lower lanthanide concentration (0.01 mol/L), the saturation point was at a higher ratio. There is a competition between the PEG and phenanthroline to coordinate the lanthanide ion.

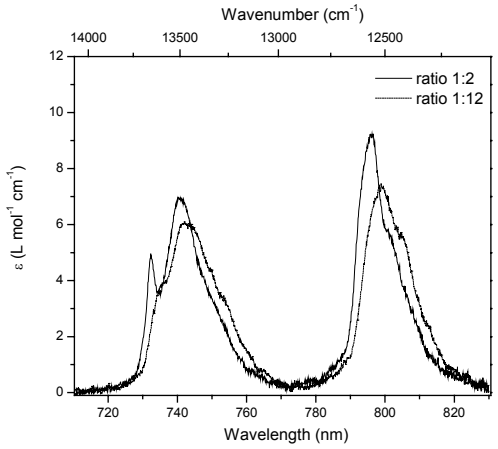

Figure 4.7: The shape of the $^4F_{5/2} \leftarrow {}^4I_{9/2}$ and $^4S_{3/2} \leftarrow {}^4I_{9/2}$ transitions of Nd(III) changes when adding 1,10-phenanthroline, at two ratios.

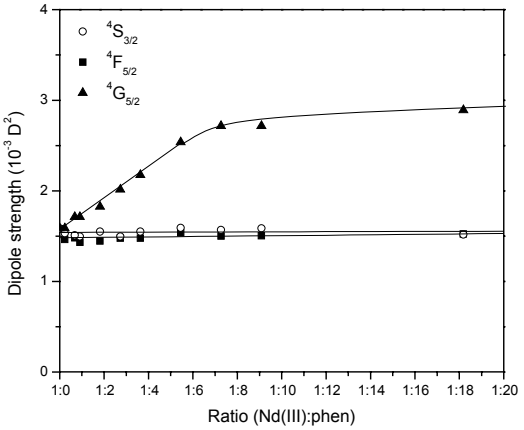

Figure 4.8: Dipole strength of three transitions: $^4F_{5/2} \leftarrow {}^4I_{9/2}$, $^4S_{3/2} \leftarrow {}^4I_{9/2}$ and $^4G_{5/2} \leftarrow {}^4I_{9/2}$ of Nd(III) (C = 0.02 mol/L) at different metal to 1,10-phenanthroline ratio (Nd(III):phen) in PEG-silica sol-gels after 1 day of drying.

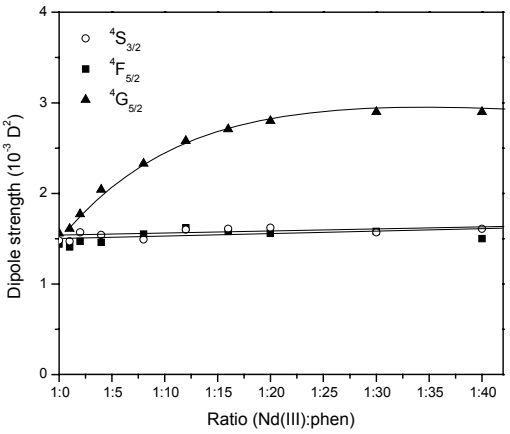

Figure 4.9: Dipole strength of three transitions: (a) $^4F_{5/2} \leftarrow {}^4I_{9/2}$, (b) $^4S_{3/2} \leftarrow {}^4I_{9/2}$ and (c) $^4G_{5/2} \leftarrow {}^4I_{9/2}$ of Nd(III) (C = 0.01 mol/L) at different metal to 1,10-phenanthroline ratio (Nd(III):phen) in PEG-silica sol-gels after 1 day of drying.

Little or no influence on the transition intensities was observed when the bipyridyl concentration was increased. The dipole strength did not change in function of the bipyridyl concentration in the concentration ranges that were tested (0.01-0.05 mol/L lanthanide). This difference in behaviour is caused by the higher solubility and the lower complexation capacity of bipyridyl. Bipyridyl is a more flexible molecule than 1,10-phenanthroline. In phenanthroline the rings are fixed and the nitrogens are in the ideal position to coordinate to the lanthanide ion. The two pyridine rings of bipyridyl can rotate with respect to one other. Complexation is not favourable in the most stable conformation where the nitrogens are positioned opposite to each other. Bipyridyl is better soluble in PEG than 1,10-phenanthroline, this also makes complexation of the lanthanide ions less favourable.

To obtain consistent calculations, samples with ratio 1:12 and concentration 0.02 mol/L were prepared for Judd-Ofelt analysis. For reference the results of samples with a ratio 1:2 were also calculated.

4.4.4 $Na_3[Ln(dpa)_3]$ doped PEG-silica sol-gels

This complex does not dissolve in acidic solutions, buffering the sol-gel was necessary. In figure 4.10, the absorption spectrum of the hypersensitive transition of Nd(III) are compared for two ligands. There is crystal-field fine structure in the spectrum of $Na_3[Nd(dpa)_3]$. Spectra of the other complexes are similar and do not show fine structure.

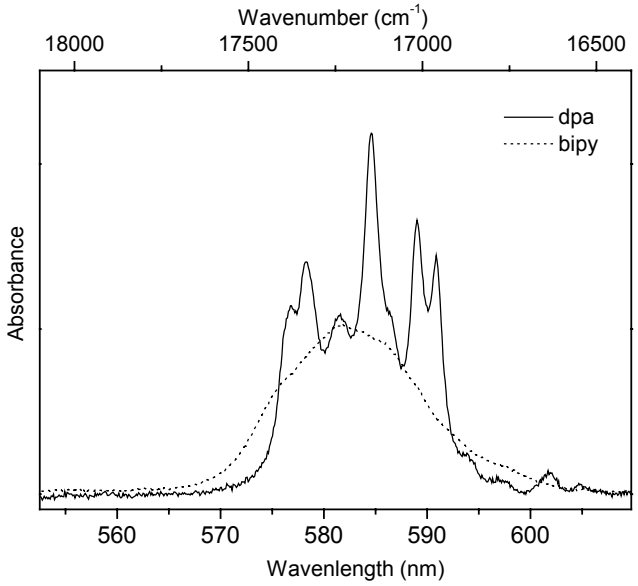

Figure 4.10: Comparison of the fine structure in the room temperature absorption spectrum of the hypersensitive transition $^4G_{5/2} \leftarrow {}^4I_{9/2}$ of $[Nd(bipy)_2]Cl_3$ and $Na_3[Nd(dpa)_3]$ in PEG-silica sol-gels.

The intensity of the transitions of the $Na_3[Ln(dpa)_3]$ complexes doped in PEG-silica sol-gels, even the hypersensitive transitions, does not vary much during drying. This was different in the other complexes. The evaporation of water has little effect on the lanthanides; this indicates that the lanthanide ions are well shielded by the dipicolinate ligands.

4.4.5 Judd-Ofelt analysis of the PEG-silica sol-gels

Hypersensitive absorption transitions in the glasses we have studied are $^4G_{5/2} \leftarrow {}^4I_{9/2}$ transition of Nd(III) (586 nm or 17300 cm^{-1}), the $^5G_6 \leftarrow {}^5I_8$ transition of Ho(III) (451 nm or 22100 cm^{-1}) and the $^2H_{11/2} \leftarrow {}^4I_{15/2}$ and $^4G_{11/2} \leftarrow {}^4I_{15/2}$ transitions of Er(III) (at 521 and 378 nm or 19200 cm^{-1} and 26400 cm^{-1} respectively). Sm(III) and Dy(III) also have hypersensitive transitions, but these transitions are situated at 1562 nm and 1298 nm where a broad absorption band of the PEG-silica sol-gel matrix is situated. It was impossible to calculate the Ω_2-parameter for these ions. No values are given for Dy(III) because the errors were too large. The parameters are in the order of 1 for the Ω_4 and 1.5 for the Ω_6.

No difference in parameter values is observed during the 24 hours of drying. Therefore only the results after 24 hours of drying are given in table 4.1-4.4. In this period the silica backbone was formed and the samples gelled. The long range-effects that influence Ω_4- and Ω_6-values are not changed. This is interesting because it indicates that the other components (water, PEG, ligand) are responsible for the transition intensities and not the silica.

Results of the complexes in pure PEG-200 and 80% PEG-200 (+ 20% water) confirm this statement because silica is absent in this case (table 4.5 p 91). The

Ω_λ-parameters in 80% PEG are similar to those for solution *C* and the gels dried for a short period. The Ω_λ-parameters of the pure PEG are similar to those of the long dried gels.

Table 4.1: Judd-Ofelt parameters of the Nd(III) doped PEG-silica sol-gels, before (1) and after a heat treatment of one month at 50°C (2).*

Ion	matrix	ligand**		Ω_2	Ω_4	Ω_6
Nd(III)	Si-PEG	dpa	(1)	4.2 ± 0.9	6.9 ± 1.5	11.1 ± 1.3
			(2)	3.9 ± 0.9	6.8 ± 1.5	11.5 ± 1.1
		phen 1:12	(1)	4.1 ± 0.7	5.9 ± 1.0	7.8 ± 0.5
			(2)	4.4 ± 1.3	6.1 ± 1.7	8.1 ± 0.9
		phen 1:2	(1)	2.2 ± 0.8	6.6 ± 1.1	8.3 ± 0.5
			(2)	2.8 ± 0.6	6.2 ± 1.0	7.9 ± 0.6
		bipy 1:12	(1)	1.6 ± 0.6	5.8 ± 0.9	7.7 ± 0.4
			(2)	2.4 ± 1.0	6.9 ± 1.2	7.8 ± 1.0
		bipy 1:2	(1)	1.2 ± 0.7	5.9 ± 1.0	7.8 ± 0.5
			(2)	2.7 ± 0.5	5.1 ± 0.7	6.5 ± 0.4
		chloride	(1)	0.7 ± 0.6	6.5 ± 0.7	7.7 ± 0.4
			(2)	2.3 ± 0.6	6.5 ± 0.8	7.3 ± 0.5

*All parameters are expressed in 10^{-20} cm^2.

** 1:12 means that the lanthanide to ligand ratio was 1 to 12

Table 4.2: Judd-Ofelt parameters of the Ho(III) doped PEG-silica sol-gels, before (1) and after a heat treatment of one month at 50°C (2).*

Ion	matrix	ligand**		Ω_2	Ω_4	Ω_6
Ho(III)	Si-PEG	dpa	(1)	6.4 ± 0.9	4.6 ± 1.4	5.0 ± 0.8
			(2)	6.6 ± 0.6	4.8 ± 0.9	5.4 ± 0.6
		phen 1:12	(1)	5.1 ± 0.7	5.5 ± 1.2	2.4 ± 0.5
			(2)	5.7 ± 0.8	4.9 ± 1.5	3.2 ± 0.6
		phen 1:2	(1)	3.4 ± 0.4	3.2 ± 0.6	3.2 ± 0.3
			(2)	3.9 ± 0.6	3.5 ± 0.9	3.8 ± 0.5
		bipy 1:12	(1)	2.8 ± 0.5	3.5 ± 0.8	3.7 ± 0.5
			(2)	3.7 ± 1.1	4.6 ± 1.5	4.1 ± 0.9
		bipy 1:2	(1)	1.6 ± 0.3	4.2 ± 0.5	2.7 ± 0.3
			(2)	3.3 ± 0.4	4.0 ± 0.7	2.3 ± 0.4
		chloride	(1)	1.4 ± 0.4	3.3 ± 0.4	3.4 ± 0.3
			(2)	4.1 ± 0.5	3.3 ± 0.8	3.6 ± 0.5

*All parameters are expressed in 10^{-20} cm^2.

** 1:12 means that the lanthanide to ligand ratio was 1 to 12

Table 4.3: Judd-Ofelt parameters of the Er(III) doped PEG-silica sol-gels, before (1) and after a heat treatment of one month at 50°C (2).*

Ion	matrix	ligand**		Ω_2	Ω_4	Ω_6
Er(III)	Si-PEG	dpa	(1)	6.5 ± 0.9	1.9 ± 1.2	3.2 ± 1.1
			(2)	6.7 ± 1.2	1.7 ± 1.0	4.0 ± 1.0
		phen 1:12	(1)	6.2 ± 0.5	1.7 ± 0.6	2.2 ± 0.4
			(2)	7.0 ± 1.2	1.8 ± 1.2	2.6 ± 1.0
		phen 1:2	(1)	3.3 ± 0.1	2.5 ± 0.2	1.4 ± 0.1
			(2)	5.2 ± 0.4	2.5 ± 0.5	1.4 ± 0.4
		bipy 1:12	(1)	4.2 ± 0.3	2.5 ± 0.3	2.1 ± 0.2
			(2)	4.7 ± 0.6	2.9 ± 0.7	2.5 ± 0.4
		bipy 1:2	(1)	3.2 ± 0.2	2.3 ± 0.3	1.6 ± 0.2
			(2)	5.1 ± 0.2	2.1 ± 0.3	1.5 ± 0.2
		chloride	(1)	2.3 ± 0.2	1.9 ± 0.3	1.5 ± 0.2
			(2)	5.5 ± 0.4	2.8 ± 0.6	2.1 ± 0.4

*All parameters are expressed in 10^{-20} cm^2.

** 1:12 means that the lanthanide to ligand ratio was 1 to 12

Table 4.4: Judd-Ofelt parameters of the Sm(III) doped PEG-silica sol-gels, before (1) and after a heat treatment of one month at 50°C (2).*

Ion	matrix	ligand**		Ω_2***	Ω_4	Ω_6
Sm (III)	Si-PEG	dpa	(1)	-	3.1 ± 0.8	6.8 ± 0.2
			(2)	-	3.5 ± 0.8	5.8 ± 0.3
		phen 1:12	(1)	-	5.3 ± 0.2	2.1 ± 0.2
			(2)	-	4.9 ± 0.5	1.2 ± 0.5
		phen 1:2	(1)	-	4.8 ± 0.2	2.1 ± 0.2
			(2)	-	4.1 ± 0.7	2.3 ± 0.3
		bipy 1:12	(1)	-	5.1 ± 0.2	2.1 ± 0.2
			(2)	-	4.9 ± 0.3	2.0 ± 0.3
		bipy 1:2	(1)	-	5.1 ± 0.2	1.6 ± 0.2
			(2)	-	6.0 ± 0.8	2.7 ± 0.4
		chloride	(1)	-	3.9 ± 0.3	1.9 ± 0.2
			(2)	-	4.1 ± 0.3	2.0 ± 0.2

*All parameters are expressed in 10^{-20} cm^2.

** 1:12 means that the lanthanide to ligand ratio was 1 to 12

*** These parameters could not be determined (see text).

The influence of the different ligands was studied. The spectra of $[Ln(bipy)_2]Cl_3$, $[Ln(phen)_2]Cl_3$ and $LnCl_3$ are very similar. On the other hand the spectrum and therefore the Ω_λ-parameters are totally different for $Na_3[Ln(dpa)_3]$. This is evident from table 4.1-4.4. Luminescence of phenanthroline and bipyridyl complexes of Tb(III) and Eu(III) in PEG-silica sol-gels was previously studied.[6] These organic ligands are used to improve luminescence yield via the antenna effect. This means that a part of the ligands has to be close enough to the lanthanide to transfer the excitation energy.[8]

Bipyridyl dissolves very well in PEG. But at high concentration (C > 0.4 mol/L) the phenanthroline complex crystallizes and there is no homogenous distribution of the lanthanide (figure 4.5). In table 4.1-4.4 little effect of complex formation is observed; the values are not much higher than those for $LnCl_3$ where the only interactions are ionic. This means that the ligands are close enough to the lanthanide to transfer energy at high concentration (C > 0.1 M bipy) but still do not bond strongly and are not able to influence the lanthanide ion much. Water and PEG dominate all the intensity parameters. Only at higher concentrations, 1,10-phenanthroline influences the hypersensitive transition of Nd(III) (figure 4.7). Beyond a metal-to-ligand ratio (Ln(III):ligand) 1:12, further addition of the ligand gives little change in dipole strength and a plateau is reached. The Judd-Ofelt parameters reach maximum values. It appears that the cation complexing capacity of PEG is too high in comparison to that of bipyridyl so that the bipyridyl ligand cannot efficiently compete with the PEG molecules for the lanthanide ion.

The parameters for the bipyridyl, phenanthroline and chloride complexes in pure silica sol-gels were discussed in chapter 3.[17,18] Because PMMA cuvettes were used in this study, the samples could not be heated to 100 °C as in chapter 3. It is therefore difficult to compare the final results. As the long-range parameters of the PEG-silica sol-gels are more determined by PEG than by the silica one can expect that the final parameters will be different. But in both cases the Ω_2-parameter value increases when water is removed.

As can be deduced from the parameter values and from figure 4.10, the dipicolinate complex molecule gives a totally different spectrum. The dipicolinate ligand crystallizes with lanthanides in a complex of D_3-symmetry.[16] According to model calculations of $Na_3[Ln(dpa)_3]$ (Ln = Nd, Ho or Er), or complexes with similar tridentate ligands like oxydiacetate in

aqueous solution, the most important contribution to the intensities of hypersensitive transitions in these ions can be correlated with the ligand polarizability.[19] Absorption and IR-luminescence of $Na_3[Nd(dpa)_3]$ has been studied in pure silica sol-gels.[20] No antenna effect was observed because the gap between energy levels of the ligand and the lanthanide ion is too large. The luminescence spectrum of $Na_3[Eu(dpa)_3]$ has also been studied in the past.[21] In present study other lanthanide complexes are doped in a PEG-silica sol-gel and Judd-Ofelt analysis has been done. The spectra of the $Na_3[Ln(dpa)_3]$ complexes (Ln = Nd, Sm, Dy, Ho, Er) in PEG-silica sol-gels still show some crystal-field fine structure and the Ω_λ-parameters differ from the other complexes. This clearly shows that dipicolinate is a better ligand than phenanthroline or bipyridyl. The Ω_2-parameters are higher than in the other systems. The tridentate dipicolinate ligand is also strong enough to shield the lanthanide from water. The Ω_4- and Ω_6-parameters are higher than those of the other ligands; the parameters are more determined by the low rigidity of the surrounding complex than by the rigidity of the PEG-silica matrix. This can be explained by efficient shielding over a long range.

Some general statements can be made for both the Ω_4- and Ω_6-parameters. The values for the lighter lanthanides are larger than those for the heavy lanthanides, with a minimum between Sm(III) and Dy(III). The radial integrals in the expressions of the Judd-Ofelt parameters decrease over the lanthanide series (no reliable Ω_λ-parameter could be determined for Eu(III), Gd(III) and Tb(III)).

Table 4.5: Judd-Ofelt parameters of different lanthanides in 80% PEG + 20% water (A) and 100% PEG (B).*

		Ω_2	Ω_4	Ω_6
Nd(III)	A	0.9 ± 0.8	6.5 ± 1.2	7.8 ± 0.7
	B	2.7 ± 0.7	5.8 ± 0.9	6.3 ± 0.5
Sm(III)	A	(**)	4.6 ± 0.4	1.9 ± 0.2
	B	(**)	5.9 ± 0.5	2.1 ± 0.3
Ho(III)	A	1.5 ± 0.5	3.3 ± 0.7	3.6 ± 0.5
	B	3.9 ± 0.6	3.3 ± 0.9	3.4 ± 0.5
Er(III)	A	2.9 ± 0.4	1.5 ± 0.6	1.6 ± 0.4
	B	4.8 ± 0.4	1.5 ± 0.5	1.3 ± 0.3

*All parameters are expressed in 10^{-20} cm^2.

** These parameters could not be determined (see text).

4.5 Conclusion

Monolithic PEG-silica hybrid sol-gels were made at a neutral pH. The sol-gels were doped with $[Ln(bipy)_2]Cl_3$, $[Ln(phen)_2]Cl_3$, $Na_3[Ln(dpa)_3]$ and $LnCl_3$ (bipy = bipyridyl, 2,2'-bipyridine, phen = 1,10-phenanthroline, dpa = dipicolinate, Ln = Nd, Sm, Dy, Ho, Er) complexes. The Judd-Ofelt theory has been used to compare the intensities of lanthanide complexes in sol-gel materials. The PEG adds flexibility to the sol-gel glass but is also able to form complexes with lanthanide ions. The Ω_2-parameters values are small in PEG. When synthesising hybrid materials, it is important to use ligands that form stable complexes with lanthanide ions. It is also important to choose an organic phase for the hybrid materials that has less complex formation capacity than the ligands in the lanthanide complex. Ligands like 1,10-phenanthroline and 2,2'-bipyridyl are not strong enough to remove the PEG molecules from the first coordination sphere of the lanthanide ions. On the other hand, dipicolinate ligands bind strongly to lanthanide ions and shield the lanthanides from PEG and water molecules. The spectrum does not change much during drying.
These PEG-silica materials are easily made and cracking is absent, long drying times are still necessary.

REFERENCES

[1] Brinker, C. J. and Scherer, G. W., *Sol-Gel Science*, Academic Press, San Diego **1990**.

[2] Sanchez, C. and Ribot, F., *New. J. Chem.*, 1994, **18**, 1007.

[3] Sanchez, C., Soler-Illia, A. A., Ribot, F., Lalot, T., Mayer, C. R., and Cabuil, V., *Chem. Mater.*, 2001, **13**, 3061.

[4] Bekiari, V., Lianos, P., and Judenstein, P., *Chem. Phys. Lett.*, 1999, **307**, 310.

[5] Bekiari, V., Pistolis, G., and Lianos, P., *J. Non-Cryst. Solids*, 1998, **226**, 200.

[6] Bekiari, V., Pistolis, G., and Lianos, P., *Chem. Mater.*, 1999, **11**, 3189.

[7] Bekiari, V. and Lianos, P., *Adv. Mater.*, 2002, **10**, 1455.

[8] Chuai, X. H., Zhang, H. J., Li, F. S., Wang, S. B., and Zhou, G. Z., *Mater. lett.*, 2002, **46**, 244.

[9] Ribeiro, S. J. L., Dahmouche, K., Ribeiro, C. A., Santilli, C. V., and Pulcinelli, S. H., *J. Sol-Gel Sci. Technol.*, 1998, **13**, 427.

[10] Bekiari, V., Lianos, P., Stangar, U. L., Orel, B, and Judenstein, P., *Chem. Mater.*, 2000, **12**, 3095.

[11] Brik, M. E., Titman, J. J., Bayle, J. P., and Judenstein, P., *J. Polymer. Sci. B*, 1996, **34**, 2533.

[12] Carlos, L. D. and Sa Ferreira, R. A., *Phys. Rev. B*, 1999, **60**, 10 042.

[13] Dahmouche, K., Carlos, L. D., de Zea Bermudez, V., Sa Ferreira, R. A., Santilli, C. V., and Craievich, A. F., *J. Mater. Chem.*, 2001, **11**, 3249.

[14] de Zea Bermudez, V., Carlos, L. D., Duarte, M. C., Silva, M. M., Silva, C. J. R., Smith, M. J., Assunçao, M., and Alcacer, L., *J. Alloys Compds.*, 1998, **275-277**, 21.

[15] Silva, M. M., de Zea Bermudez, V., Carlos, L. D., Passos de Almeida, A. P., and Smith, M. J., *J. Mater. Chem.*, 1999, **9**, 1735.

[16] Van Meervelt, L., Binnemans, K., Van Herck, K., and Görller-Walrand, C., *Bull. Soc. Chim. Belg.*, 1997, **106**, 25.

[17] Driesen, K., Görller-Walrand, C., and Binnemans, K., *J. Mater. Sci. Eng. C*, 2001, **18**, 255.

[18] Driesen, K., Lenaerts, F., Binnemans, K., and Görller-Walrand, C., *Phys. Chem. Chem. Phys.*, 2002, **4**, 552.

[19] Devlin, M. T., Stephens, E. M., Richardson, F. S., Van Cott, T. C., and Davis, S. A., *Inorg. Chem.*, 1988, **27**, 1517.

[20] Lai, D. C., Dunn, B., and Zink, J. I., *Inorg. Chem.*, 1996, **35**, 2152.

[21] Huskowska, E., Gawryszewska, P., Legendziewicz, J., Maupin, C. L., and Riehl, J. P., *J. Alloys Compds.*, 2000, **303-304**, 325.

5.1 Introduction

Recently much attention has been paid to the research of *near-infrared luminescence* (NIR-luminescence) of lanthanide ions. Several lanthanides show luminescence in the telecommunication low-loss NIR-regions of silica (1250-1350 nm, 1450-1600 nm and to a lesser extent 900-1100 nm). Candidates for luminescence in these regions are the trivalent Nd, Pr, Sm, Er, Ho, Dy and Yb ions. Some important NIR-luminescence transitions are given in table 5.1. The optical properties of Nd(III) doped glass obtained by the sol-gel method were first studied by Pope *et al.*.[1] These authors reported a method of preparation for silica glass which contained Nd(III). Fujiyama *et al.* investigated the luminescence properties of Nd(III) in SiO_2 and SiO_2-Al_2O_3 glass made by the sol-gel method.[2]

The observation of NIR-luminescence is hampered by quenching of the excited states by vibronic coupling with the vibration of hydroxyl groups (in Si-OH and H_2O). In wet xerogels the concentration of hydroxyl groups is high. The most common method to decrease the quenching is to dry the sol-gel materials at high temperatures (> 900°C). This method was successfully demonstrated for sol-gel processed optical fibers and thin films.[3,4,5] Different compositions (e.g. SiO_2, SiO_2-TiO_2, SiO_2-Al_2O_3, SiO_2-TiO_2-P_2O_4) in addition to silica have been used to enhance the luminescence.[6,7,8] By heating, annealing and sintering all water is evaporated and most of the Si-OH or M-OH (M = transition metal) groups have been removed by condensation reactions.

Table 5.1: Common lanthanide NIR-luminescence transitions and their wavelength.

Ion	Transition	Wave-length (nm)	Transition	Wave-length (nm)
Nd(III)	$^4F_{3/2} \rightarrow {}^4I_{9/2}$	880	$^4F_{3/2} \rightarrow {}^4I_{13/2}$	1320
	$^4F_{3/2} \rightarrow {}^4I_{11/2}$	1064	$^4F_{3/2} \rightarrow {}^4I_{15/2}$	1945*
Pr(III)	$^3P_0 \rightarrow {}^3F_4$	908*	$^1G_4 \rightarrow {}^3H_5$ and $^1D_2 \rightarrow {}^1G_4$	1326, 1364, 1406, 1460*
	$^1D_2 \rightarrow {}^3H_5$	1014*	$^1G_4 \rightarrow {}^3F_2$ and $^3H_6 \rightarrow {}^3H_4$	2300*
Sm(III)	$^4G_{5/2} \rightarrow {}^6H_{15/2}$	896*	$^4G_{5/2} \rightarrow {}^6F_{9/2}$	1162*
	$^4G_{5/2} \rightarrow {}^6F_{5/2}$	963*	$^4G_{5/2} \rightarrow {}^6F_{11/2}$	1376*
	$^4G_{5/2} \rightarrow {}^6F_{7/2}$	1022*		
Dy(III)	$^4F_{9/2} \rightarrow {}^6H_{5/2}$	934	$^4F_{9/2} \rightarrow {}^6F_{3/2}$	1294
	$^4F_{9/2} \rightarrow {}^6F_{7/2}$	1000	$^4F_{9/2} \rightarrow {}^6F_{1/2}$	1384
	$^4F_{9/2} \rightarrow {}^6F_{5/2}$	1170		
Er(III)	$^4S_{3/2} \rightarrow {}^4I_{13/2}$	847*	$^4I_{13/2} \rightarrow {}^4I_{15/2}$	1530
	$^4I_{11/2} \rightarrow {}^4I_{15/2}$	977*	$^4I_{11/2} \rightarrow {}^4I_{13/2}$	2719*
	$^4S_{3/2} \rightarrow {}^4I_{11/2}$	1219*		
Ho(III)	$^5S_2 \rightarrow {}^5I_6$	1015*	$^5S_2 \rightarrow {}^5I_4$	1953*
	$^5I_6 \rightarrow {}^5I_8$	1154, 1191*	$^5I_7 \rightarrow {}^5I_8$	2039*
	$^5S_2 \rightarrow {}^5I_5$	1381*	$^5I_6 \rightarrow {}^5I_7$	2848*
Yb(III)	$^2F_{5/2} \rightarrow {}^2F_{7/2}$	977		

* Values in fluorozirconate glass.[9] Other values were found in PEG-silica sol-gels.

A disadvantage of such lanthanide-doped glasses is the low absorbance of the lanthanides. The antenna effect of organic ligands cannot be used because the sensitizers decompose at the high drying temperatures.

Another method to avoid luminescence quenching is to shield the metal ion from the deactivating groups.[e.g.[10]] Luminescence of neodymium in sol-gel monoliths processed at room temperature was demonstrated by Lai *et al.* for the tris(dipicolinato)neodymate(III) complex $Na_3[Nd(dpa)_3]$.[11] The absorption properties and Judd-Ofelt theory for this complex was already discussed in chapter 4. In that paper by Lai *et al.*, the sol-gel material used was a pure silica gel. In this work, NIR-luminescence is presented for $Na_3[Ln(dpa)_3]$ (with Ln = Nd, Er, Ho, Pr, Dy) in PEG-silica sol-gels. The dipicolinate molecule absorbs light around 260 nm. The positions of the ligand energy levels are too high for energy transfer to the lanthanide energy levels, the antenna effect does not work for Nd(III), Er(III), Dy(III), Pr(III), Ho(III) and Sm(III).

Calcein is a successful water soluble sensitizer for NIR-luminescent lanthanide ions. The triplet levels are situated around 500 nm. The Yb(III) complex has been used as a NIR-luminescent label in fluoroimmunoassay.[12] Silica sol-gel coatings doped with calcein were prepared by Garcia *et al.* for use as pH sensor.[13] The luminescence of calcein is pH-dependent. Here the NIR-luminescence of PEG-silica sol-gels doped with lanthanide-calcein complexes are studied.

5.2 Preparation of the samples

5.2.1 Dipicolinate complex

The preparation of dipicolinate complexes is described in chapter 4.

5.2.2 Calcein complex

Calcein is a ligand combining a fluorescein group and an EDTA group.
Two isomers can be purchased: *4',5'-bis[N,N-bis(carboxymethyl) aminomethyl]-fluorescein* (noted as calc45) and *2',7'-bis[N,N-bis(carboxymethyl)aminomethyl]-fluorescein* (noted as calc27). Calc45 was purchased from Molecular Probes, Inc.. The calc27 was purchased from Fluka. Calcein forms water soluble 1:1 complexes with trivalent lanthanides. The stability of the calc45 complex is high (figure 5.2).[14] The *N*,*N*-bis(carboxymethyl)aminomethyl groups are very flexible and the calc27 isomer can also form complexes with calcium or lanthanide ions and is therefore used as an indicator. The complexation by calc27 is not as favorable as in calc45. Dimerization by linking a lanthanide ion to two *N*,*N*-bis(carboxymethyl)aminomethyl groups of different ligands is possible and cannot be excluded.
In contrast to previous methods, no pure solid complex was prepared to avoid losses of the very expensive ligands. Instead solutions containing an exact amount of ligand and lanthanide were prepared. Fresh solutions were directly

used in the preparation of the sol-gels. The solutions were prepared by dissolving equimolar amounts of the ligand and the lanthanide ion in a solution containing a triethylammoniumacetate (TEAAc) buffer. The TEAAc concentration was 0.1 mol/L and pH 8. Adding the metal ion to the solution quenches the luminescence of the ligand as the complex is formed.

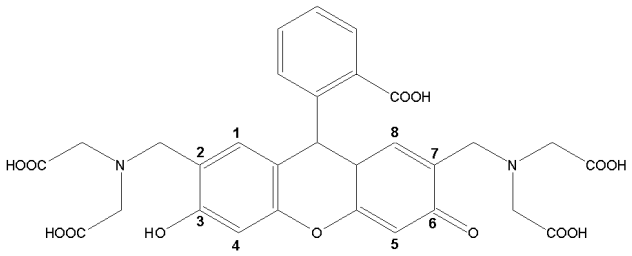

(a)

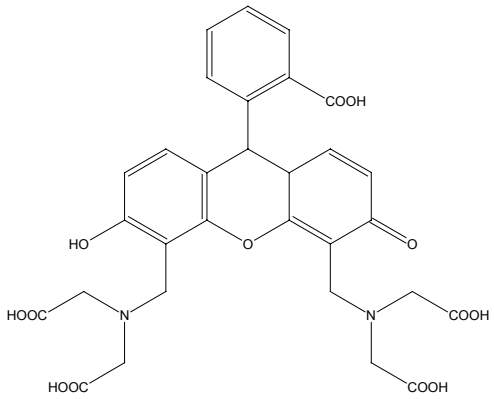

(b)

Figure 5.1: Structure of calcein (a) 2',7'-bis[*N*,*N*-bis(carboxymethyl)aminomethyl]fluorescein or calc27 (b) 4',5'-bis[*N*,*N*-bis(carboxymethyl)aminomethyl]fluorescein or calc45.

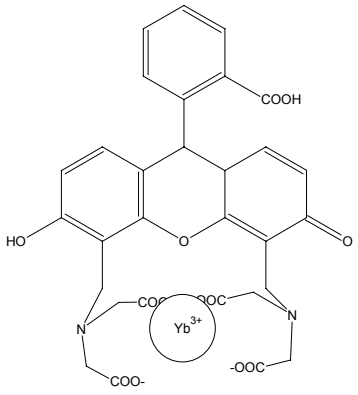

Figure 5.2: Structure of the Yb(calc45) complex.

5.3 Preparation of the PEG-silica sol-gels

5.3.1 Introduction

This type of sol-gel was used because the preparation is very fast and the pH can be adjusted to neutral pH. Samples can be poured into a microcuvette. This is very convenient when luminescence intensities have to be compared. The disk-like silica sol-gel glasses are more difficult to position in the spectrofluorimeter.

Silica sol-gel coatings doped with calcein were prepared by Garcia *et al.* for use as pH sensor.[13] The luminescence of calcein is pH dependent. The authors describe a procedure where the thin film samples were prepared from: TMOS,

water (pH = 2, HCl) and methanol in a 1:4:8 molar ratio. The film was doped with 2 wt.% calcein. The lanthanide complexes do not dissolve in such an acid environment.

5.3.2 $Na_3[Ln(dpa)_3]$ doped PEG-silica sol-gels

The synthesis of the dipicolinate-doped sol-gels is described in chapter 4.

5.3.3 [Ln(calc)] doped PEG-silica sol-gels

These doped sol-gels were not prepared by dissolving a dried complex in the starting solutions. A buffered solution containing 1.10^{-3} mol/L of the complex was prepared. The PEG-silica sol-gels were synthesized by hydrolysis and polymerization of the monomeric precursor tetramethylorthosilicate (TMOS, purchased from Fluka) with water and PEG-200 (purchased from Fluka).[15] First, a solution *A* was made by mixing 8 mL of TMOS with 2 mL of water containing hydrochloric acid or nitric acid to obtain pH = 2. This solution was stirred for 1 hour. For solution *B*, 0.50 mL of the buffered complex solution was mixed with 1.50 mL of destilled water and 8.00 g of PEG-200. The final solution *C* was prepared by mixing 1 mL of solution *A* with 5 mL of solution *B*. Stirring was continued for 20 min. 2 mL portions of solution *C* were poured in disposable PMMA (polymethylmethacrylate) UV-microcuvettes. All volumes were exactly pipetted. Parafilm® was used to seal the cuvettes for direct measurement and aluminium foil was used for the cuvettes in the oven (50°C). The solutions gelled after a few hours.

5.4 The lanthanide NIR-spectra

5.4.1 $Na_3[Ln(dpa)_3]$ doped PEG-silica sol-gels

The dipicolinate molecule is strongly bonded to the lanthanide ions. This was discussed in more detail in chapter 4. The NIR-luminescence was tested for several lanthanide ions. The first candidate was Nd(III). This ion has a strong luminescence at 1064 nm. Lai *et al.* published the luminescence of this complex in a pure silica glass with a drying time of more than 11 weeks.[11] In figure 5.3 the luminescence of $Na_3[Nd(dpa)_3]$ in a PEG-silica sol-gel is presented. The samples gelled in a few hours, were dried for one month and were not degassed prior to the measurement.

For $Na_3[Eu(dpa)_3]$ doped silica glass the ligand excitation can be used because the energy levels of europium ($^5L_6$ multiplet) that are used to pump the luminescence are situated around 390 nm.

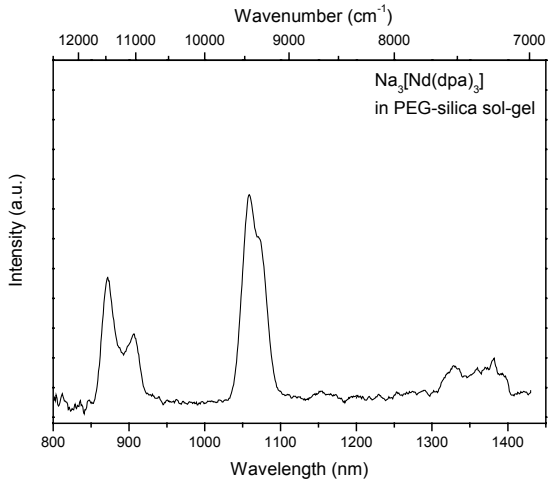

Figure 5.3: NIR-luminescence for $Na_3[Nd(dpa)]_3$ in a PEG-silica sol-gel.

Here a Xe-arch lamp is used to excite the Nd(III) at 580 nm, whereas Lai *et al.* used a Kr ion laser. Direct excitation in the lanthanide energy levels ($^4G_{5/2} \leftarrow {}^4I_{9/2}$) was used because the ligand energy levels (~ 260 nm) are too high for most NIR-luminescent lanthanides to use the antenna effect. $Na_3[Dy(dpa)]_3$ showed NIR-luminescence in a PEG-silica sol-gel by direct excitation at 390 nm (figure 5.4). NIR-luminescence was also tested for $Na_3[Ln(dpa)_3]$ with Ln = Pr, Sm, Er, Ho and Yb. The Pr, Sm, Er and Ho complexes did not show NIR-luminescence.

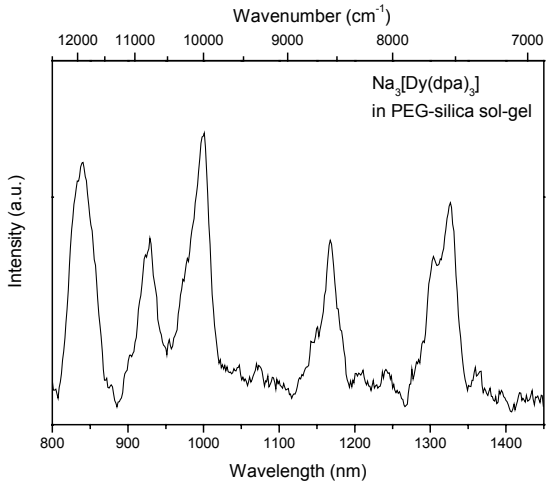

Figure 5.4: NIR-luminescence for $Na_3[Dy(dpa)]_3$ in a PEG-silica sol-gel (excited at 390 nm).

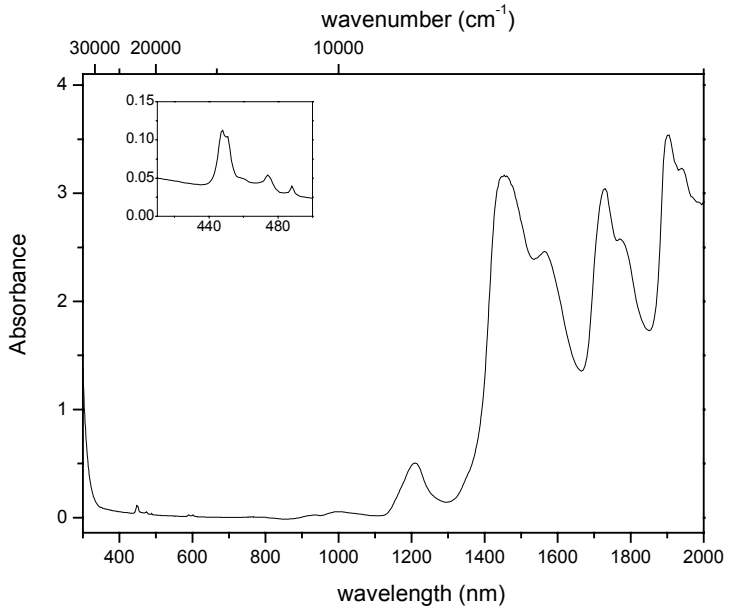

Figure 5.5: Absorbance spectrum of the $Na_3[Pr(dpa)_3]$. A detail of the $^3P_{0,1,2} \leftarrow {}^3H_4$ and $^1I_6 \leftarrow {}^3H_4$ transitions of Pr(III) is shown.

A possible explanation is that these lanthanide ions have intense transitions in the spectrum where the present water molecules or Si-OH vibration overtones can absorb or quench the luminescence. The absorption spectrum of $Na_3[Pr(dpa)_3]$ is displayed in figure 5.5. Intense and broad absorption bands appear in the NIR-region of all the PEG-silica sol-gels.

An excitation mechanism different from the antenna effect is possible for Yb(III), as was already explained in the first chapter. Yb(III) has a low reduction potential, -1.05 V versus the normal hydrogen electrode compared to an average of -3 V for most other lanthanides. If there is *ligand-to-metal charge transfer* (LMCT) the charge recombination (ligand$^+$-Yb(II) to ligand-Yb(III)*) leaves Yb(III) in an excited state.[16] The mechanism is shown in

figure 5.6. Although the ligand energy levels are far above the energy levels of Yb(III), situated at 977 nm, an intense transition is observed (figure 5.7). Excitation at 300 nm was used.

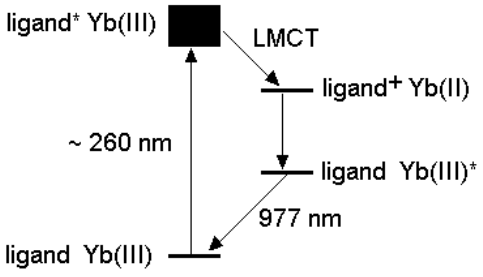

Figure 5.6: Yb(III) luminescence mechanism.

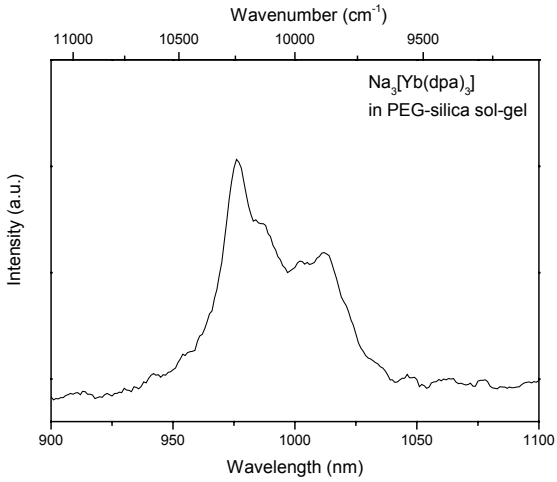

Figure 5.7: NIR-luminescence for $Na_3[Yb(dpa)]_3$ in a PEG-silica sol-gel (excited at 300 nm).

5.4.2 [Ln(calc)] doped PEG-silica sol-gels

Advantage of the dipicolinate molecule is an excellent shielding of the lanthanide ion, avoiding quenching by the abundant OH vibrations. The three tridentate dipicolinate molecules allow the lanthanide ion to obtain coordination number 9 and to saturate the first coordination sphere without the need of water molecules. NIR-luminescence can be observed. However the energy levels of dipicolinate are too far in the UV to sensitize lanthanide ions, except Yb(III). This is a major disadvantage. Therefore other water-soluble complexes were searched that can act as an antenna to sensitize the NIR-luminescence of lanthanide ions and at the same time shield the lanthanide from the surroundings. It was demonstrated by Werts *et al.* that lanthanide-calcein complexes of Yb(III) and Nd(III) show good luminescence in water.[14,17,18] Therefore these ligands were ideal if they dissolve in a sol-gel matrix. Calcein (4',5'-bis[*N*,*N*-bis (carboxymethyl)aminomethyl]fluorescein or 2',7'-bis[*N*,*N*-bis(carboxymethyl) aminomethyl]fluorescein) forms water soluble 1:1 complexes with calcium. Calcein is commercially available. This ligand is used as a fluorescent indicator for calcium, hence its name. The ionic radius of calcium resembles the radius of the trivalent lanthanides. The binding site for the lanthanide ion is closely situated to the fluorescein chromophore. Formation constants of the 1:1 complexes at pH = 8 are around 1.10^{12}.[19] The stability of the complexes is less than that of lanthanide ion-EDTA complexes but still high. Judd-Ofelt parameters could not be calculated because the intensity is too low. There is also a broad absorption band of the ligand around 485 nm that prohibits detection of lanthanide absorption (f-f transitions).

Addition of trivalent lanthanide ions to a solution containing calcein quenches the fluorescence of the ligand. This is due to enhancement of intersystem

crossing by the paramagnetic and the heavy atom effect (enhanced spin-orbit coupling).[20,21] By enhanced spin-orbit coupling the wavefunction of the ligand singlet and triplet levels do not remain pure singlet or triplet wavefunctions. A part of the singlet wavefunctions is mixed into that of the triplet wavefunction and vice versa, therefore the triplet level character achieved some singlet character. The absorption spectra of the complexes are slightly different for each lanthanide ion.[14,18]

The concentration of the calcein complex in the not-dried sol-gel is around 5.10^{-5} mol/L whereas the concentration of the dipicolinate complexes was much higher (1.10^{-3} mol/L). This concentration is too low for direct excitation of the lanthanide (e.g. 580 nm for Nd(III)). The lanthanide f-f transitions are very weak in comparison with the ligand absorption bands (figure 5.8). The broad intense peak at 485 nm is due to calcein.

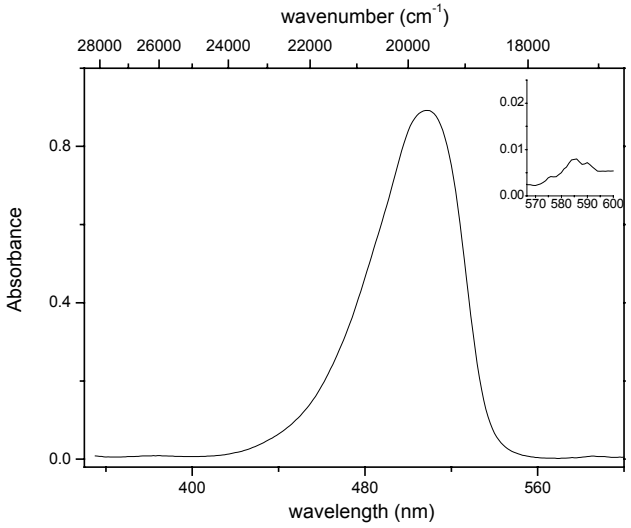

Figure 5.8: Absorption spectrum of [Nd(calc45)].
A detail of the $^4G_{5/2} \leftarrow {}^4I_{9/2}$ transition is shown.

A Xe-arch lamp was used to excite the ligand. The samples were not degassed prior to the measurement. The luminescence spectra of the [Nd(calc)] complexes before and after drying are shown in figure 5.9. The transitions were very intense despite the low concentration of the neodymium. The antenna effect works and the complex did not dissociate in the sol-gel matrix.

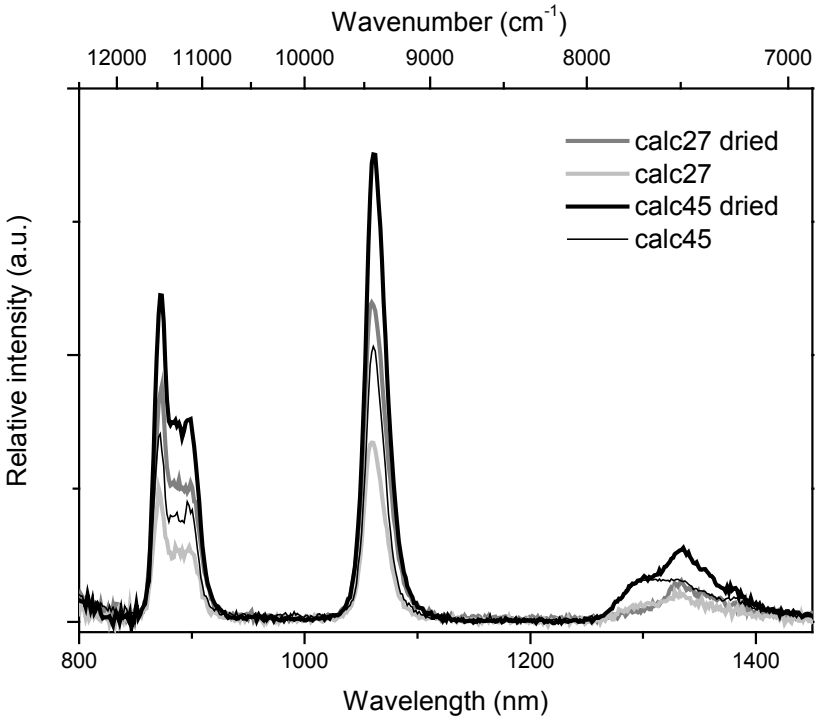

Figure 5.9: NIR-luminescence of [Nd(calc27)] and [Nd(calc45)] before and after drying in a PEG-silica sol-gel.

The intensity of the Xe-arch lamp varies over the region 450-520nm. To compare intensities of the two isomeric complexes [Nd(calc27)] and [Nd(calc45)] the ligands were excited at a position where the ligands showed the same or similar absorbance, but lower than 0.5 Absorbance units. The

spectra were corrected for the small differences in absorption and the emission correction file of the spectrofluorimeter.

The intensity of the [Nd(calc45)] is higher than that of the [Nd(calc27)] complex. A possible explanation is the better coordination to the lanthanide. Especially the $^4F_{3/2} \rightarrow {}^4I_{13/2}$ transition at 1340 nm is more intense (table 5.2). This transition is at a longer wavelength and therefore more susceptible to quenching of OH vibrations.

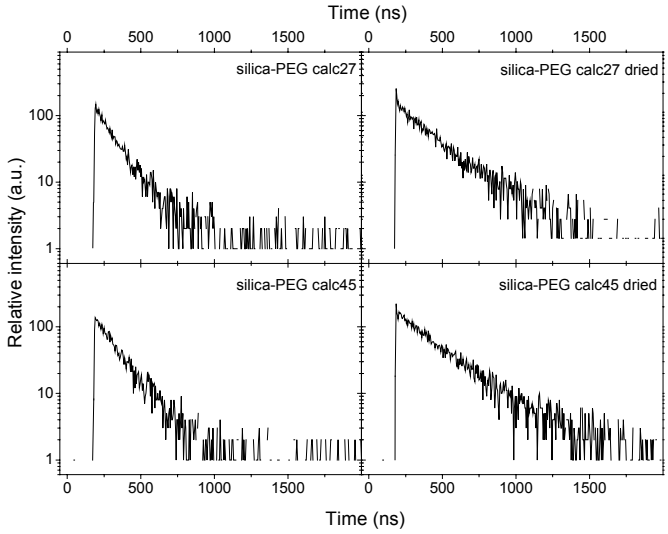

Figure 5.10: NIR-luminescence lifetime of the transition at 1064 nm of [Nd(calc)] in PEG-silica sol-gel.

NIR-luminescence lifetime of the transition at 1064 nm was tested (figure 5.10 and table 5.2). These results confirm the results in figure 5.9. The lifetime is longer in the dried sol-gels because the quenching by water is decreased. The difference between the calc45 and calc27 complexes is due to better shielding.

Table 5.2: Approximate relative intensity for the Nd(calc) complexes.

Transition	λ (nm)	I(calc27)	I(calc45)	I(calc27) dry	I(calc45) dry
$^4F_{3/2} \rightarrow {}^4I_{9/2}$	800	1	1.4	1.9	2.5
$^4F_{3/2} \rightarrow {}^4I_{11/2}$	1064	1	1.4	1.9	2.5
$^4F_{3/2} \rightarrow {}^4I_{13/2}$	1340	1	1.8	1.3	2.8

Table 5.3: Luminescence lifetime of the Nd(III) transition at 1064 nm.

Sample	τ (ns)
Nd27sol	124 ± 4
Nd27dry	222 ± 6
Nd45sol	139 ± 4
Nd45dry	280 ± 4

Yb(III) is a special case when NIR-luminescence is studied. The ion has only one absorption peak around 977 nm. The luminescence is also observed at 977 nm (resonance luminescence, no Stokes shift). Photosensitized near infrared luminescence of Yb(III) occurs mainly via an internal redox process.[16] The light absorbed by calcein can be transferred to Yb(III) as demonstrated by Werts *et al.*.[12] The Yb(III) complex has been used as a NIR-luminescent label in fluoroimmunoassay. This intense luminescence can also be observed in the PEG-silica sol-gel (figure 5.11).

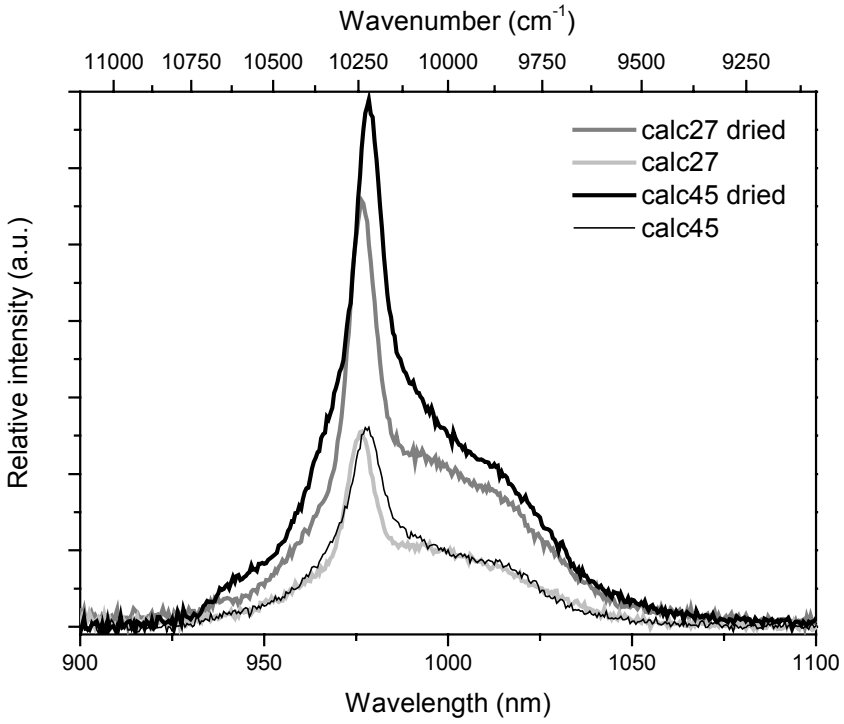

Figure 5.11: NIR-luminescence of [Yb(calc27)] and [Yb(calc45)] before and after drying PEG-silica sol-gel.

Table 5.4: Approximate relative intensity for the Yb(calc) complexes.

Transition	λ (nm)	I(calc27)	I(calc45)	I(calc27) dry	I(calc45) dry
$^2F_{5/2} \rightarrow {}^2F_{7/2}$	977	1	1.1	2.2	2.8

The transition is more intense in the calc45 complex in comparison with the calc27 complex before drying and after drying. NIR-luminescence lifetime of

the transition at 977 nm was tested (figure 5.12 and table 5.5). The lifetime is longer in the dried sol-gels because the quenching by water is decreased. The difference between the calc45 and calc27 complexes is due the better shielding.

Table 5.5: Luminescence lifetime of the Yb(III) transition at 977 nm.

Sample	τ (ns)
Yb27sol	1760 ± 20
Yb27dry	3215 ± 25
Yb45sol	1832 ± 16
Yb45dry	3720 ± 20

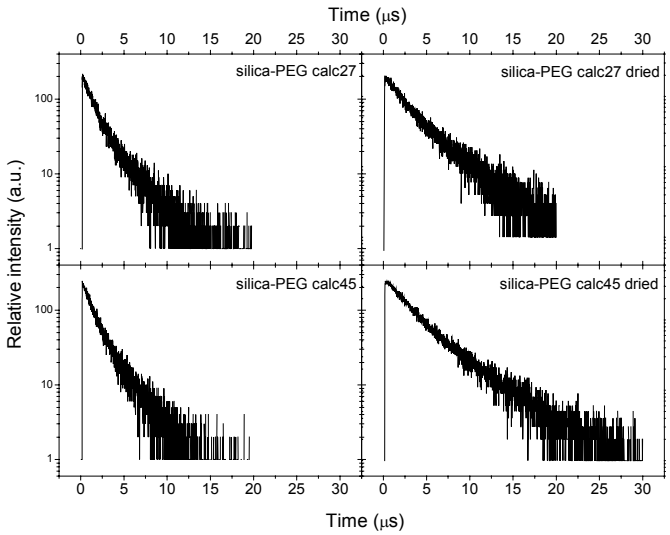

Figure 5.12: NIR-luminescence lifetime of the transition at 677 nm of the wet and dried Ybcalc complexes in PEG-silica sol-gel.

The most interesting lanthanide for NIR-luminenscence is Er(III). The transition at 1530 nm is at the right position for telecom applications (erbium doped fiber amplifiers). This transition was not observed in the dipicolinate complex. Here a Xe-arch lamp was used to obtain the spectrum in figure 5.13. Although the intensity is very low, a transition can be observed at 1525 nm. This is remarkable because no laser was used and the sample was not dried. The difference between the two isomers is not calculated because the intensity was too low to make a good comparison.

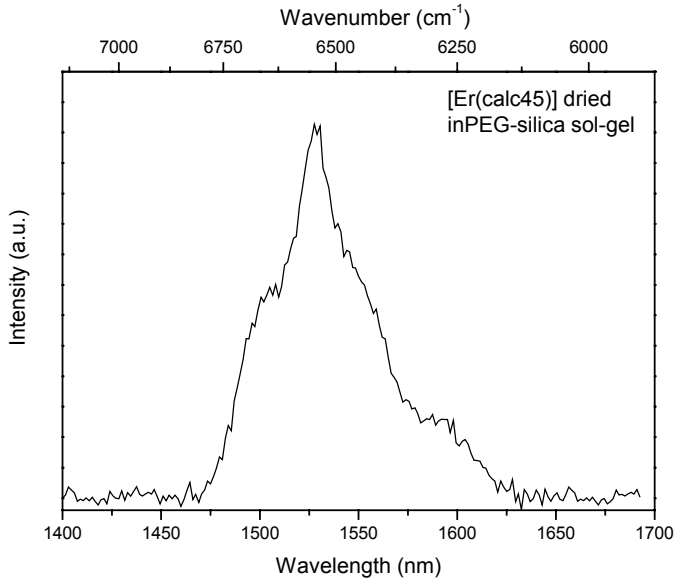

Figure 5.13: Typical NIR-luminescence of Er(calc)
in a PEG-silica sol-gel at 1530 nm.

Other lanthanide-calcein complexes did not show NIR-luminescence. The sensitization is not ideal for these lanthanides. Dy(III) and Sm(III) have no energy levels in the 520-830 nm region. A problem occurs if the energy levels of the ligand are situated close to the emitting levels of the lanthanide. The energy can go back to the ligand. Pr(III) and Ho(III) have intense transitions in the spectrum where the water molecules or Si-OH groups can absorb the light or quench the luminescence.

5.5 Conclusion

NIR-luminescence of dipicolinate complexes was detected in PEG-silica sol-gels. $Na_3[Dy(dpa)]_3$ and $Na_3[Nd(dpa)]_3$ showed NIR-luminescence by direct excitation with a Xe-arch lamp at 390 nm and 580 nm respectively. Although the dipicolinate energy levels are far above the energy levels of Yb(III), situated at 977 nm, an intense transition is observed by excitation at 300 nm. Luminescence of other lanthanides was not detected.

The calcein complexes with Nd(III) and Yb(III) show good luminescence because of the antenna effect. Also Er(III) luminescence was detected. Differences between calc45 and calc27 were observed in intensity and lifetime. Calc45 is more able to shield the lanthanide ions from their environment. The intensities and lifetimes of the NIR-transitions are higher. Water is used in the synthesis method; drying increases the intensity and lifetimes become higher. However the quenching by OH vibrations remains high.

REFERENCES

[1] Pope, E. J. A. and Mackenzie, J. D., *J. Non-Cryst. Solids*, 1988, **106**, 236.

[2] Fujiyama, T., Hori, M., and Sasaki, M., *J. Non-Cryst. Solids*, 1990, **121**, 273.

[3] Pawlik, E. M., Strek, W., Derén, P. J., Wojcik, J., Malaskevich, G. E., and Gaishun, V. E., *Spectrochimica Acta A*, 1999, **55**, 369.

[4] Strek, W., Pawlik, E. M., Derén, P. J., Bednarkiewicz, A, Wojcik, J., Gaishun, V. E., and Malashkevich, G. E., *J. Alloys Compds.*, 2000, **300**, 459.

[5] Fonseca, L. F., Resto, O., Soni, R. K., Buzaianu, M., Weisz, S. Z., Gomez, M., and Jia, W., *Mater. Sci. Eng. B*, 2000, **72**, 109.

[6] Gaponenko, N. V., Mudryi, A. V., Sergeev, O. V., Borisenko, V. E., Stepanova, E. A., Baran, A. S., Rat'ko, A. I., Pivin, J. C., and McGilp, J. F., *Spectrochimica Acta A*, 1998, **54**, 2177.

[7] Strohhöfer, C., Fick, J., Vasconcelos, H. C., and Almeida, R. M., *J. Non-Cryst. Solids*, 1998, **226**, 182.

[8] Duverger, C., Montagna, M., Rolli, R., Ronchin, S., Zampedri, L., Fossi, M., Pelli, S., Righini, G. C., Monteil, A., Armellini, C., and Ferrari, M., *J. Non-Cryst. Solids*, 2001, **280**, 261.

[9] Davey, S. T. and France, P. W., *Br. Telecom. Technol. J.*, 1989, **7**, 58.

[10] Viana, B., Koslova, N., Aschehoug, P., and Sanchez, C., *J. Mater. Chem.*, 1995, **5**, 719.

[11] Lai, D. C., Dunn, B., and Zink, J. I., *Inorg. Chem.*, 1996, **35**, 2152.

[12] Werts, M., Woudenberg, R., Emmerink, P., van Gassel, R., Hofstraat, J., and Verhoeven, J., *Angew. Chem. Int. Ed. Engl.*, 2000, **39**, 4542.

[13] Garcia, M., Paje, S. E., Villegas, M. A., and Llopis, J., *Appl. Phys. A*, 2002, **74**, 83.

[14] Werts, M., Verhoeven, J., and Hofstraat, J., *J. Chem. Soc. Perkin Trans.*, 2000, **3**, 433.

[15] Bekiari, V., Pistolis, G., and Lianos, P., *J. Non-Cryst. Solids*, 1998, **226**, 200.

[16] Horrocks, W., Bolender, J., Smith, W., and Supkowsky, R., *J. Am. Chem. Soc.*, 1997, **119**, 5972.

[17] Werts, M., *Luminescent Lanthanide Complexes*, Universiteit van Amsterdam, PhD thesis **2000**.

[18] Werts, M., Hofstraat, J., Geurts, F, and Verhoeven, J., *Chem. Phys. Lett.*, 1997, **276** , 196.

[19] Berregi, I., Del Campo, G., Durand, J., and Casado, J. A., *Anal. Lett.*, 2000, **33**, 277.

[20] Guldi, D., Mody, T., Gerasimchuk, N., Magda, D., and Sessler, J., *J. Am. Chem. Soc.*, 2000, **122**, 8289.

[21] Tobita, S., Arakawa, M., and Tanaka, I., *J. Phys. Chem.*, 1985, **89**, 5649.

6.1 Introduction

Dispersed liquid crystal displays are a newer type of LCD. This type of LCD involves micrometer-sized droplets of a nematic liquid crystal in a solid, isotropic matrix. The first thin *sol-gel glass dispersed liquid crystal* (GDLC) films were prepared by mixing water, TEOS, *4-pentyl-4'-cyanobiphenyl* (5CB) and an organoalkoxysilane *triethoxyethylsilane* (TEES). This procedure was demonstrated by Levy and Otón.[1,2] The material has dispersed droplets filled with 5CB and with droplet diameter 0.1 to 15 μm. The Si-CH_2-CH_3 groups from TEES make the orienting surface on the pore cage. Newer studies proposed different precursors to lower the voltage and to decrease the differences between the refractive index of the matrix and the liquid crystal.[3,4,5,6,7,8,9,10] A patented method uses a mixture of organoalkoxysilanes with other metal alkoxides, the oxide of the added metal alkoxide must have a refractive index larger than 1.52.[8] Amine sidegroups make the orienting surface in the droplets.

GDLC films were already doped with dyes.[11,12] Rhodamine 6G, fluorescein and oxazine-1 were used as matrix dopant. The liquid crystal microdroplets were doped using a B3 dye specifically designed for liquid crystal doping.

Well-known display phosphors are Eu(III) compounds. Eu(III) has an intense red luminescence line around 612 nm. The most simple types of GDLC were used to test the application of lanthanide doped luminescent GDLCs. The liquid crystal formation of the sol-gel film and the solubility of some β-diketones were tested. Luminescence spectra were recorded.

6.2 Synthesis of the complexes

6.2.1 [Eu(BA)$_3$]

The complex was formed by adding an equivalent amount of $EuCl_3.6H_2O$ to a water-ethanol mixture of *benzoylacetone* (BA) at pH 7. The complex was filtrated and dried in a vacuum oven for three days. The purity was verified by CHN-analysis.

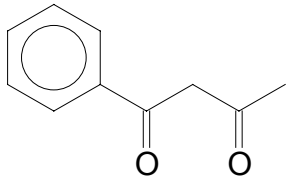

Figure 6.1: Benzoylacetone (BA).

6.2.2 [Eu(DBM)$_3$gly]

This complex was synthesized from a slightly changed procedure described by Evans *et al*.[13] Monoglyme (gly, 1,2-dimethoxyethane, 6.24 mmol) was added to a suspension of Eu_2O_3 (2.74 mmol) in 30 mL of toluene. *Dibenzoylmethane* (DBM, 14.96 mmol) was slowly added to the vigorously stirred suspension. The mixture was heated at reflux for one week. Toluene was removed under vacuum and the solids were dried for three days in a vacuum oven. The purity was verified by CHN-analysis.

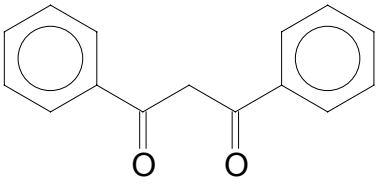

Figure 6.2: Dibenzoylmethane (DBM).

6.3 Synthesis of the GDLC

6.3.1 SiO_2-GDLC

To test the doping with lanthanide complexes the most simple sol-gel GDLCs were chosen, described by Levy and Otón.[1,2] Advantage of these materials is that no nitrogen chamber is necessary (no fast hydrolising components like titanium alkoxides are present). Major disadvantage is the low transmittance because the refractive index of the glass matrix ($n \approx 1.35$) and that of the liquid crystals ($n = 1.52$) differ greatly. GDLC films were prepared by mixing water, ethanol, TMOS, 5CB and TEES. Levy and Otón propose a wide range of volume ratios that results in films with liquid crystal droplets.[1] Some of these results were checked and one optimal procedure was chosen:

4 mL of ethanol is added to a mixture of 3 mL of TMOS and 1 mL of TEES. Slowly 1 mL of distilled water is pipetted to the stirred mixture. After three days of stirring 0.250 mL of 5CB (purchased from Merck) is added. The solution remained clear. After one day the lanthanide complex was dissolved in

the solution. When the complex was dissolved totally, the mixture was rested for a few hours. Now GDLC films could be made. Films were made by dipping one side of a glass substrate in the solution or pipetting a small volume on a flat surface. The films were put in a sealed glass vial and aged 12 h. The film was then dried in an oven at 50°C. The dried films showed a lot of cracks depending on the drying temperature. It was difficult to avoid cracking. Other authors working with similar materials also reported this.[8,8]
A reference sample was prepared by drying 2 mL of the GDLC mixture in a small glass vial. After one month of drying a crack-free monolith was formed.

6.3.2 SiO_2-TiO_2-GDLC

This type of GDLC was prepared similar to a patented method by Whang.[8] The material composition of the patented GDLCs include three- and two-organofunctional silanes. Amine sidegroups make the orienting surface in the droplets. To change the refractive index of the glass matrix to a value similar of the liquid crystal, a metal alkoxide is added (the refractive index of the oxide of the metal must be higher than 1.52).
The samples were prepared by mixing 1 mL of *N*-(2-aminoethyl)-3-aminopropyl-trimethoxysilane with 0.2 mL of *tetraethylorthotitane* (TEOT) in a nitrogen chamber. TEOT is very easily hydrolyzed in open air to form a white powder. The mixture was stirred for several minutes. 0.2 mL of the liquid crystal 5CB was added to this solution.
Up to 25 mg of the $[Eu(DBM)_3gly]$ can be dissolved giving a clear yellowish solution. The lanthanide doped mixture was taken out of the nitrogen chamber for further processing. Films were made by dipping one side of a glass

substrate in the solution or pipetting a small volume on a flat surface. The coated glass substrates were put in small glass vials. These vials were placed in a large beaker containing a small volume of distilled water. The beakers were covered with a glass plate. The metal alkoxides hydrolyze and polymerize in this humid atmosphere. Turbid gels were formed at room temperature in two days and the beakers were placed in an oven at 60 °C. After two days of drying lanthanide doped GDLCs were formed with good film integrity.
A reference sample was prepared by making a film with the same procedure but no liquid crystal was added. The reference samples were transparent and crack-free.

6.4 Detection of the switching capacity

6.4.1 Introduction

The mechanism of a GDLC doped with luminescent dyes is different from a GDLC based on transmission of (colored) light. The transmission type of GDLC is explained in chapter 1. In this type of GDLC the light cannot pass in the OFF stage (dark) because it is scattered due to the difference of the refractive index between the glass matrix (n_g) and the unaligned LC droplets ($n_g \neq n_{//}$). If the layer is in the ON stage, all the liquid crystals are aligned by an external field along the direction of the light. The refractive index encountered by the light is n_g in the matrix and $n_\perp = n_g$ in the droplets. The light passes (light or color).

Labes and coworkers studied luminescent Eu(III) dyes in nematic liquid crystal electro-optic cells that roughly consist of a nematic liquid crystal between two transparent electrodes.[14,15,16] The mechanism is expected to be similar in GDLCs doped with luminescent dyes. This is explained in figure 6.3. UV light is used to excite the luminescent dye. Due to the large internal scattering of the UV-light in the OFF stage (A) the absorption by the luminescent dyes is enhanced because the pathlength of the light increases. This gives the layer a visible color. In the ON position (B) the UV-light passes the layer with less absorption and thus less luminescence.

6.4.2 Experimental setup

5CB is a crystalline solid at room temperature (18°C) and becomes liquid-crystalline at 22.5 °C (nematic phase) and an isotropic liquid at 35.0 °C. Once it is melted, the 5CB remains liquid-crystalline at room temperature. The liquid crystal in the nematic phase is turbid due to the anisotropy that causes birefringence (double refraction). In a GDLC film the droplets containing LC cause the whole sample to be turbid. Incident light is scattered.
Besides applying an electrical field to make de film transparent along the direction of the electrical field, another way to make the GDLC film transparent is to heat the sample above the liquid crystal-liquid transition (clearing point, $T_{clearing}$) at 35.0 °C. The whole film becomes transparent if the refractive index of the isotropic liquid (n_i) is similar to that of the glass (figure 6.3 C).

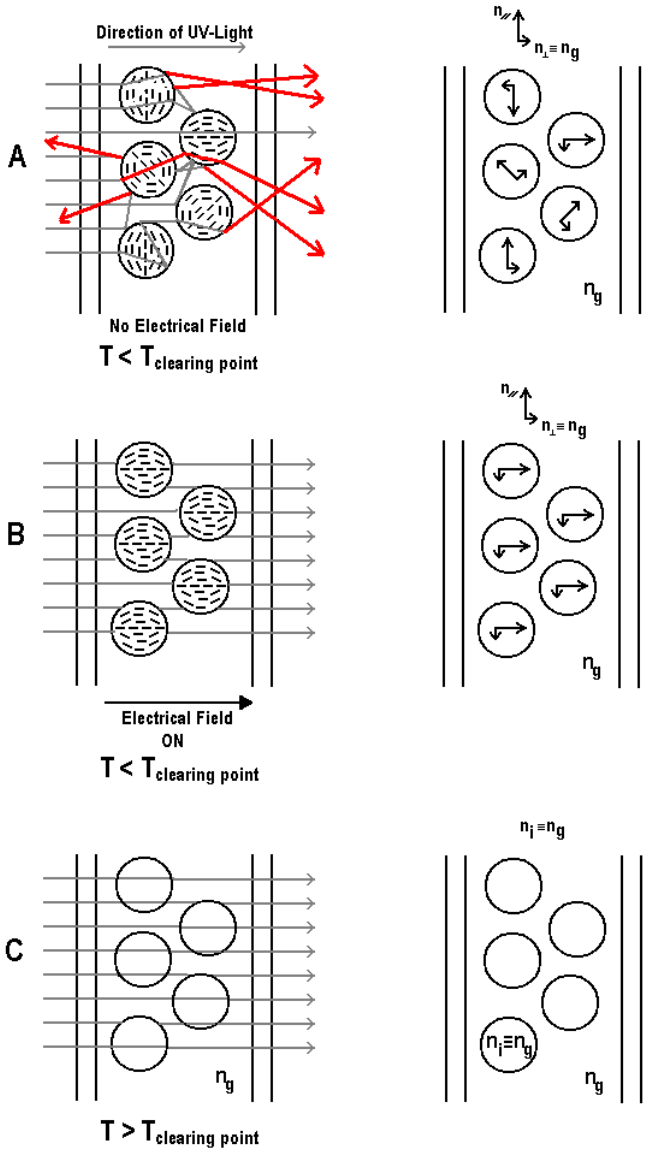

Figure 6.3: Mechanism of a GDLC doped with a luminescent dye: without electrical field and below $T_{clearing}$ (A), with electrical field and below $T_{clearing}$ (B) and $T_{clearing}$ (C). The refractive indexes of the liquid crystal ($n_{\perp}$ and $n_{//}$) and the glass (n_g) are indicated on the right side.

The change of luminescence intensity in Eu(III) doped GDLCs was indirectly tested by heating a GDLC film from room temperature to 50°C while monitoring the luminescence. The experimental setup of the spectrofluorimeter is given in figure 6.4.

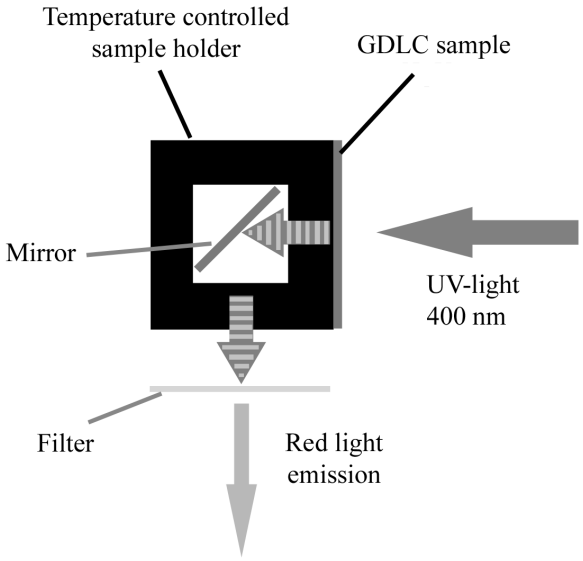

Figure 6.4: Experimental setup for the spectrofluorimeter.

6.5 SiO_2-GDLC

6.5.1 [$Eu(BA)_3$]

Portions ranging from 2.0 mg to 20 mg of the complex were added to 2 mL of the starting solution. After vigorous stirring the complex dissolved. In comparison to the non-doped solutions the doped solutions needed a long resting period. If the films were made directly after dissolving, no liquid crystal properties appeared. The liquid crystal droplet size varied greatly in the sample and even between samples made from the same solution.

Liquid-crystalline behavior can be tested with a thermo-optical microscope or polarizing optical microscope. The sample is placed on a temperature controlled heating device between crossed polarizers. Due to the anisotropy of the sample, the polarization direction of incoming polarized light is changed. A fraction of the light can pass through the second polarizer. In a typical liquid crystal the change in polarization direction is not constant over the entire sample. Some areas appear light and others appear dark. By heating the sample, the liquid-crystal to isotropic liquid phase transition can be monitored. In figure 6.5 a photograph of a $Eu(BA)_3$ doped SiO_2-GDLC film placed in a polarizing optical microscope (300 x magnification) is shown. Maltese crosses are observed. This is typical for nematic phases. The liquid-crystal to liquid phase transition appeared around 31 °C depending on the diameter of the droplets. Smaller droplets became isotropic liquids faster than large droplets. Partial dissolving of other components, like methanol, in the 5CB can also lower the clearing point. The samples were tested for their Eu(III) luminescence. A spectrum is shown in figure 6.6.

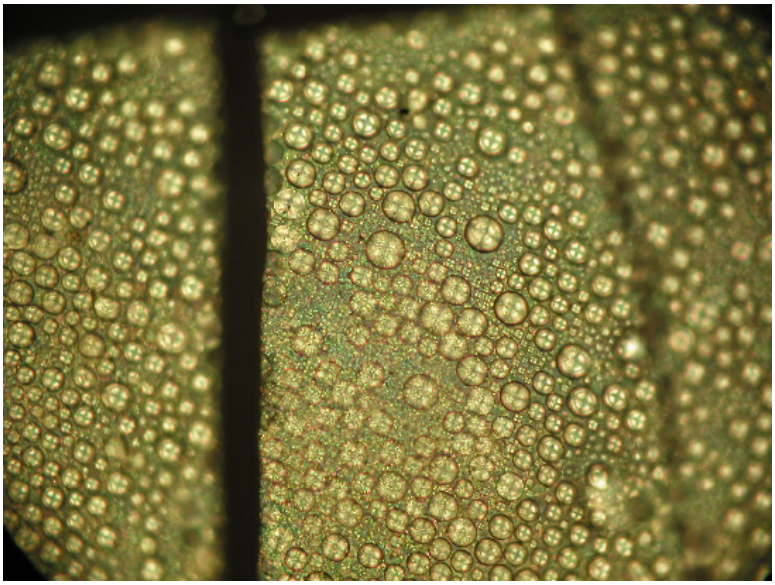

Figure 6.5: Photograph of a $Eu(BA)_3$ doped SiO_2-GDLC film placed in a polarizing optical microscope (300 x enlarged).

The antenna effect was used to excitate the Eu(III) ions but the sample had still a low intensity and therefore a long measuring time was necessary. The spectrum also did not show fine structure. The starting solution was already highly doped with $Eu(BA)_3$ and more complex could not be dissolved. Therefore a better luminescent complex was chosen.

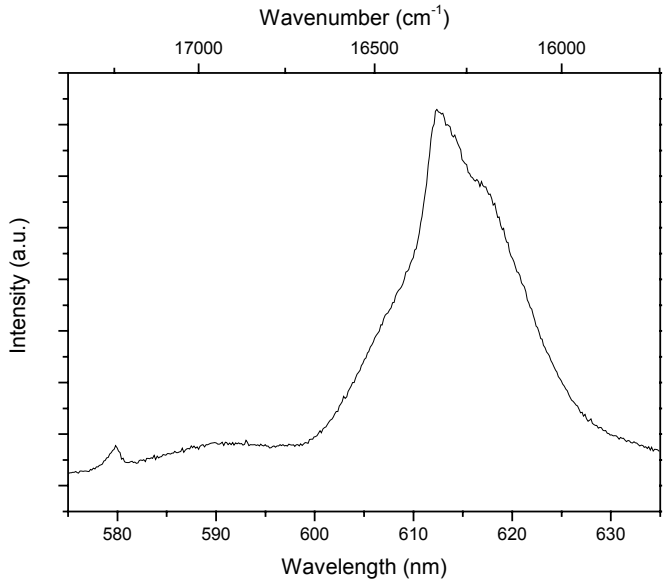

Figure 6.6: Luminescence spectrum of a $Eu(BA)_3$ doped SiO_2-GDLC.

6.5.2 [Eu(DBM)$_3$gly]

This [$Eu(DBM)_3$gly] β-diketone complex is better luminescent than the [$Eu(BA)_3$] complex thanks to the monoglyme molecule that prohibits other molecules (like water) to coordinate to the lanthanide ion and quench the luminescence. The triplet energy levels of DBM are also situated lower than those for BA. There is a better match with the energy levels of Eu(III). This is not the case for Tb(III) where the triplet energy levels of DBM are situated below the lanthanide levels. Doped SiO_2-GDLC samples have been prepared. A digitally enlarged picture is shown in figure 6.7.

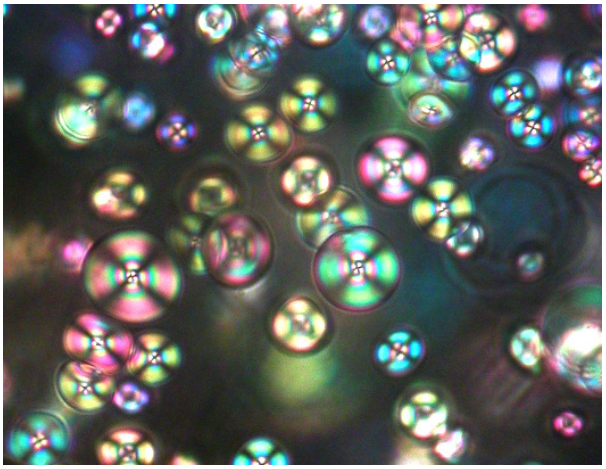

Figure 6.7: Digitally enlarged picture of an $Eu(DBM)_3gly$ doped SiO_2-GDLC film.

The colours of the samples can differ; this depends on external factors like sample thickness. Figure 6.8 shows the luminescence spectrum of a $Eu(DBM)_3gly$ SiO_2-GDLC film. The luminescence intensity is very high in comparison with the BA doped films. The fine structure has also been improved. For reference, a 2 mL solution with the same composition was dried in a glass vial at room temperature. After five weeks the thick sample was crack-free, transparent and did not have liquid crystal droplets. The luminescence spectrum is also shown in figure 6.8 and is similar to the SiO_2-GDLC spectrum.

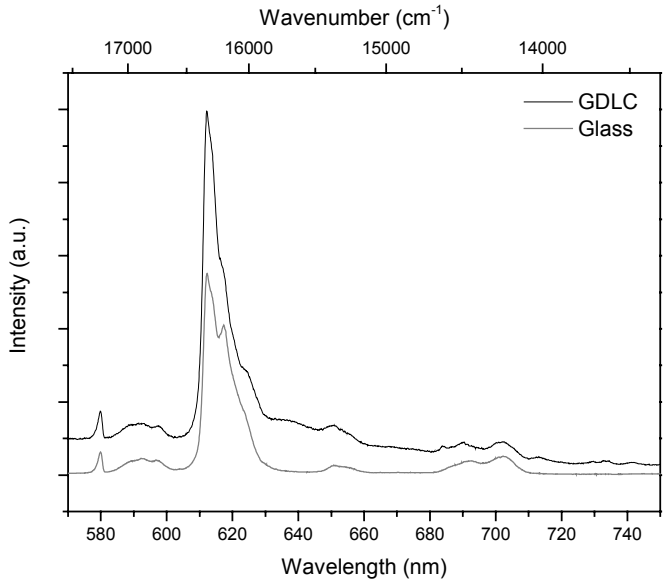

Figure 6.8: Spectra of $Eu(DBM)_3gly$ doped SiO_2-GDLC film and glass.

The luminescence intensity of the lanthanide doped SiO_2-GDLC film was measured as a function of the temperature (figure 6.9). Only the intensity of the hypersensitive $^5D_0 \rightarrow {}^7F_2$ transition was measured. This transition accounts for around 70% of the total intensity. A short scan was used to lower the time of the measurement because excitation during a longer period can influence the temperature of the sample.

The intensity of the Eu(III) complex itself decreases in function of the temperature because quenching by non-radiative decay is improved at higher temperature. Therefore all spectra were corrected for this decrease in intensity.

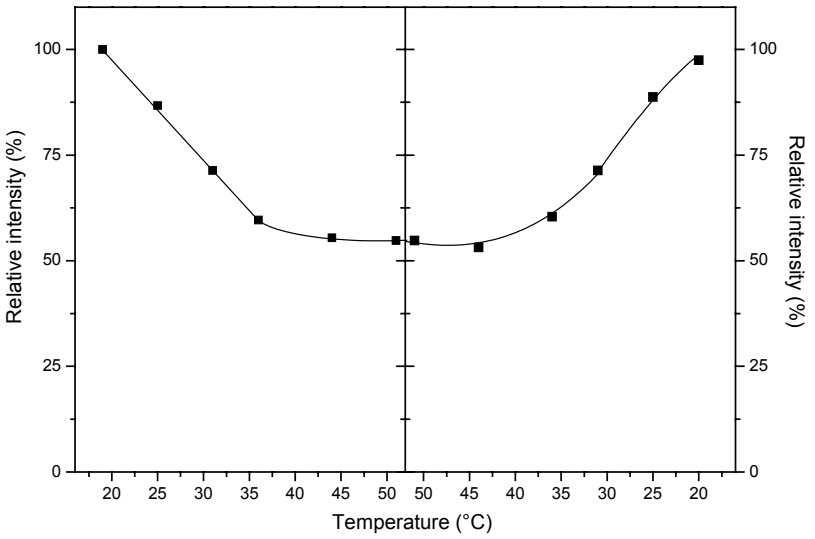

Figure 6.9: The relative intensity of a $Eu(DBM)_3gly$ doped SiO_2-GDLC film as a function of the temperature.

The intensity after the clearing point is roughly the half of the intensity at room temperature. Already at 28 °C the intensity decreased by 25%. There is no sharp change of intensity around the clearing point at approximately 31 °C.

The decrease in intensity before the clearing point can be explained by the temperature dependence of the refractive index and the anisotropy of the liquid crystalline phase. The anisotropy and the birefringence decrease with increasing temperature.[17] The temperature dependence is pronounced at the clearing point. The change in refractive index is mainly influenced by the temperature dependence of the polarizability.[18]

The small change in intensity (ratio 1:2) and the small change at the clearing point in these SiO_2-GDLC films can be attributed to the large difference between the refractive indices of the ORMOSIL and the 5CB, 1.35 versus 1.52 respectively. The samples are not fully transparent at temperatures above the clearing point; the high scattering is responsible for the remaining high luminescence intensity (approximately 53 % of the initial intensity). The difference in refractive index must be lowered to achieve better results.

6.6 SiO_2-TiO_2-GDLC

A photograph of a SiO_2-TiO_2-GDLC film (noted as TiO_2-GDLC) placed in a polarizing optical microscope (300 x enlarged) is given in figure 6.10. A luminescence spectrum of the GDLC film doped with $[Eu(DBM)_3gly]$ is shown in figure 6.11. The clearing point is situated at 34 °C. The TiO_2-GDLC films are more suitable than the pure SiO_2-GDLC films. When the turbid samples (at room temperature) are placed in an oven at 60 °C the samples become transparent. This change was not as clearly observed in the case of a SiO_2-GDLC sample.

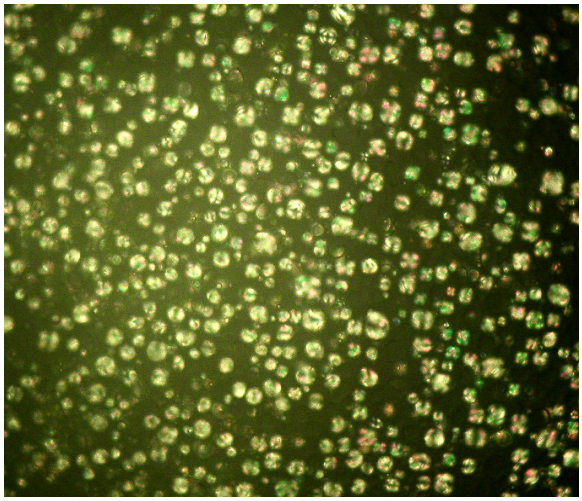

Figure 6.10: photograph of a TiO_2-GDLC film placed in a polarizing optical microscope (300 x enlarged).

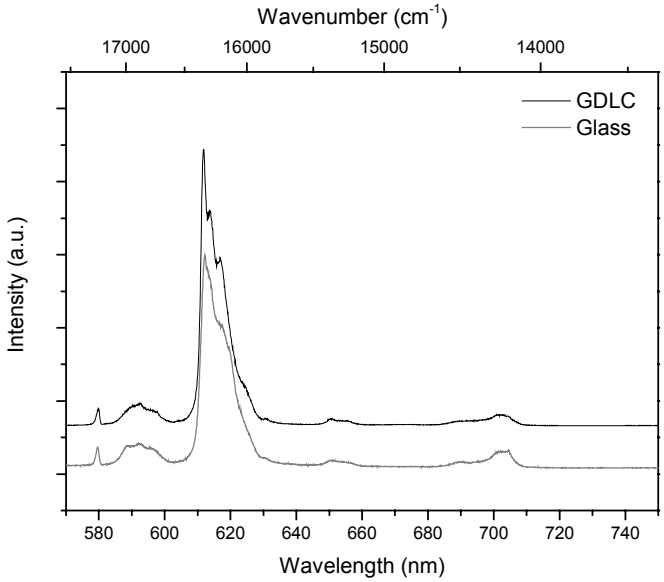

Figure 6.11: Luminescence spectrum of $[Eu(DBM)_3gly]$ in the SiO_2-TiO_2-GDLC film and in a SiO_2-TiO_2 sample.

As mentioned before, the intensity of the Eu(III) complex itself decreases in function of the temperature because quenching by non-radiative decay is improved at higher temperature. The influence of the temperature on the intensity of the $^5D_0 \rightarrow {}^7F_2$ transition in a SiO_2-TiO_2 sample containing no liquid crystal is shown in figure 6.12.

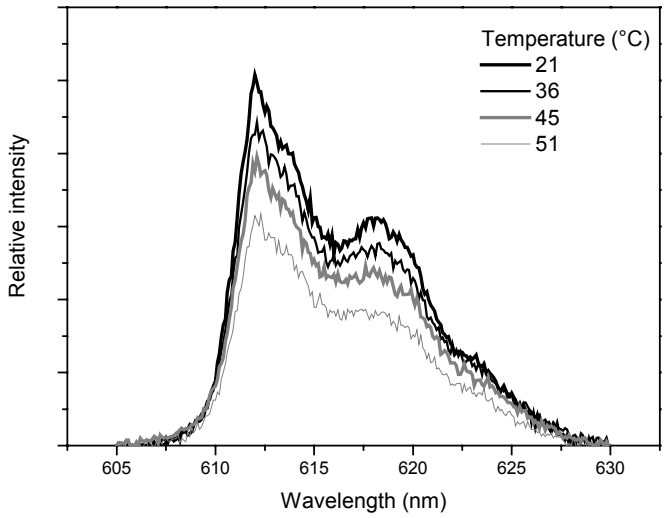

Figure 6.12: influence of the temperature on the intensity of the $^5D_0 \rightarrow {}^7F_2$ transition of [Eu(DBM)$_3$gly] in a SiO_2-TiO_2 sample.

The increase and decrease in intensity of the [Eu(DBM)$_3$gly] in a TiO_2-GDLC is shown in figure 6.13. All spectra were corrected for the decrease in intensity in a [Eu(DBM)$_3$gly] doped SiO_2-TiO_2 sample.

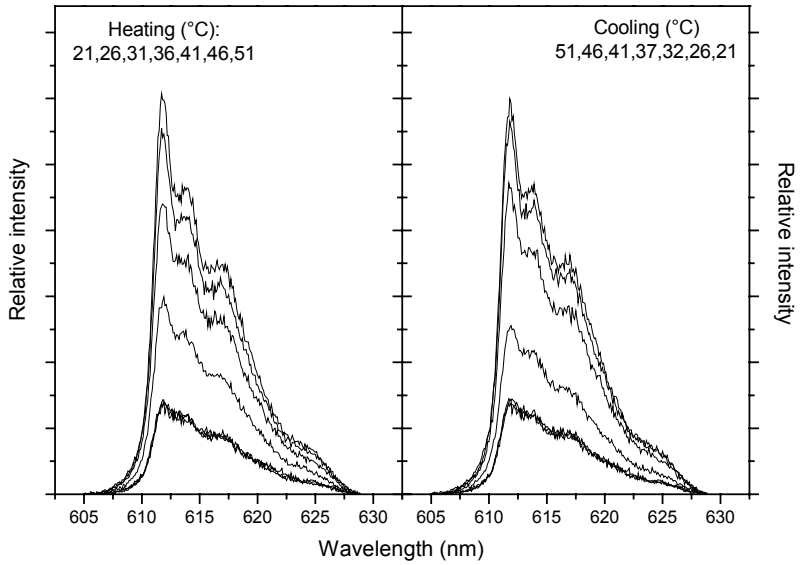

Figure 6.13: Corrected intensity of a [Eu(DBM)$_3$gly] doped SiO_2-TiO_2-GDLC film during a heating and cooling cycle. The intensity decreases with increased temperature.

The calculated intensity of the $^5D_0 \rightarrow {}^7F_2$ transition in function of the temperature is shown in figure 6.14. The contrast ratio, between the luminescence of the sample heated at 50 °C (dispersed isotropic 5CB) and the luminescence of the sample at room temperature (dispersed nematic 5CB), is around 1:4. The intensity decrease around the clearing point at 34 °C is sharper than in the SiO_2-GDLC. Intensity decrease caused by the change in the refractive index (< 30 °C) is smaller. The TiO_2-GDLC benefits from the better match between the refractive indices of the matrix and the liquid crystal. The temperature corrected luminescence remains stable after the clearing point.

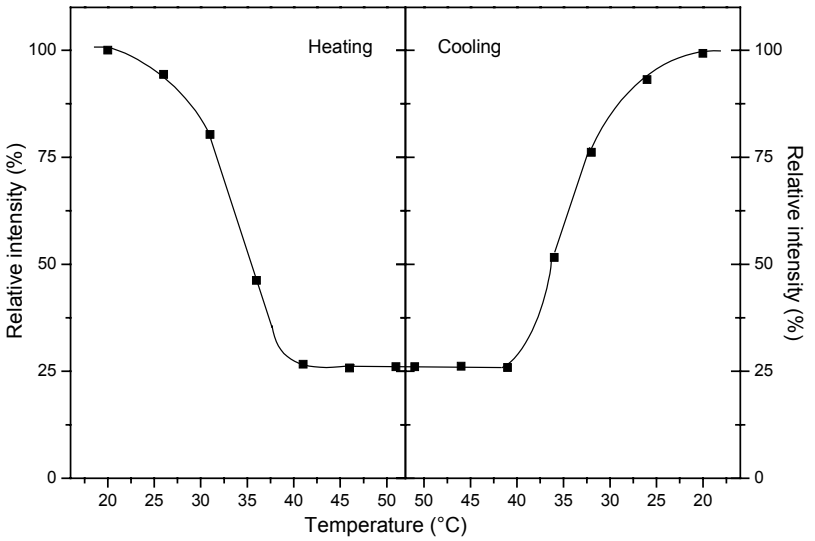

Figure 6.14: The relative intensity of Eu(III) doped TiO_2-GDLC film as a function of the temperature.

The samples were not optimized for layer thickness and phosphor concentration. These parameters can be useful to improve the contrast ratio. It is also interesting to investigate the influence of different lanthanide complexes in these GDLC films.

6.7 Conclusion

Luminescent GDLC films doped with Eu(III) phosphors were prepared successfully. Intense lanthanide luminescence can be measured for [$Eu(DBM)_3$gly] but not for [$Eu(BA)_3$]. The better shielding by the monoglyme and the better overlap between the DBM triplet energy level and Eu(III) energy levels increased the intensity.

LCD switching capacity of the samples was tested indirectly. The intensity decrease between the ON and OFF state was measured by recording the luminescence intensity while heating the samples from room temperature to above the clearing point. The SiO_2-TiO_2-GDLC films have a better contrast ratio than the SiO_2-GDLC films when heated (1:4 versus 1:2) and show a sharper decrease in intensity near the clearing point.

The samples were not optimized for layer thickness and phosphor concentration. Further investigation is required. It is also interesting to investigate the influence of different lanthanide complexes in these GDLC films. These parameters can be useful to improve the contrast ratio.

REFERENCES

[1] Levy, D., Serna, C. J., and Oton, J. M., *Mater. lett.*, 1991, **10**, 470.

[2] Oton, J. M., Serrano, A., Serna, C. J., and Levy, D., *Liq. Cryst.*, 1991, **12**, 733.

[3] Levy, D., Pena, J. M. S., Serna, C. J., and Oton, J. M., *J. Non-Cryst. Solids*, 1992, **147-148**, 646.

[4] Levy, D., *J. Non-Cryst. Solids*, 1992, **147-148**, 508.

[5] Levy, D., Serrano, A., and Oton, J. M., *J. Sol-Gel Sci. Technol.*, 1994, **2**, 803.

[6] Levy, D. and Esquivias, L., *Adv. Mater.*, 1995, **7**, 120.

[7] Pena, J. M. S., Olias, E., Quintana, X., and Oton, J. M., *Mol. Cryst. Liq. Cryst.*, 1997, **299**, 337.

[8] Whang, W., *Gel-glass dispersed liquid crystals*, 1997, US patent 5,702,636.

[9] Hori, M. and Toki, M., *J. Sol-Gel Sci. Technol.*, 2000, **19**, 349.

[10] Levy, D., *Mol. Cryst. Liq. Cryst.*, 2000, **354**, 159.

[11] Levy, D., Del Monte, F., Quintana, X., and Oton, J. M., *J. Sol-Gel Sci. Technol.*, 1997, **8**, 1063.

[12] Haruvy, Y. and Webber, S. E., *Chem. Mater.*, 1991, **10**, 470.

[13] Evans, W. J., Giarikos, D. G., Johnston, M. A., Greci, M. A., and Ziller, J. W., *J. Chem. Soc. , Dalton Trans.* , 2002, 520.

[14] Labes, M. M., *Fluorescent liquid crystal display*, 1977, US patent 4.176.918.

[15] Hochbaum, A., Yu, L. J., and Labes, M. M., *J. Appl. Phys.*, 1980, **51**, 867.

[16] Sato, S. and Labes, M. M., *J. Appl. Phys.*, 1981, **52**, 3941.

[17] Bogi, A. and Faetti, S., *Liq. Cryst.*, 2001, **25**, 729.

[18] Demus, D., Goodby, J., Gray, G. W., Spiess, H. W., and Vill, V., *Handbook of Liquid Crystals*, Wiley-VCH, Weinheim **1998**, 132.

General conclusion and summary

In this PhD thesis, the spectroscopic properties of lanthanide ions in silica-based hybrid materials were studied. Several hybrid materials were prepared by the sol-gel method starting from silicon alkoxides. Due to the low processing temperatures, these materials can be doped with organic lanthanide coordination complexes.

To start the study of lanthanide spectroscopy in silica-based materials the absorption properties of lanthanide ions doped in *pure silica sol-gel glasses* were investigated. Silica sol-gel glasses were doped with $[Ln(bipy)_2]Cl_3$, $[Ln(phen)_2]Cl_3$ and $Ln(NO_3)_3$ complexes (bipy = bipyridyl, 2,2'-bipyridine, phen = 1,10-phenanthroline, Ln = Nd, Sm, Dy, Ho, Er). Cluster formation was tested and was found to be absent in the measured concentration range. Judd-Ofelt parameters have been calculated. The Ω_λ-parameters describe the intensity of the *induced electric dipole transitions*. The Ω_2-parameter, linked to short-range effects, increased upon heat treatment due to a change in the coordination sphere of the Ln(III). This is caused by water molecules leaving the sol-gel glass and the first coordination sphere around the lanthanide ions. The Ω_4- and Ω_6-parameters, linked to long-range effects, remain constant during heat treatment and are more influenced by matrix effects than by the surrounding ligands. Almost total recovery of the initial intensity occurs when the samples are exposed to air at room temperature after the heat treatment. It was demonstrated that Judd-Ofelt parameters are not only of interest to compare results between different materials or different complexes, but that

these parameters can also be used to detect structural changes within one material.

Lanthanide complexes with large basic ligands, like dipicolinate, are often not soluble in the pure silica sol-gel glasses that are prepared at pH 2. Therefore silica-based hybrid materials were made with the sol-gel method at a neutral pH. The PEG-silica materials are easily made and cracking is absent. The sol-gels were doped with $[Ln(bipy)_2]Cl_3$, $[Ln(phen)_2]Cl_3$, $Na_3[Ln(dpa)_3]$ and $LnCl_3$ complexes (dpa = dipicolinate, Ln = Nd, Sm, Dy, Ho, Er). Ligands like 1,10-phenanthroline and 2,2'-bipyridyl are not strong enough to remove the water and PEG molecules from the first coordination sphere of the lanthanide ions. On the other hand, dipicolinate ligands bind strongly to lanthanide ions and shield the lanthanides from PEG and water molecules. This is interesting for the luminescence of lanthanides in the near-infrared region of the spectrum where quenching by OH vibrations limits the luminescence intensity severely.

Both lanthanide ions and silica-based materials are currently used for near-infrared data transfer. NIR-luminescence was detected in PEG-silica sol-gel glasses for $Na_3[Ln(dpa)_3]$ and [Ln(calc)] (calc = calcein) complexes. $Na_3[Dy(dpa)]_3$ and $Na_3[Nd(dpa)]_3$ showed NIR-luminescence by direct excitation with a Xe-arch lamp at 390 nm and 580 nm respectively. Although the dipicolinate energy levels are far above the energy levels of Yb(III), situated at 977 nm, an intense transition is observed by excitation at 300 nm. Luminescence of other lanthanides was not detected.
The calcein complexes with Nd(III) and Yb(III) show good luminescence when excited in the ligand absorption band. Er(III) luminescence was also detected. To our knowledge, this is the first time that an organic ligand is used

to sensitize the NIR-luminescence of erbium(III) in a silica sol-gel material. Differences between calc45 and calc27 were observed in intensity and lifetime. Calc45 is more able to shield the lanthanide ions from their environment. The intensity and lifetime of the NIR-transitions are higher. Water is used in the synthesis method; drying increases the intensity and the lifetime becomes higher. However, the quenching by OH groups in the material remains high.

Glass dispersed liquid crystal (GDLC) displays are a newer type of LCD. This type of LCD involves micrometer-sized droplets of a nematic liquid crystal in a glass matrix. GDLC films were prepared with the sol-gel method and doped with lanthanide phosphors. Intense lanthanide luminescence could be measured for [Eu(DBM)$_3$gly] (DBM = dibenzoylmethane en gly = monoglyme). LCD switching capacity of the samples was tested indirectly. The intensity decrease between the OFF and ON state was measured by recording the luminescence intensity while heating the samples from room temperature to above the clearing point. The SiO_2-TiO_2-GDLC films have a better contrast ratio than the SiO_2-GDLC films when heated (1:4 versus 1:2) and show a sharper decrease in intensity near the clearing point. The samples were not optimized for layer thickness and phosphor concentration. Further investigation is required. It is also interesting to investigate the influence of different lanthanide complexes in these GDLC films. These parameters can be useful to improve the contrast ratio.

The sol-gel synthesis is an excellent route to prepare hybrid silica materials and lanthanide ions have good visible- and NIR-luminescence. It was shown that interesting optical materials can be prepared by combining silica sol-gel synthesis and lanthanides.

Samenvatting

De lanthaniden zijn de 4f-elementen met atoomnummer 57 tot 72. De driewaardige lanthanide-ionen zijn gekend voor hun goede optische eigenschappen. Materialen gedoteerd met lanthaniden kennen reeds vele optische toepassingen. Een klassiek voorbeeld is de rode fosfor $Y_2O_2S:Eu^{3+}$ in de *Cathode Ray Tube*-beeldschermen. De rode luminescentie komt van de *geïnduceerde elektrisch dipool* (ED)-transities binnen de f-schil van europium. Een ander lanthanide, erbium, luminesceert in het nabije infrarood en wordt daarom gebruikt in infraroodlasers voor optische datacommunicatie.

De "sol-gel methode" is een geschikte methode om hoogwaardige optische materialen te maken bij lage temperatuur. Siliciumalkoxiden reageren met water, waarbij ze hydrolyseren en condenseren ter vorming van een sol. Een typisch voorbeeld is *tetraethylorthosilicaat* (TEOS). Door verdere condensatiereacties wordt een anorganisch netwerk gevormd met colloïdale dimensies (gel). Naargelang de reactiecondities (pH, verhouding water/precursor, temperatuur) en de verwerkingsmethode kan men bijvoorbeeld glasvezels, dunne films, hoogdisperse materialen of bulkglazen maken. Ook kunnen *hybride materialen*, een combinatie van anorganische en organische materialen, worden gemaakt door de grote verscheidenheid aan precursoren zoals organoalkoxysilanen. In dit werk werden de spectroscopische eigenschappen van lanthanide-gedoteerde silica sol-gelmaterialen bestudeerd.

Eerst werden zuivere silica (SiO_2) sol-gelglaasjes gemaakt, gedoteerd met enkele lanthanidecomplexen: $Ln(Cl)_3$, $[Ln(bipy)]Cl_3$ en $[Ln(phen)]Cl_3$ (met Ln = Nd, Sm, Dy, Ho, Er en bipy = dipyridyl of 2,2'-bipyridine, phen = 1,10'-fenanthroline). De Judd-Ofelt-theorie werd gebruikt om de intensiteit van de geïnduceerde ED-transities te bestuderen. De Ω_2-parameters, die in verband staan met interacties over korte afstand en de hypersensitieve overgangen, veranderen sterk wanneer de glaasjes worden gedroogd. Dit komt omdat tijdens het drogen water wordt verwijderd uit de eerste coördinatiesfeer. De Ω_4- en Ω_6-parameters staan in verband met lange-afstandsinteracties en veranderen weinig.

Er werd ook onderzoek gedaan op een hybride materiaal bestaande uit silica en *polyethyleenglycol* (PEG). Deze sol-gels kunnen worden gemaakt in neutraal midden waarin ook het dipicolinaat (dpa)-complex oplost. De PEG-silica sol-gels werden gedoteerd met: $Ln(Cl)_3$, $[Ln(bipy)]Cl_3$, $[Ln(phen)]Cl_3$ en $Na_3[Ln(dpa)_3]$. Uit een analyse van de Ω_λ-parameters blijkt dat niet alleen de rol van water belangrijk is, maar ook die van het PEG, dat complexerende eigenschappen heeft. Het dpa-complex daarentegen schermt het lanthanide goed af van water en PEG.

In een volgende reeks van experimenten werden lanthanide-gedoteerde PEG-silica sol-gels getest op nabije infraroodluminescentie (NIR-luminescentie). Sol-gels gedoteerd met $Na_3[Nd(dpa)_3]$ en $Na_3[Dy(dpa)_3]$ geven luminescentie door rechtstreekse excitatie in lanthanide f-f transities. $Na_3[Yb(dpa)_3]$ geeft intense luminescentie door een ladingsoverdracht-mechanisme tussen het dpa en Yb(III). De PEG-silica sol-gels werden ook gedoteerd met een lanthanide-calceïne complex. Intense NIR-luminescentie werd waargenomen voor Yb(III)

en Nd(III) door excitatie in het ligand. Energie geabsorbeerd door het calceïne wordt overgedragen naar het lanthanide-ion. Ook Er(III) luminescentie werd waargenomen. De invloed van twee isomeren van calceine werd onderzocht. Betere complexatie zorgt er voor dat de lanthanide-ionen beter worden afgeschemd van quenchende OH-groepen die in de gel aanwezig zijn. De intensiteit en leeftijden van de transities verbeteren. Ook intenser drogen van de stalen zorgt voor een verhoging van de NIR-luminescentie en vervalleeftijden.

Gedispergeerde vloeibare kristallen zijn toepasbaar als een nieuwer type van LCD. Glas-gedispergeerde vloeibare kristallen (GDLCs) kunnen gemaakt worden via de sol-gel methode. Films werden gedoteerd met een europium-complex [$Eu(DBM)_3gly$] (met DBM = dibenzoylmethaan en gly = monoglyme). Een contrastverhouding van 4:1 werd gemeten tussen luminescentie bij kamertemperatuur en bij 51 °C. Dit is een temperatuur boven het klaarpunt van het gebruikte vloeibaar kristal. De invloed van de matrix werd onderzocht.

De sol-gel methode is zeer geschikt voor de bereiding van hybride materialen. Er werd aangetoond dat lanthanide-gedoteerde hybride silica sol-gelmaterialen interessant zijn voor optische toepassingen.

List of publications

[1] Driesen, K., Binnemans, K. and Görller-Walrand, C., "Spectroscopic properties of monolithic sol-gel glasses doped with lanthanide bipyridyl complexes", *Materials Science and Engineering C*, 18 (2001) 255-258.

[2] Binnemans, K., Malykhina, L., Mironov, V., Haase, W., Driesen, K., Van Deun, R., Fluyt, L., Görller-Walrand, C. and Galyametdinov, Y., "Probing the magnetic anisotropy of lanthanide-containing metallomesogens by luminescence spectroscopy", *ChemPhysChem*, 11 (2001) 680-683.

[3] Driesen, K., Lenaerts, P., Binnemans, K. and Görller-Walrand, C., "Influence of heat treatment on the intensities of f-f transitions in lanthanide-doped sol-gel glasses", *Physical Chemistry Chemical Physics*, 4 (2002) 552-555.

[4] Galyametdinov, Y., Malykhina, L., Haase, W., Driesen, K. and Binnemans, K., "Luminescent lanthanide complexes with liquid-crystalline properties", *Liquid Crystals*, 29 (2002) 1581-1584.

[5] Driesen, K., Fourier, S., Görller-Walrand, C. and Binnemans, K., "Judd-Ofelt analysis of lanthanide doped silica-PEG hybrid sol-gels", *Physical Chemistry Chemical Physics*, 5 (2003) 198-202.

[6] Driesen, K. and Binnemans, K., "Temperature-driven luminescence switching of europium(III) in a glass dispersed liquid crystal film", *Adv. Mater.* (submitted).

[7] Driesen, K., Van Deun, R., Görller-Walrand, C. and Binnemans, K., "Near-infrared luminescence of lanthanide-calcein complexes doped into a silica-PEG hybrid material", *Chem. Mater.* (submitted).